A new approach to identifying behaviour in animals using tiger sharks, *Galeocerdo cuvier*, as a test species.

Wallis May James, Marine Biology BSc

Submitted to Swansea University in fulfilment of the requirements for the Degree of MRes Biosciences.

Swansea University

2022

Declarations

This work has not previously been accepted in substance for any degree and is not being concurrently submitted in candidature for any degree.

Signed.. [redacted] .....

Date.....16/08/22.....

This thesis is the result of my own investigations, except where otherwise stated. Other sources are acknowledged by footnotes giving explicit references. A bibliography is appended.

Signed [redacted] .....

Date.....16/08/22.....

I hereby give consent for my thesis, if accepted, to be available for photocopying and for inter-library loan, and for the title and summary to be made available to outside organisations.

Signed... [redacted] .....

Date.....16/08/22.....

The University's ethical procedures have been followed and, where appropriate, that ethical approval has been granted.

Signed... [redacted] .....

Date.....16/08/22.....

STATEMENT OF EXPENDITURE

No costs were incurred during the production of this work.

STATEMENT OF CONTRIBUTIONS

R.P. Wilson conceived and developed the idea. Dr. M. Meekan collected the data, M. Holton developed the software while W. M. James conducted the major part of the analysis. W. M. James completed the writing of the manuscript, with critical feedback from R. P. Wilson.

ACKNOWLEDGEMENTS

Firstly, this work was made possible by Dr. Mark Meekan, of the Australian Institute of Marine Science (AIMS), generously sharing his tag data with me, for which I am extremely grateful. The superb guidance and support from Rory Wilson undoubtedly contributed to the progress and completion of this work. Additionally, I would like to express my gratitude to Mark Holton for his remarkable software, as well as his devotion to helping users understand its intricacy. Finally, thanks to my fellow Biosciences MRes peers Milz, Abi and Cindy who provided a virtual support community during the production of this work under COVID lockdown circumstances.

ETHICS APPROVAL

Project Ethics Assessment Confirmation|Cadarnhad o Asesiad Moeseg Prosiect

CE cosethics@swansea.ac.uk
To JAMES W. [redacted]
Cc Wilson R.P.

Reply | Reply All | Forward | ...
Thu 28/01/2021 20:01

This is an automated confirmation email for the following project. The Ethics Assessment status of this project is: APPROVED

Applicant Name: Wallis James
Project Title: A new approach to identifying behaviour in animals using sharks as a test taxon.
Project Start Date: 25/01/2021
Project Duration: 8-9 months
Approval No: SU-Ethics-Student-280121/3695

NOTE: This notice of ethical approval does not cover aspects relating to Health and Safety. Please complete any relevant risk assessments prior to commencing with your project.

Neges awtomataidd yw hon ar gyfer y prosiect canlynol. Statws Asesiad Moeseg y prosiect hwn yw: APPROVED

Enw'r Ymgeisydd: Wallis James
Teitl y Prosiect: A new approach to identifying behaviour in animals using sharks as a test taxon.
Dyddiad Dechrau'r Prosiect: 25/01/2021
Hyd y Prosiect: 8-9 months
Rhif y Gymeradwyaeth: SU-Ethics-Student-280121/3695

SYLWER: Nid yw'r hysbysiad hwn o gymeradwyaeth foesegol yn cynnwys agweddau sy'n ymwneud ag Iechyd a Diogelwch. Dylech gwblhau unrhyw asesiadau risg perthnasol cyn dechrau eich prosiect.

Risk Assessment			
College/ PSU	**College of Science**	**Assessment Date**	**28/01/2021**
Location	**SO53/TW2/SA2**	**Assessor**	**Wallis James**
Activity	**Desk Study**	**Review Date (if applicable)**	**NA**
Associated documents	**NA**		

Part 1: Risk Assessment

What are the hazards?	Who might be harmed?	How could they be harmed?	What are you already doing?	S	L	Risk (SxL)	Do you need to do anything else to manage this risk?	S	L	Risk (SxL)	Additional Action Required
Eye fatigue/strain	Student/supervisor	Can cause tiredness and muscle ache and difficulty sleeping.	Taking regular breaks.	1	5	5	Regular breaks, exercise and stretches.	1	4	4	Switch display settings to “dark mode” and reduce brightness.
Back/neck strain.	Student/supervisor	Discomfort, reduced mobility, difficulty sleeping.	Take regular breaks to walk and stretch.	3	5	15	Use a suitable work chair, sit with good posture.	3	3	9	See doctor/physio if problems persist. Core Strengthening exercises.
General household injuries (i.e. trips, slips,	Student/supervisor	Damage to skin, limbs, head, body.	Take care when moving around.	5	4	20	Take care when moving around	5	2	10	Wear suitable foorwear.

What are the hazards?	Who might be harmed?	How could they be harmed?	What are you already doing?	S	L	Risk (SxL)	Do you need to do anything else to manage this risk?	S	L	Risk (SxL)	Additional Action Required
burns).							and completing tasks, keep pathways clear and clear up spillages.				
Repetitive strain injury (RSI).	Student/supervisor	Discomfort, reduced mobility, difficulty sleeping.	Take regular breaks to walk and stretch.	3	5	15	Use a suitable work chair, sit with good posture.	1	5	5	See doctor/physio if problems persist.
Damage to equipment.	Equipment (i.e. computers, laptops)	Water damage, screen damage.	Cautious with liquids and moving equipment.	2	5	10	Limit fluids around equipment, use protective cases.	2	2	4	Use cups with lids, clear pathways and wear suitable footwear to avoid trips when moving equipment around.
Electric shocks/fire.	Student, supervisor, equipment (i.e. computers, laptops).	Check all wiring is intact with no loose/exposed connections and that sockets are safe. Ensure equipment does not overheat.	Replace damaged cables and	5	1	5	Turn off equipment and allow to cool down if too hot and fans are straining.	5	1	5	Potentially get electrics tested regularly by a professional.

What are the hazards?	Who might be harmed?	How could they be harmed?	What are you already doing?	S	L	Risk (SxL)	Do you need to do anything else to manage this risk?	S	L	Risk (SxL)	Additional Action Required
Loss of data/files.	Data and files.	Latest progress could be accidentally deleted and unretrievable.	Save work regularly and have backups.	1	3	3	Save to online source (e.g. OneDrive).	1	2	2	Save and email new versions of documents regularly.

Part 2: Actions arising from risk assessment

Actions	Lead	Target Date	Done Yes/No
Ensured wiring/cables and sockets for all electrical equipment is undamaged and safe.	Wallis James	28/01/2021	Yes
Ensured desk chair is suitable/comfortable.	Wallis James	28/01/2021	Yes
Undergoing regular breaks/exercise to reduce likelihood/impacts of eye fatigue, back and neck strain and RSI.	Wallis James	28/01/2021 (continuous).	Yes
Check workspace is clear and tidy.	Wallis James	28/01/2021 (continuous).	Yes
Install and set up online document saving service (OneDrive) and transfer necessary files here.	Wallis James	28/01/2021	Yes

Risk Matrix

		Consequences				
		1 Insignificant No injuries/ minimal financial loss	**2 Minor** First aid treatment/ medium financial loss	**3 Moderate** Medical treatment/high financial loss	**4 Major** Hospitalised/ large financial loss	**5 Catastrophic** Death/ Massive Finanical Loss
Likelihood	**5 Almost Certain** Often occurs/ once a week	5 Moderate	10 High	15 High	20 Catastrophic	25 Catastrophic
	4 Likely Could easily happen/ once a week	4 Moderate	8 Moderate	12 High	16 Catastrophic	20 Catastrophic
	3 Possible Could happen/ happen once a year	3 Low	6 Moderate	9 Moderate	12 High	15 High
	2 Unlikely Hasn't' yet happened but could happen	2 Low	4 Moderate	6 Moderate	8 High	10 High
	1 Rare Conceivable but 1/100 year event	1 Low	2 Low	3 Low	4 Moderate	5 Moderate

CONTENTS

LIST OF TABLES

LIST OF FIGURES

DEFINITIONS OF ABBREVIATIONS

BB	Behaviour Builder (a function within DDMT)
CATS	Customised Animal Tracking Solutions
DBA	Dynamic Body Acceleration
DD	Daily Diary
DR	Dead Reckoning
DDMT	Daily Diary Multiple Trace (software)
GPS	Global Positioning System
GTR	Galvanic Timed Release
ML	Machine Learning
ODBA	Overall Dynamic Body Acceleration (*g*)
REM	Rapid Eye Movement
SD	Standard Deviation
TS	Timeseries (a function of BB within DDMT)
TS#	Tiger Shark followed by tag identification number
VeDBA	Vector of Dynamic Body Acceleration (*g*)
VeSBA	Vector of Static Body Acceleration (*g*)

ABSTRACT

There are many advantages in determining animal behaviour for conservation initiatives seeking to protect species impacted by the changing planet. However, for many years, direct observation of elusive or dangerous animals in challenging habitats precluded the acquisition of representative, non-biased behavioural data. Recently though, animal-attached tag technology incorporating accelerometers, magnetometers and pressure sensors, has greatly advanced our abilities to document the behaviour of a numerous vertebrate species (e.g. birds, reptiles, fish, mammals), even when they cannot be observed. For this, supervised and unsupervised machine learning are often used to categorise behaviours by identifying patterns within the biotelemetry data. However, supervised machine learning requires training data, which is not always available, and both methods are driven by machine-based software with no explicitly defined parameters associated with behaviours which can be cross-checked. This work aimed to use a proper physics-based understanding of triaxial accelerometer-, magnetometer- and pressure data taken from electronic tags deployed on tiger sharks, *Galeocerdo cuvier,* to interpret patterns and group them into behaviours. As part of this, multi-modality in frequency distributions of parameters was investigated, on the premise that different behaviours can result in different frequency distributions in particular metrics. Following examination, algorithms using defined numerical limits were created to isolate distinct behaviours and these used to detect the extent of identified patterns within entire data sets and across individuals. A total of 12,338 minutes of tag data was processed, from which 10 behaviours were identified. Seven of these were successfully described using numerical metric limits from recorded and/or derived data including; ‘descent’, ‘ascent’, ‘burst power’, etc. However, frequency distributions showed a continuum rather than multiple distinct modes, indicating that this approach is likely to be more complex than thought. The use of physical principles seems a promising method for interpreting accelerometer, magnetometer and pressure data to identify behaviours that occur in study animals that cannot be directly observed. Although these algorithms are specific to tiger sharks in this work, this method is likely to be applicable to other species in aerial, aquatic or terrestrial habitats and could inform a broad range of conservations initiatives in the future.

LAY SUMMARY

The way an animal interacts with, and moves within, its natural environment can provide insight into its physiological condition, the space it uses (e.g. for feeding, resting, mating) and its energy expenditure (and therefore its energy/feeding requirements), along with many other factors. An in-depth knowledge of an animal's behaviour is therefore crucial to informing conservation programs that hope to ensure the survival of species.

A previous challenge with gathering behavioural information from animals was that visual observation was needed. Wild animals are often elusive, dangerous or live in habitats unsuitable for humans (e.g. oceans) and observing a captive animal is not the same as studying a wild counterpart. The presence of humans can influence the behaviours presented by animals and behaviours may be so subtle (e.g. jaw position) or occur on too large a timescale (e.g. migrations) for humans to notice or observe wholly. Tiger sharks are endangered, extremely difficult to follow and are also a danger to humans. They live in a marine environment in which they can travel large three-dimensional distances so visual observation to determine behaviours is unrealistic.

By fitting specialist recording hi-tech tags to the dorsal fins of 10 wild tiger sharks at Ningaloo Reef, Australia, we were able to remotely study the behaviour of wild tiger sharks. The tags recorded metrics such as acceleration, magnetic orientation and pressure at high rates (i.e. 20 time per second), which provide detailed information on behaviours *via* changes in the sharks' body postures, headings and depths etc. Previously, computer driven 'machine learning' has been used to process this type of data and categorise patterns into behaviours. However, supervised machine learning generally requires that the study animals be observed to 'ground truth' the data. This is not possible for tiger sharks. Another analysis option, 'unsupervised machine learning', also driven by a machine-based software, does not require 'training data' but provides no defined numerical limits of the machine-categorised behaviours that can be cross-checked with data from other sharks. In addition, once unsupervised machine learning categories are identified, they still require human interpretation to decipher what behaviour the data refer to.

Instead, a proper understanding of the sensory outputs of the tags allowed me to reconstruct behaviours, as if I was watching the animal, and define them using numerical limits. Figure 1 shows how three of the behaviours were defined and distinguished from one another using these limits. Of 10 behaviours that I identified, seven were numerically defined. The numerical

limits were used to construct search formulae to extract the behaviour from each individual tiger shark's data. Interestingly, examination of the behaviour metrics from the extracted data revealed that the sharks did not always distinctly switch between one mode of a behaviour to another, sometimes showing 'intermediate' behaviours.

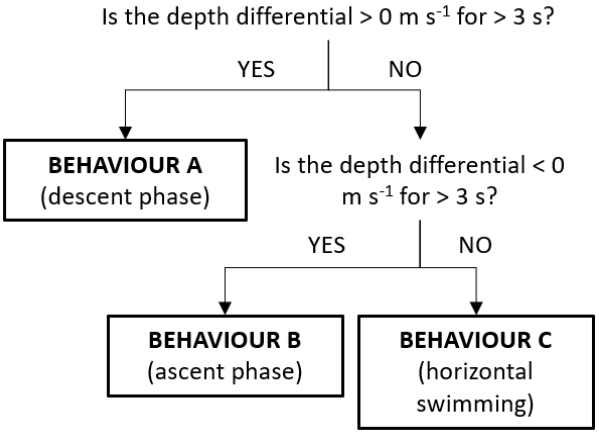

Figure 1 – The initial steps of the decision tree in which the 10 identified behaviours are distinguished and the key metrics that define them are summarised.

This is a successful and viable method for categorising behaviours from multi-sensor tag data. Further development could identify more behaviours and formulae to identify them within the data sets created. Although the formulae I produced are specific to tiger sharks, this method could certainly be applied to a range of other species and provide vital information to conservation and management initiatives, not only for protecting the species but to implement animal control programs to ensure the safety of humans as well.

INTRODUCTION

Global vertebrate populations and biodiversity have continuously declined throughout the past century (Butchart *et al.,* 2010) due to overexploitation, climate change and a loss of habitats and resources caused by direct and indirect anthropogenic activity (Stevens *et al.,* 2000; Block *et al.,* 2011; Hoffman *et al.,* 2010). There are 9,914 vertebrate species currently threatened by the risk of extinction, making up almost 14% of the estimated total number of extant vertebrate species described, although this proportion is potentially higher due to only 75% of described vertebrate species having been assessed (IUCN, 2021). Strengthened conservation efforts are necessary to address and stem this biodiversity crisis and aid the recovery of endangered species (Butchart *et al.,* 2010; Hoffman *et al.,* 2010; Cooke, 2008).

Identification and understanding of animal behaviour can play a pivotal role in helping conservation initiatives (Cooke *et al.,* 2004; Cooke, 2008; Greggor *et al.,* 2016). For example, Sutherland (1998) summarises numerous areas in which the study of animal behaviour can be used to help solve conservation problems including overexploitation, minimum reserve area, minimum habitat requirements and predicting consequences of environmental change, to name a few. Behaviour, characterised by patterns in body posture and body motion (Shepard *et al.,* 2008b), is an animal's response to its environment and physiological condition (Shepard *et al.,* 2008a, 2008b). It can provide direct insight into its physical state (Williams *et al.,* 2017; Shepard *et al.,* 2008b), space use, activity (or quiescence) (Cooke *et al.,* 2004), inter- and intra-specific interactions (Broell *et al.,* 2013; Herrera & Nunn, 2019) and life-history traits (e.g. mating behaviour; Whitney *et al.,* 2010). Thus, an in-depth understanding of animal behaviour is essential to coordinating and implementing many effective conservation management schemes.

Advances in animal-attached tag technology have begun to overcome the difficulties of observing behaviour in intractable animals (Cooke, 2008; Schneirla, 1950; Godley & Wilson, 2008; Brown *et al.,* 2013; Ferreira *et al.,* 2017; Bestley *et al.,* 2013; Stankowich & Blumstein, 2005) and have developed into sophisticated systems for the remote monitoring of free-roaming animals in the wild (Broell *et al.,* 2013; Wilson *et al.,* 2006, Rutz & Hays, 2009). Initially, biologging and biotelemetry were most frequently used to document the spatial ecology of animals (Cooke, 2008). However, the use of animal-attached accelerometers and magnetometers in particular, has since provided fine-scale measurements of animal body movements (Yoda *et al.,* 2001) and allowed workers to quantify animal behaviour and been

used to identify and monitor poorly understood behaviours of free-living animals in their natural habitat (Yoda *et al.,* 1999; Wilson *et al.,* 2002; Whitney *et al.,* 2010; Naito *et al.,* 2010; Block *et al.,* 2011; Owen *et al.,* 2016). This has also led to the ability to estimate energy expenditure (Halsey, Shepard & Wilson, 2011; Wright *et al.,* 2014; Wilson *et al.,* 2020; Gleiss, Wilson & Shepard, 2011) and activity-specific metabolic rate in wild animals (Wilson *et al.,* 2006; Gleiss *et al.,* 2009), as well as assess the risk of infectious disease and parasite transmission (Herrera & Nunn, 2019), among other uses. A broad range of free-living vertebrate species from fish, through reptiles to birds, and mammals, has now been equipped with triaxial accelerometer tags (Wilson, Shepard & Liebsch*,* 2008; Wilson *et al.,* 2018).

Triaxial accelerometers, which sense acceleration in the three orthogonal axes of space, measure 'static' acceleration (due to the Earth's gravitational field and the tag's relative orientation) and thereby indicate an animal's posture (Shepard et al. 2008a), but they also sense 'dynamic' acceleration (due to the animal's movement (Wilson et al. 2020)), which provides additional information useful in determining behaviour (Shepard *et al.,* 2008a, 2008b). Triaxial magnetometers measure the strength of the Earth's magnetic field and the orientation of the tag in relation to the direction of the field lines, also over three orthogonal axes (Williams et al. 2017). Consequently, triaxial accelerometer and magnetometer data has been increasingly used to identify behavioural modes (e.g. sitting, walking) with quantifiable metrics (e.g. Dynamic Body Acceleration – DBA (Wilson *et al.,* 2020)).

Supervised and unsupervised machine-learning (ML) algorithms have been successfully and routinely used to classify patterns within accelerometer data into behavioural categories (e.g. *m-prints,* Williams *et al.,* 2017; state-space models, Nathan *et al.,* 2012; hidden Markov models, Wang, 2019; *k*-means cluster methods, Sakamoto *et al.,* 2009; random walk models, Morales *et al.,* 2004). However, supervised ML requires training data such as synchronised visual observations for the algorithms (Nathan *et al.,* 2012) to 'label' the data, which can be difficult or impossible to obtain for elusive or cryptic species or those moving widely within expansive environments (Wang *et al.,* 2019). Conversely, unsupervised ML can detect and categorise unknown patterns in 'unlabelled' data. However, human interpretation is still required to identify what any categorised patterns potentially mean in terms of putative behaviours, without prior training data (Valetta *et al.,* 2017). Furthermore, unsupervised learning often fails to describe and cluster behavioural patterns amongst data recorded over longer time scales due to variation in the individual's movement behaviour pattern and requires the use of numerous complex models (Morales *et al.,* 2004). This may be unsuitable; a) for

data sets recorded over longer periods to get a more whole depiction of an animal's long term behavioural movements, such as migratory species or species with expansive home ranges and b) when trying to assess multimodality within behaviours of the same category. Tsuda *et al.* (2009) successfully categorised nine spawning behaviours of female chum salmon, *Onchorynchus keta,* solely using acceleration data, without the assistance of machine learning. However, in a manner similar to that of other studies, video-recorded observations synchronised with the acceleration data were first used to confirm each behaviour. Thus, there is a need for biologists to consider how animal behaviour might be categorised from acceleration and magnetometer data (and metrics derived from them) for conditions when visual observation is not possible.

Furthermore, whilst such methods can identify and categorise discrete behavioural modes, modality or variation of parameters used to describe individual behavioural categories is less often considered. Uni-modality would indicate that a behaviour can be described by a single set of limits on a recorded parameter with little or no variation. A behaviour with bi- or multi-modality would indicate that there are two or more modal groups with separate metric limits within a behaviour category. Multimodality has been documented in the communication displays and/or vocalisations of wolf spiders (Uetz, Roberts & Taylor, 2009; Gordon & Uetz, 2011) and some bird, canid, and primate species (Sebeok, 1993), but less so within other behaviours. However, by assessing the distributions of the metrics that describe each behaviour, the modality can be determined. Separating out the data based on the distributions around the metrics can produce behavioural cascades following a Boolean approach (Wilson et al., 2018) that provides multiple metric behaviour divisions.

The main thrust of this work was to attempt to identify behaviours adopted by tiger sharks, *Galeocerdo cuvier,* equipped with animal-attached multi-sensor tags, solely using the data provided by the tags and without validation from visual observations. Indeed, it is virtually impossible to observe tagged wild tiger sharks for any length of time and this species is likely to be particularly constrained in its behavioural repertoire in captivity (Cooke, 2017; Hart, Reynolds & Troxell-Smith, 2021). However, tag-derived metrics can be used to define many of the characteristics used by people to define behaviours directly by visual observation (Tinbergen, 1960). Thus, for example, body posture can be determined by pitch and roll and movement effort (including speed) can be derived from the Dynamic Body Acceleration (Halsey *et al.* 2011, Bidder *et al*., 2012) so careful examination of tag-derived metrics can produce a physical framework analogous to direct visual observations. Thus, I aimed to

quantify, as far as possible, as many behaviours as I could using this approach. My principal objective was to define each behaviour by stated limits in tag-derived metrics, which could be used to construct bespoke algorithms to identify and extract specific behaviours from continuous data obtained from wild tiger sharks, without the use of machine-learning or assistance of visual observations. The extracted data from each behaviour were to be used to produce frequency distributions of descriptive metrics to assess the modality (uni-, bi- or multi-modality or a continuum) of each identified behaviour to assess whether simple consideration of frequency distributions of select metrics would allow behaviours to be differentiated. Finally, I attempted to determine what my identified behaviours may signify.

Large predatory sharks are imperative for maintaining healthy ocean ecosystems globally (Stevens *et al.,* 2000; Heithaus 2001; Simpfendorfer, Goodreid & McAuley, 2001; Ferretti *et al.,* 2010), yet many species are under threat from a myriad of environmental and anthropogenic factors. Indeed, elasmobranchs are experiencing severe population declines worldwide (Ferretti *et al.,* 2003; Dulvy *et al.,* 2014), with 36% of assessed shark, ray and chimaera species being threatened with the risk of extinction (IUCN, 2021). As a result, their conservation has become a focal point for ecosystem management (Stevens *et al.,* 2000; Gleiss *et al.,* 2009), making them an obvious threatened species archetype for the focus of this research. Their elusiveness and difficulty to observe in the wild also makes them an excellent test species for this new approach.

MATERIALS AND METHODS

Data Collection

The tagging process and subsequent data collection was carried out by Andrzejaczek *et al.* (2019). During April-May 2017, tiger sharks, were captured inside the reef lagoon at Ningaloo Reef (approximately 23° 00’ S, 113° 48’ E), Australia. A series of three drumlines were each equipped with a single 20/0 circle hook baited with fish scraps and deployed ~100 m apart between 07:00-16:00. Lines were checked for captures hourly and once caught, sharks were secured alongside a 5.8 m vessel, measured (pre-caudal length, fork length, total length, and maximum girth) and sexed. Finally, a multi-sensor biologging tag (see below) was clamped to the base of the dorsal fin and photographed for identification purposes, and to assess any potential physiological effects of tags.

The tags were attached using a stainless-steel spring clamp (CATS, Australia - https://www.cats.is/products/cats-diary/) *via* a docking pin and a corrodible galvanic timed

release (GTR, Ocean Appliances, Australia - http://oceanappliances.com.au/index.php). The GTR dissolved between seven and 48 hours later, releasing the tag and allowing it to float to the surface, to be located using a hand-held VHF receiver and collected by boat (Lear & Whitney, 2016). After approximately seven days, a magnesium sleeve on the clamp itself dissolved, detaching the clamp and leaving no tagging equipment fixed to the shark. For further details, see Andrzejaczek *et al.* (2019). In this study, tag data from 10 tiger sharks was used, totalling 205 hours and 38 minutes of sensor data for processing.

Biologging Tags

The tags used were CATS Diary tags (Customised Animal Tracking Solutions, https://www.cats.is/products/cats-diary/), equipped with triaxial accelerometers (illustrated in figure 1), triaxial magnetometers, gyroscopes and depth, temperature, and light sensors (all parameters were continuously recorded at 20 Hz). Speed sensors were present, but not functional and the light and temperature readings were not functional in the data processing software used. CATS Cam tags were also deployed on some of the tiger sharks, but the video footage was not analysed in this study.

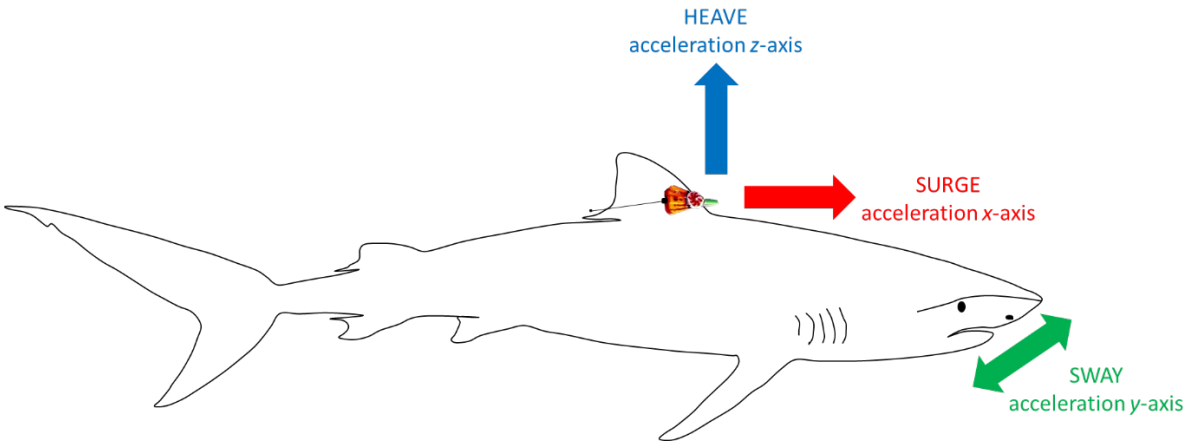

Fig. 2. Schematic diagram of G. cuvier equipped with a multi-sensor tag at the base of the dorsal fin. A major sensor within the tag was a triaxial accelerometer, which recorded acceleration along three orthogonal axes. The red arrow illustrates the x-axis, recording forward and backwards movements (surge). The green arrow shows the y-axis, which records side-to-side acceleration (sway). The blue arrow illustrates the z-axis, recording the dorso-ventral movements (heave).

The data channels directly recorded by the tag sensors are described in table 1. Once the tags had been retrieved and the data had been imported into a processing software (DDMT, discussed in the next section), additional metrics were derived from the data channels recorded by the tags (table 2), which provided further means of quantifying behaviours.

Table 1. Descriptions of the metrics directly recorded by the CATS tag and stored on the SD card whilst it was attached to the shark, before retrieval.

Recorded data channel characteristics:	
Duration	The duration of recording is recorded as decimal seconds, seconds, minutes, hours and days and presented as DD:HH:MM:SS.ss.
Acceleration *x*	Surge (triaxial accelerometer axis 1). Measures the linear longitudinal acceleration of the shark (0-6 *g*), as well as centripetal acceleration and the static acceleration of the Earth's gravitational field.
Acceleration *y*	Sway (triaxial accelerometer axis 2). Perpendicular to axis 1. Measures the linear lateral acceleration of the shark (0-6 *g*), as well as centripetal acceleration and the static acceleration of the Earth's gravitational field.
Acceleration *z*	Heave (triaxial accelerometer axis 3) of the triaxial accelerometer. Perpendicular to axis 1 and 2. Measures the linear dorso-ventral acceleration of the shark (0-6 *g*), as well as centripetal acceleration and the static acceleration of the Earth's gravitational field.
Mag *x*	Axis 1 of the triaxial magnetometer. Measures magnetic field intensity in milligauss (mG), ranging to the maximum of the earth's magnetic field.
Mag *y*	Axis 2 of the triaxial magnetometer. Same measurements as axis 1.
Mag *z*	Axis 3 of the triaxial magnetometer. Same measurements as axis 1.
Water pressure	The sensor measures water pressure (mbar) which can be converted into depth within DDMT.

Acceleration occurs with or against the force of gravity, with an immobile tag's total acceleration across the three orthogonal axes having a vectorial sum of 1 *g* (equal to the Earth's gravitational field). As the tag is moved with the animal's trunk, the recorded animal-generated acceleration values are superimposed on the static values, generating higher or lower values independently and simultaneously at any point, depending on the movement type (Wilson et al., 2020). The tag also records a series of other data channels (table 1), from which other metrics can be derived (table 2).

Data Processing

Daily Diary Multiple Trace Software (DDMT – Wildbyte Technologies, http://www.wildbytetechnologies.com/), developed at Swansea University, was used for data inspection. DDMT was originally designed for reading data recorded via Daily Diary (DD) Tags (Wildbyte Technologies, http://www.wildbytetechnologies.com/) but the CATS tag data were converted to make them readable within DDMT. In addition, the original imported shark heading (with respect to the Earth's magnetic field and given values between 0 and 359°) data (calculated using the accelerometer and magnetometer data (Gunner et al. 2021)) were found to be flawed, but the errors could be corrected within DDMT to calculate true shark heading.

Metadata (Appendix III) was used to identify each tag's recording start time and date, following the deployment of the tags onto the sharks and their subsequent release. This information was also input individually into DDMT for each tag, alongside the magnetometry corrections and saved as a 'Time Date Offset' or '.tdo' file, to be reloaded into DDMT each time the file was inspected. This ensured that the correct time/date data was associated with the data, and that any heading data was correct. Shark body pitch data was also examined, to assess whether each tag had been correctly oriented during attachment to the sharks. This was done by finding periods during which the sharks maintained a constant water depth and examining the pitch recorded by the tag (table 2). If the pitch angle was approximately zero degrees when the shark was swimming horizontally, it indicated that the tag was likely oriented correctly, and no corrections were needed. This proved to be the case for all tags in this study.

Each file was inspected for patterns within various data channels (tables 1 and 2) that may be produced by a particular behaviour. This is a tag-based visualisation approach that may be likened to the standardized simple observation of animals (e.g. Tinbergen, 1960) since the tag data are quantified metrics for movement and body posture. VeDBA was a key metric for describing several behaviours. VeDBA (Vectorial sum of the Dynamic Body Acceleration) is a derivation of Dynamic Body Acceleration (DBA), a proxy used for rate of energy expenditure in animals and humans (Wilson *et al.,* 2020; Wright *et al.,* 2014; Qasem *et al.,* 2012). The equation (shown in table 2) removes the acceleration imposed by the Earth's gravitational field by subtracting the smoothed (over 2 s) acceleration data of each orthogonal axis from the corresponding raw acceleration data, leaving the dynamic acceleration for each axis that is produced by the animal's movement. The values of the three axes are then summed vectorially to calculate the Vectorial Dynamic Body Acceleration (VeDBA) (Gleiss, Norman & Wilson, 2011; Wilson *et al.,* 2020; Shepard *et al.,* 2008a). Once a behaviour pattern was identified, numeric values of parameters (see Tables 1 & 2) were ascribed to describe the limits within which the behaviour occurred. These limits could then be used to construct Boolean algorithms (Wilson et al. 2018) to find the behaviour within continuous shark data using the 'Behaviour Builder' function within DDMT.

Table 2. Derived metrics from data channels directly recorded by the tag. These metrics enabled further description of the behaviours. These metrics were provided by DDMT.

Derived metrics characteristics:	
Date/time	The recording start times and dates were manually input into DDMT for each individual tag using metadata as reference and saved as '.tdo' files, which could be reloaded into DDMT. Date was presented as dd/mm/yy,

	and time the same as duration. The duration then continued from the input start date and time, so that the data was associated with the correct time, also allowing day and night to be distinguished.
Body pitch	Derived from the accelerometer data, the pitch angle (°) is the static component of the surge (*x*) axis and is essentially the tilt on the *x*-axis given by; Pitch = sin($AccX_{sm}$) where $AccX_{sm}$ is the surge acceleration smoothed over 2 s (see above). Parallel to the water's surface, the shark's pitch angle was expected to be zero and therefore measured as 0° (see text). A negative pitch indicated that the shark was angled downwards, and a positive value suggested the shark was angled upwards (e.g. a value of -90° being straight down and 90° being directly upward, perpendicular to the surface).
Roll	Roll angle (°) is the static component of the sway (*y*) axis, similar to pitch and surge above, given by: Roll = sin($AccY_{sm}$) where $AccY_{sm}$ is the sway acceleration smoothed over 2 s (see above). Roll depicts the angle at which the shark is rolling or banking to the left or right, along the body's longitudinal (*y*) axis. Roll angle to the left ranged 0° to 180° and roll to the right had an identical but negative range to easily distinguish between the two directions.
VeDBA	The vector of the dynamic body acceleration (VeDBA) shows the dynamic acceleration implemented by the shark at any time. It is calculated using: $\text{VeDBA} = ((AccX - AccX_{sm})^2 + (AccY - AccY_{sm})^2 + (AccZ - AccZ_{sm})^2)^{0.5}$ Where $AccX$ is the raw *x* axis (surge) acceleration data, $AccX_sm$ is the smoothed *x* axis acceleration data. $AccY$ is the raw *y* axis (sway) acceleration data, $AccY_{sm}$ is the smoothed *y* axis acceleration data. $AccZ$ is the raw *z* axis (heave) acceleration data and $AccZ_{sm}$ is the smoothed z axis acceleration data. The subtraction of the smoothed acceleration from the raw acceleration provides the dynamic acceleration (Wilson *et al.* 2020).
Heading	Heading was derived from the magnetometry *x, y* and *z* axes after taking into account the pitch and roll angles of the shark (see above) (details in Gunner et al. 2021). Heading ranges from 0° to 359° and portrays the heading of the individual in relation to magnetic north. A circular mean of the heading can also be viewed in DDMT to remove the vertical line created by the individual crossing over north.
Angular velocity	Angular velocity was derived from a combination of the rate of change of three data channels: heading, pitch, and roll (° s^{-1}). Angular velocity provides a rate of change of angular position of the overall rotation of the body (see Gunner et al. 2020).
Depth	Depth (m) was derived from pressure data assuming that the density of seawater is 1.03 g/mL. DDMT can visually invert this channel (e.g.,

	increasing depth slopes downwards and *vice-versa*) to reflect the animal's direction of movement in the water column.
Differentials	Differential channels were used to extract the rates of change of existing recorded and derived channels. For example, creating a differential channel for depth (m) provided the rate of change of depth [= vertical velocity] ($m.s^{-1}$) at any given time. Within DDMT, the range (length of time) over which the differential is calculated is set by the user but is over 5 consecutive data points by default, and I used this setting unless otherwise stated.
Dead reckoning	The dead-reckoning option within DDMT provides a three-dimensional visualisation of the shark's track derived by using vectors on animal speed, heading and change in the vertical dimension over time (Gunner et al. 2021). Within my analysis, the heading (°) provided a two-dimensional track over time, whilst incorporating pressure (mbar) *via* depth (m) provided the vertical axis, making the track three dimensional (for example see later in figure 30).

Data Analysis

The 'Behaviour Builder' (hereafter termed BB) function within DDMT allowed the user to construct algorithms using a metric or combination of metrics that best described an identified behaviour. DDMT would run the algorithm and search a specified section or the entire data file using a Boolean approach to identify and 'mark' any data points (hereafter referred to as 'events') with metrics that fit the requirements of the algorithm. For example, when searching for events where the depth of the shark was increasing, the algorithm was inputted as '*If* (Diff_Chan (Depth (R=5)) > 0) *then* 'Mark Events'. This algorithm thus searched for a mean rate of change of depth greater than 0 m s^{-1}, over five consecutive depth data points (therefore lasting 0.25 s in my 20 Hz dataset). Minor disturbance or 'noise' was visible in the recorded data channels when observed on a small scale, possibly due to tag disturbance during movement through the water. To reduce noise within the differential channels, they were smoothed over 80 events (2 s) before defining limits within them to construct algorithms. This period was chosen since, by inspection, it minimized noise (generated, for example, in the acceleration data due to tag wobble on the sharks as they swam) while not obviously changing underlying trends. Thus, all differential channels were smoothed before running algorithms in each data file to search for events that fitted within the algorithm's defined limits. Over-smoothing can result in a loss of information, so a smoothing limit was set and to ensure consistency. However, to avoid over-smoothing and loss of detail, 'noise' could not always be eliminated entirely.

Depth, and rate of change of depth, are particularly important parameters for defining the behaviours of marine animals (e.g. Gleiss *et al.,* 2013; Ritter, 2020; Owen *et al.,* 2016) and so are considered in more detail here. In particular, algorithms were developed to highlight the whole descent and ascent phases of dives as a complete behaviour (see e.g. Nakamura *et al.,* 2011), rather than transient changes in depth of approximately <0.2 m that may only represent minor momentary changes (possibly resulting from tag disturbance via stability on the fin). To eliminate such transience, the 'Timeseries' function within DDMT (hereafter referred to as TS) was used to 'bookmark' events that matched the BB algorithm requirements over a certain timescale or number of events. For instance, the algorithm; 'Diff_Chan Depth > 0, present for 100 events, %time 100, with next expression starting from range 100, flexibility after of 10' instructed DDMT to search for and bookmark sections of data that had a rate of change of depth > 0 m s^{-1} for a duration of at least 100 events or 5 s (as the data was recorded at 20 Hz). Once the bookmarked events were converted to 'marked events', this data was exported to excel for further examination.

The overall aim within the behavioural identification was to construct algorithms for each behaviour that could be applied across whole data files of any tiger shark and successfully detect each identified behaviour. Once an algorithm was run and had marked the data within the limits, the data was exported. Graphs were constructed to illustrate the key defining metrics of each behaviour category clearly and provide a visual description for future analysis using similar tags, software, and metrics. Frequency distributions were also produced to demonstrate whether there was multi-modality within the initial behaviour categories, shown in the following section.

RESULTS

A total of 10, non-mutually exclusive, behavioural categories were identified from the tag data of the 10 tiger sharks (TS8, TS12-19 & TS24) using the methods described. All behaviours are described in detail below before being summarized in table 3 where key metrics for Boolean search terms are provided. Some of the behaviours were more straightforward to describe using recorded and derived metrics than others, so not all are numerically defined.

BEHAVIOURS BASED ON DEPTH

Behaviour A – 'Descent'

Key metrics

'Descent' of the water column was manifest by a continuous increase in depth (and pressure). Rate of change of depth was > 0 m s^{-1} for > 3 s.

Example behaviour

Examination of the data showed that when the rate of change of depth was positive (e.g. figure 3c) and the body pitch angle of the shark was mostly < -5° (e.g. figure 3d), this was indicative of the shark's position descending through the water column (e.g. figure 3a). The graphed example in figure 3 spanned 205 seconds, during which time the depth increased to about 93 m. The mean rate of change of depth throughout this particular descent was 0.09 m s^{-1} (±0.04, SD). The mean pitch angle of the example dive was -24.6° (±9.5). The smoothed VeDBA (*g*) mostly remained below 0.05 *g* (mean 0.03 *g* ±0.02), excluding some peaks that coincided with the dive initiation or increases in body pitch angle steepness and rate of change of depth (figure 3b). The peaks in VeDBA indicated that the shark sometimes powered its descent with tailbeats. It took approximately 2 to 2.5 s to complete one full tailbeat.

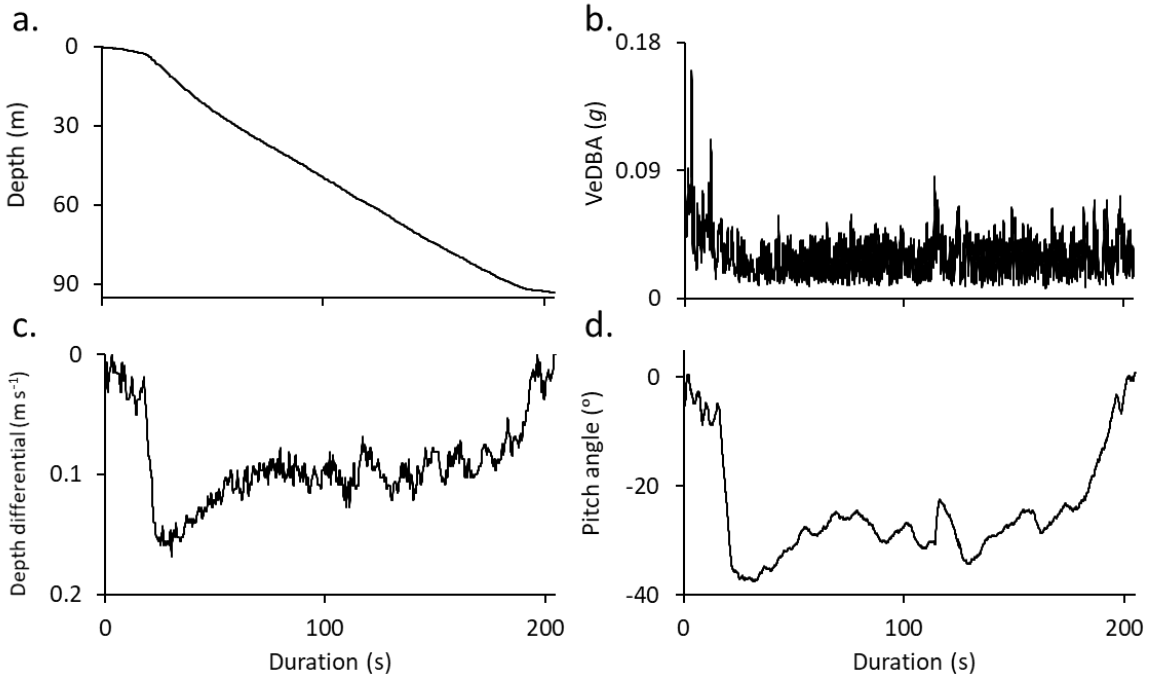

Figure 3. Time series plots of key metrics associated with Behaviour A (descent), including a) depth (m), b) VeDBA (g), c) rate of change of depth (m s^{-1}) and d) body pitch angle (°). Metrics smoothed over 2 s.

Multiple examples of the behaviour within an individual

The frequency distributions from TS8's Behaviour A data are graphed in figure 4, to show general patterns across descents. Here, the mean rate of descent was 0.09 m s^{-1} (±0.04), with almost 25% of cases occurring between 0.02 and 0.03 m s^{-1} (figure 4a). The data were distributed in a single continuum. The mean pitch angle was -11.3° (±5.9), with the most frequently occurring pitch angles during TS8's descents ranging between -6° and -8°. Mean smoothed VeDBA values were 0.02 *g* (±0.02) with almost 40% of all values ranging between 0.001 and 0.002 *g*. These metrics also displayed continuum distributions, with no distinct separation between potential behavioural modes.

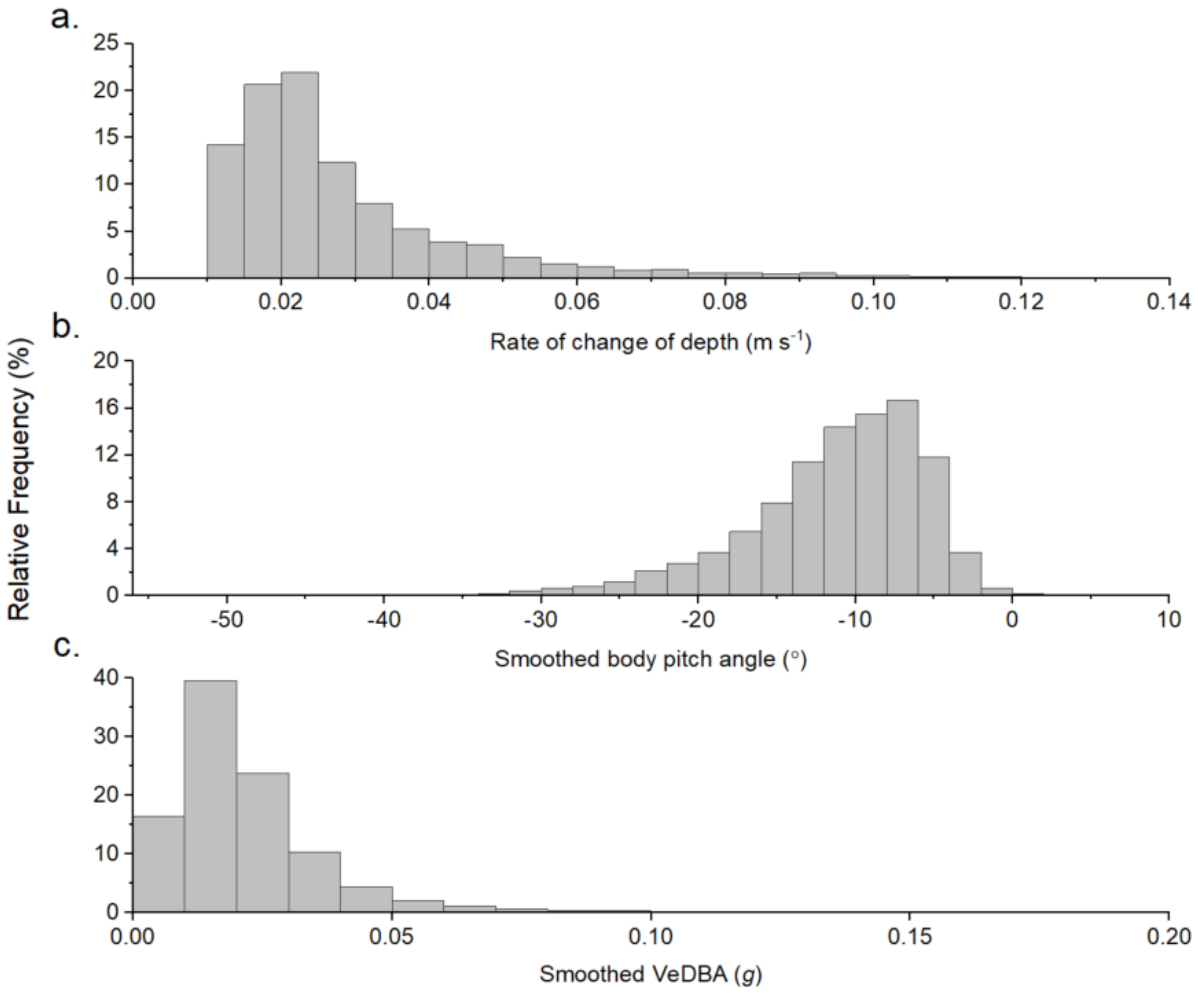

Figure 4. Frequency distributions of key derived metrics from the extracted descent data of TS8, including a) rate of change of depth (m s^{-1}), b) body pitch angle (°) and c) VeDBA (g). The maximum VeDBA value was 0.595, however the frequency of values in bins from 0.1 g onwards were negligible and not shown. Metrics smoothed over 2 s.

Patterns across individuals

All tiger sharks observed in this work participated in Behaviour A, but the rates of descent varied between them (figure 5a). The rate of change of depth of all descending tiger sharks values bar one (TS18) generally ranged between 0 and 0.05 m s^{-1}. However, some of the maximum values greatly exceeded this. For example, TS13 had a maximum rate of change of depth of 0.37 m s^{-1}, compared with a median value of 0.025 m s^{-1}, as well as the greatest range of values. TS13 also exhibited the highest proportion of time spent descending through the water column (figure 5b) of all sharks, although there is no evidence that this was specifically due to the greater range of values in the descent rate. The proportion data for descent includes all activities (identified below) that may have occurred during descent phases. Examples include straight swimming, undulatory swimming and circling during descents (see

below). Most of the tiger sharks displayed a minimum rate of change of depth value below zero, despite the algorithm searching for values greater than zero. This is because a search flexibility value of 10 was enabled for all algorithms to avoid exclusions of descent events due to unexpected values potentially caused by tag disturbance.

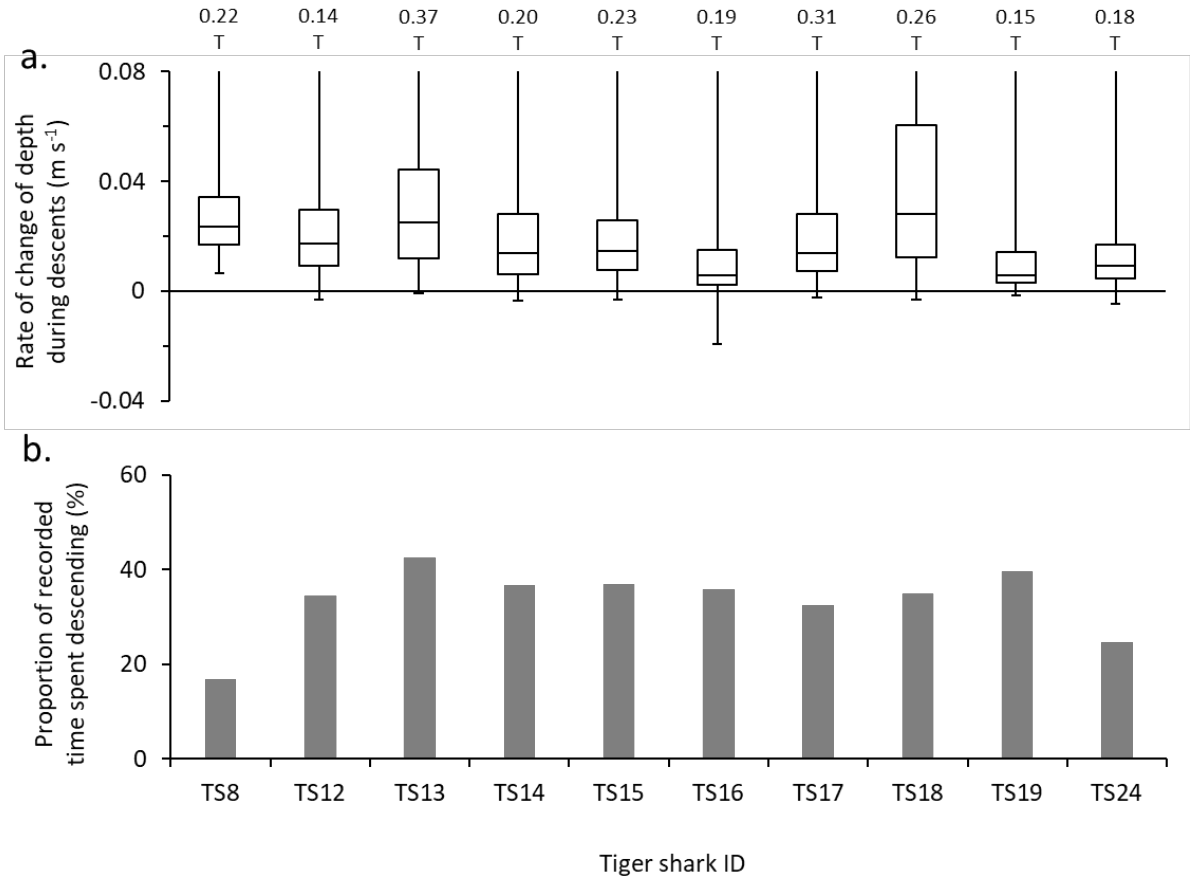

Figure 5. a) Box whisker plot of the rates of descent for all tiger sharks exhibiting Behaviour A (horizontal lines show medians, boxes quartiles and whiskers limits). The y axis was limited to 0.08 m s^{-1} to give a more precise view of the interquartile ranges. Maximum values are included above. The same occurs in other box whisker plots later on. b) The proportion of recorded time each shark dedicated to this behaviour.

Behaviour B – 'Ascent'

Key metrics

'Ascent' of the water column was manifest by a continuous decrease in depth. Rate of change of depth was < 0 m s^{-1} for > 3 s.

Example behaviour

A negative rate of change of depth and a body pitch angle > 5° were key indications of a decrease in depth or 'ascent' of the water column (e.g. figure 6a). The example below spanned 192 s, during which time the shark's depth in the water column decreased by 92.3 m. The rate of change of depth (figure 6c) values remained mostly negative, (mean -0.10 m s^{-1} ±0.04) and the body pitch angle (figure 6d) remained mostly positive with a mean of 20.7° (±9.3). The mean smoothed VeDBA (figure 6b) was 0.06 *g* (±0.06).

However, after approximately 25 seconds, the rate of change of depth increased to a maximum of 1.94 m s^{-1} and the pitch angle became positive simultaneously, resulting in increasing depth. Furthermore, the smoothed VeDBA demonstrated substantial increases in total acceleration, a few seconds prior to the periods when the depth differential and body pitch angle developed considerably steeper gradients. Throughout the rest of the ascent phase, the rate of change of depth was not constant and appeared as a series of increases and decreases.

This pattern indicates that ascent phases were not achieved using a continuous acceleration effort. Instead, the sharks alternated between 'climb' and 'rest' periods (although these periods are not as distinct as this, as discussed below for figure 7). The climb periods consisted of increased acceleration and steeper body pitch angles, which produced steeper negative depth differential values and faster rates of ascent. They were then followed by rest periods of decreased acceleration, shallower pitch angle and slower rates of ascent. Table 3 describes both Behaviour A (descents) and Behaviour B (ascents) to be 'continuous increases or decreases (respectively) in depth' from start to finish. However, within the general criterion of rates of change of depth being either negative or positive, sharks frequently levelled-off or even momentarily changed descent for ascent and *vice versa* during either behaviour (these moments are not marked by the relevant algorithms).

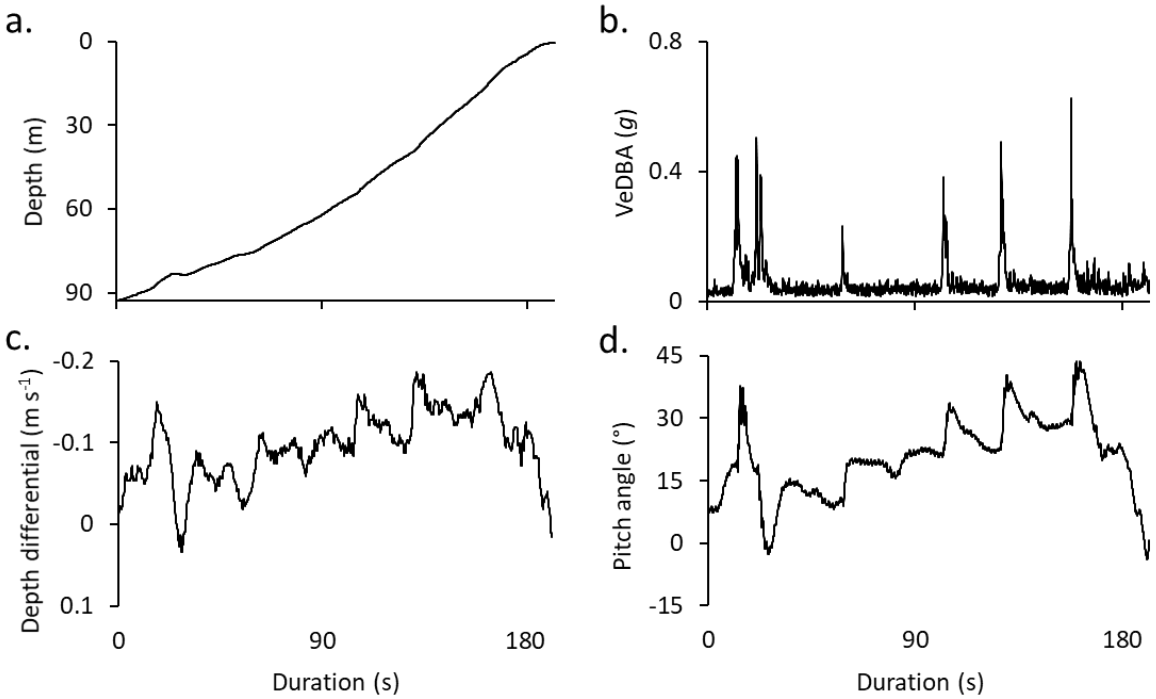

Figure 6. Time series plots of key metrics associated with Behaviour B, including a) depth (m), b) VeDBA (g), c) rate of change of depth (m s^{-1}) and d) pitch angle (°). Metrics smoothed over 2 s.

Multiple examples of the behaviour within an individual

Patterns within the derived data channels suggested that Behaviour B consisted of 'climb' and 'rest' periods. However, when all the ascent data was extracted and the key metrics were graphed as frequency distributions for each shark, this pattern was not apparent. When observed collectively as frequency distributions, the data showed skewed continua, rather than the bimodality that would be expected if ascent phases were a combination of distinct climb and rest periods. Figure 7 shows the frequency distributions of a) rate of change of depth (m s^{-1}), b) smoothed body pitch angle (°) and c) smoothed VeDBA (*g)* for the Behaviour B data from TS12. The most frequently occurring rate of change of depth values ranged between -0.005 and -0.01 m s^{-1} (figure 7a), yet the mean was -0.02 m s^{-1} (±0.01). Smoothed body pitch angle most frequently ranged between 4° and 6° (figure 7b) and the mean 6.8° (±5.0). Smoothed VeDBA most frequently ranged between 0.01 and 0.02 *g* (mean 0.03 ±0.02 *g*).

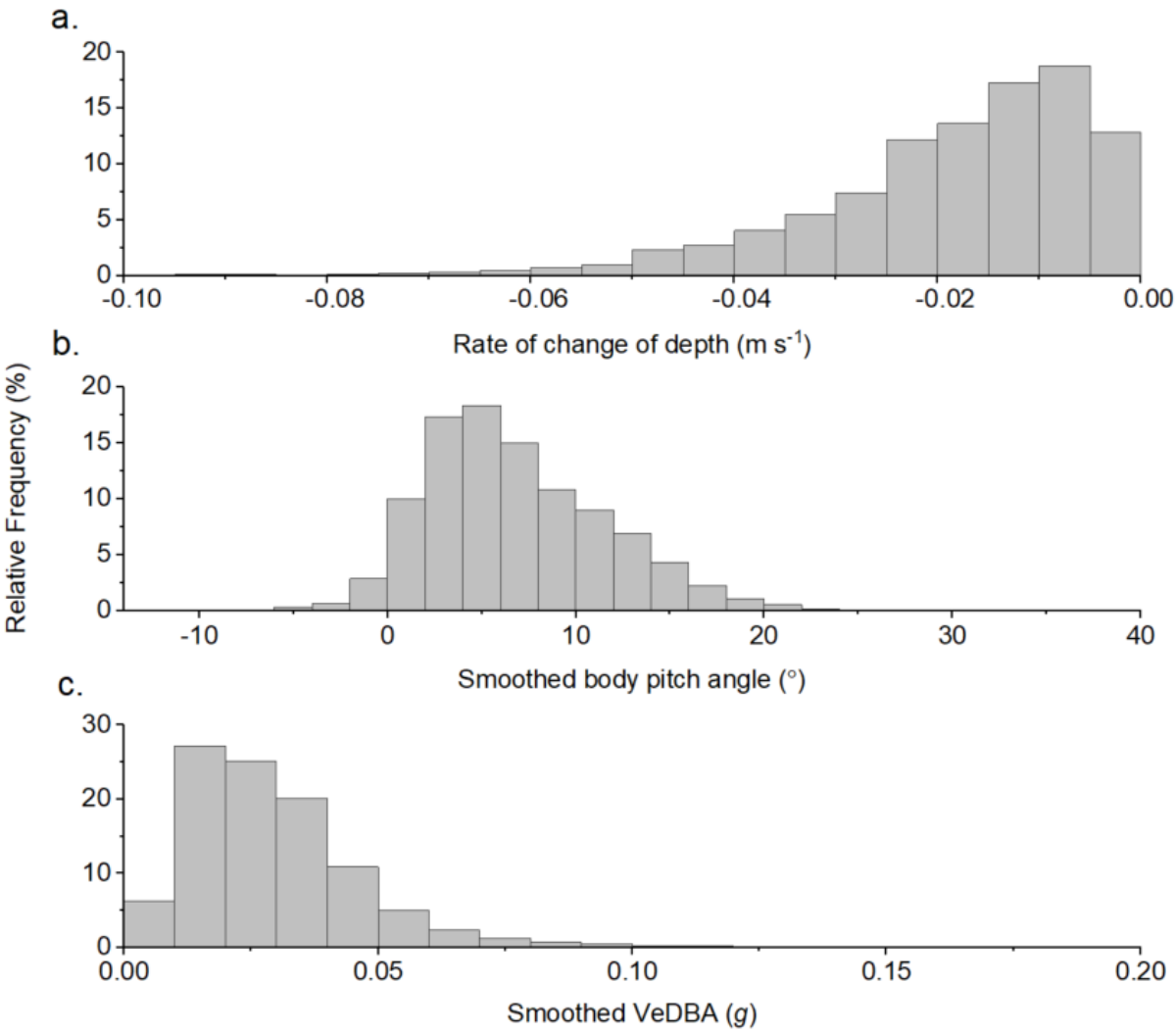

Figure 7. Frequency distributions of key derived metrics from the extracted Behaviour B of TS12, including a) rate of change of depth (m s^{-1}), b) pitch angle (°) and c) VeDBA (g). Metrics smoothed over 2 s. Rate of change of depth reached a maximum decrease rate of -0.16 m s^{-1}, however the frequency of values occurring between this value and -0.1 m s^{-1} was minimal. The maximum pitch angle exhibited by this shark during ascents was 78.52° but values this extreme rarely occurred. Smoothed VeDBA reached 0.54 g but values greater than 0.15 were also uncommon.

Patterns across individuals

Figure 8a shows that the spread of rates of change of depth performed by the sharks during Behaviour B followed a relatively similar pattern to one another, that was not normally distributed. For all sharks, the rate of ascent mostly ranged between 0 and -0.05 m s^{-1}, a similar (but negative) gradient range to the rates of descent in Behaviour A. However, despite all sharks exceeding these values on occasion (TS18 performed a maximum rate of change of depth of -0.24 m s^{-1}), overall ranges and maximum values of Behaviour B ascent rates were slower than that of Behaviour A descent rates. Despite the larger range of values for Behaviour A, when

the mean rates of change of depth were compared between both behaviours and across all sharks, very little difference was observed (figure 9).

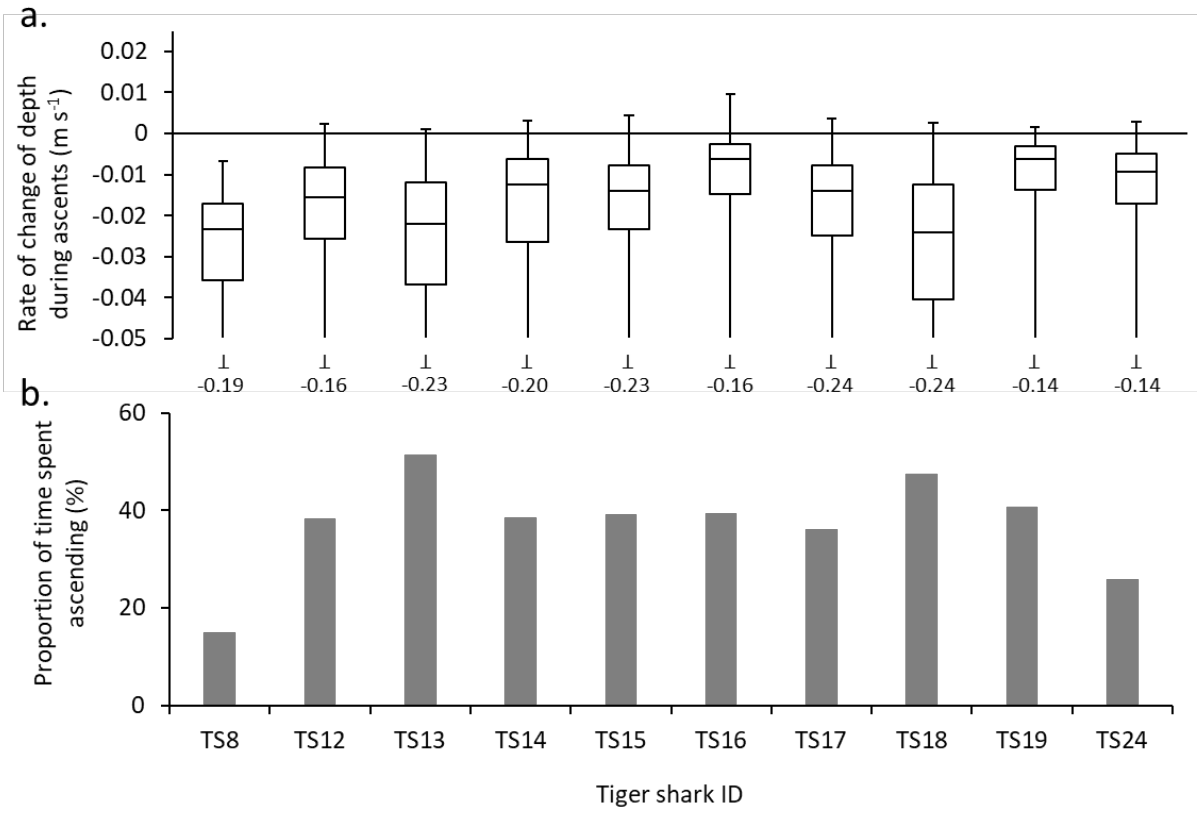

Figure 8. a) Comparisons of extracted rate of change of depth (m s^{-1}) data between sharks during Behaviour B (horizontal lines show medians, boxes quartiles and whiskers limits). b) compares the proportion of recorded time each shark dedicated to this behaviour.

The bar heights in figure 8b displays an almost identical pattern to that in figure 5b, between individuals' proportion of time spent exhibiting Behaviours A and B. For example, TS8 spent the smallest proportion time both descending (16.9%) and ascending (15.1%) and TS13 spend the greatest proportion of time both descending (42.4%) and ascending (51.4%). All sharks, except for TS18, spent more time exhibiting behaviours engaged in ascents, than descents.

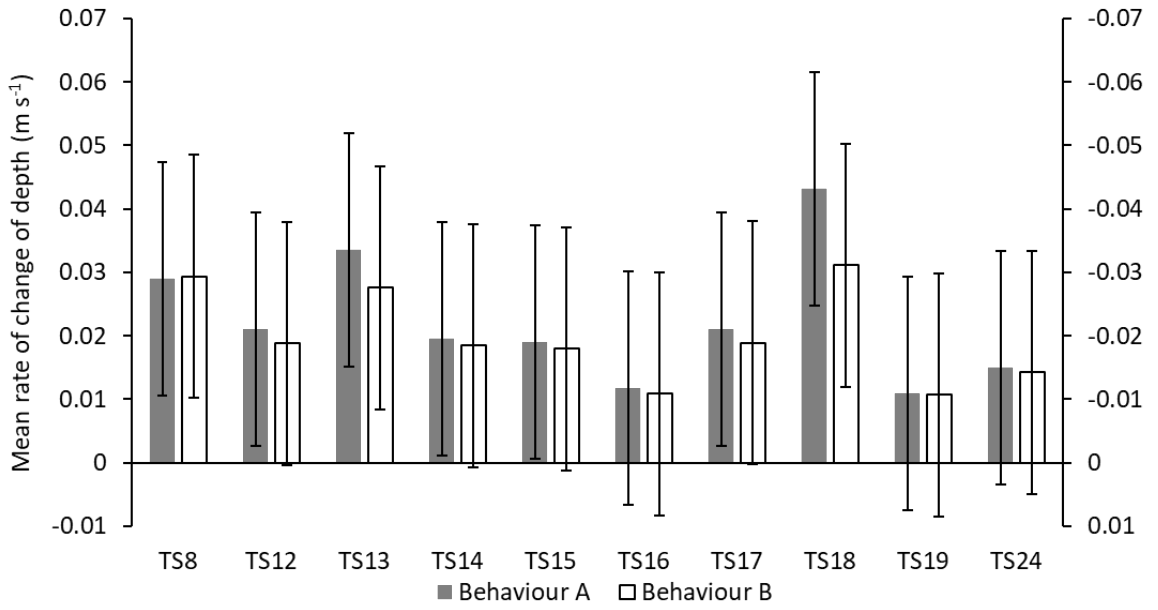

Figure 9. Comparisons of the mean rates of change of depth (m s^{-1}) for Behaviour A and Behaviour B. Although Behaviour A's values are positive and B's values are negative, they represent the gradient at which the sharks increased or decreased depth respectively. Thus, the secondary axis (reading Behaviour B's rate of change of depth values) is reversed to allow for easy comparison. Error bars show standard deviation.

Figure 9 shows that the mean rates of change of depth were slightly higher during Behaviour A than Behaviour B for all sharks except TS8. This is unsurprising if the sharks returned to a depth that was approximately the same as the initial depth prior to the descent phase, during the ascent phase of a dive which had slower mean rates of change of depth. Thus, faster rates of descent would be expected to result in less time dedicated to descents than ascents. However, the standard deviation bars indicate that each shark's data deviates greatly from the means and any significant difference between the gradient of the two behaviours and also between individual sharks is unlikely. Additionally, over all ascents and descents for all sharks, the mean VeDBA values (descents 0.032 *g* ±0.027, ascents 0.033 *g* ±0.025) were not significantly different ($t = 0.49$, unpaired t-test at 0.05 level).

Figure 10a represents the first 60 seconds of a single dive descent phase, reaching a maximum depth of 93.16 m. During the first 60 seconds, the depth increased by 29.407 m at a mean rate of 0.098 ±0.053 m s^{-1}. Based on the second half of the data from this dive section (due to more regular visible tailbeats), the tailbeat frequency was approximately 0.433 tailbeats s^{-1} and the mean smoothed VeDBA was 0.034 ±0.020 *g*. Figure 10b represents the first 60 seconds of the corresponding ascent phase of the same dive, following a bottom phase. During the first 60 seconds of the ascent, the depth decreased by 17.204 m at a mean rate of -0.057

±0.035 m s^{-1}. Again, based on the second half of the first minute of ascent, the tailbeat frequency was approximately 0.567 tailbeats s^{-1} and the mean smoothed VeDBA was 0.063 ±0.072 *g*.

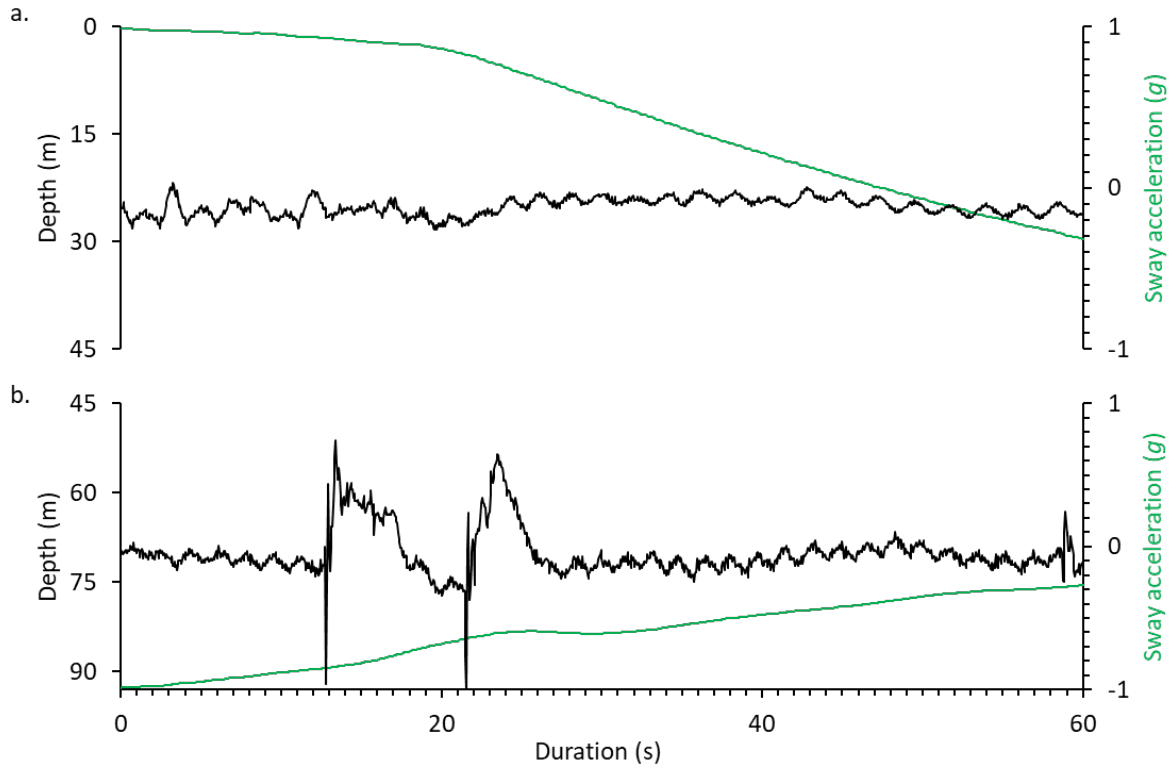

Figure 10. The first 60 seconds of a) a descent phase and b) an ascent phase of the same dive, taken from TS18's tag data. The green lines showing continuous decrease and increase represent depth (m, smoothed over 2 s). The black oscillating lines represent sway acceleration (g) from the acceleration y axis.

Data from only the first 60 seconds of each phase was used in this example to provide a clearer view of the TS18's tailbeats, visible in the sway acceleration (*g*) axis. This data suggests that the shark's tailbeats were slightly irregular when initiating both a descent and an ascent. During the descent phase (figure 10a), TS18's tailbeats began with greater magnitude but became smaller and more uniform after the first 24 s, when the depth began to increase more steeply. During the ascent (figure 10b), between approximately 0-3 s, 13-27 s and 58-60 s, there are some obvious irregularities in the tailbeats, some of which appear to coincide with changes in the gradient of the depth line. Between 27 and 58 s, the tailbeat frequency and amplitude are more regular as the gradient of the depth line decreases more steadily. The tailbeat frequency was higher and amplitude greater during the ascent phase compared to the descent phase.

Behaviour C – 'Horizontal Swimming'

Key metrics

'Horizontal swimming' was manifest when the rate of change of depth was equal to 0 m s^{-1} for > 3 s.

Example behaviour

A rate of change of depth of <0.01 and >-0.01 m s^{-1} for a prolonged period (> 3s) indicated that there was no change in depth and that the sharks were maintaining their horizontal position in the water column. Behaviour C was relatively short-lived in all occurrences, for example TS14 maintained a constant depth of 8.3 m for just over three seconds (figure 11a). During this period, the smoothed pitch angle (figure 11b) changed very little, with a range of only 1.3° within a mean of 0.3° ±0.3°. The mostly positive body pitch during this behaviour suggests that the shark's body was pitched slightly upwards. The smoothed VeDBA (*g*) varied slightly during this short period, ranging between 0.005 *g* and 0.371 *g* (mean 0.03 ±0.01 *g*). The current algorithm only detected the occurrence of Behaviour C amongst the data of two sharks (figure 13).

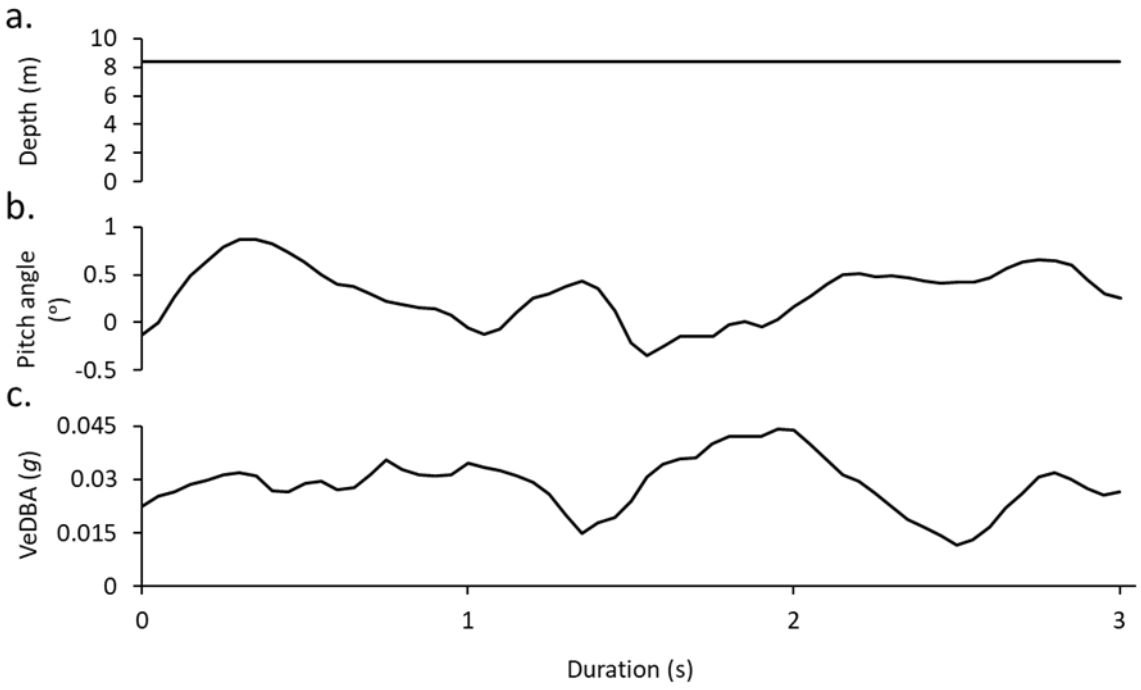

Figure 11. Time series plots illustrating the key features of Behaviour C within derived metrics, including a) depth (m) and b) pitch angle (°) and c) VeDBA (g). Metrics smoothed over 2 s.

Multiple examples of the behaviour within an individual

For TS14, Behaviour C most frequently occurred at depths between 0.5 and 0.1 m and at a mean depth of 2.91 m (±3.68). Depths < 1 m were considered to be at the water's surface. Body pitch angle values had a mean of -0.4° (±1.1) however, both positive and negative body pitch angles were observed during this behaviour (figure 12b). The most frequently occurring negative pitch angles ranged between 0° and -0.5° and the most frequently occurring positive pitch angles ranged between 0° and 0.5°. Figure 12c shows a continuum in the distribution of VeDBA values for Behaviour C and the most frequently occurring values ranged between 0.01 *g* and 0.02 *g,* with a mean value of 0.06 ±0.01 *g*.

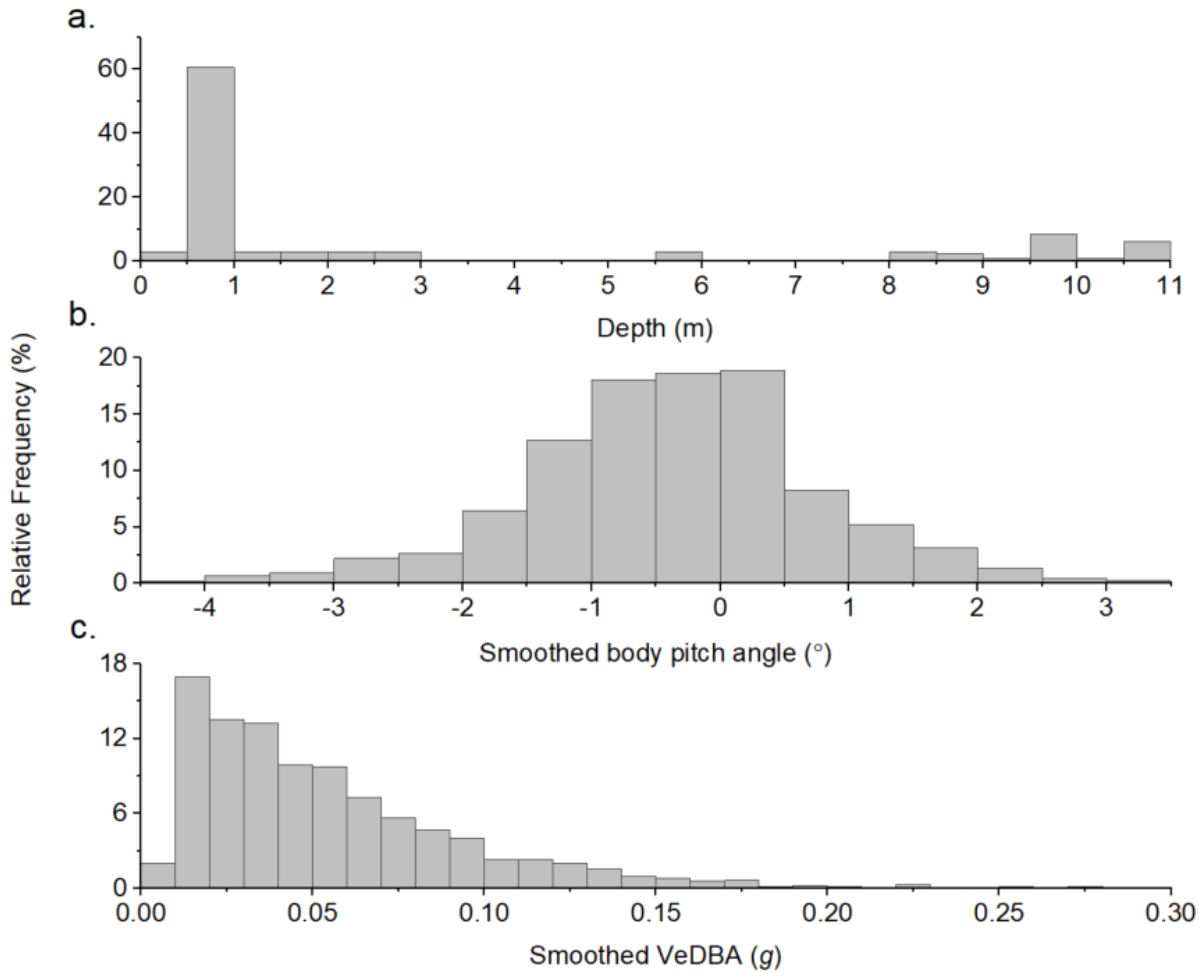

Figure 12. Frequency distributions of extracted a) rate of change of depth (m s^{-1}) data, b) pitch angle (°) data and c) VeDBA (g) data for TS14 during Behaviour C. VeDBA reached 0.37 g but were rarely greater than 0.2 g. Metrics smoothed over 2 s.

Patterns across individuals

For both sharks that showed Behaviour C, body pitch angle was mostly positive (or upwards) (figure 13a). Pitch angle was never less than -5° and never exceeded 5°, markedly shallow compared with the ranges seen in Behaviours A and B (figures 5b and 8b). The proportion of time dedicated to horizontal swimming was also minimal (figure 13b). Both sharks dedicated less than 1% of the recorded time to Behaviour C, indicating that maintenance of a perfectly constant depth was uncommon and most sharks did not do so at all within their monitored periods.

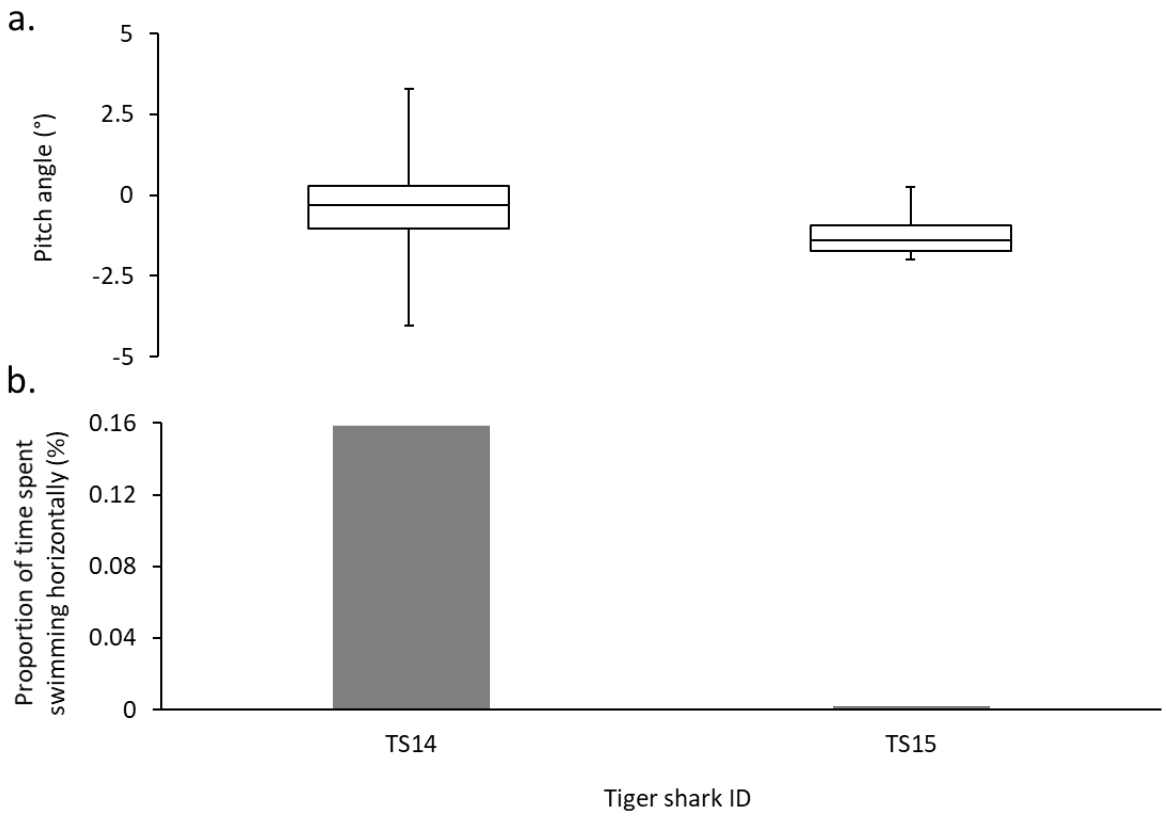

Figure 13. Comparisons of extracted a) body pitch angle (°) data (smoothed over 2 s) between sharks during Behaviour C (horizontal lines show medians, boxes quartiles and whiskers limits). b) compares the proportion of recorded time each shark dedicated to this behaviour.

Behaviour D – 'Surface Swimming'

Key metrics

'Surface swimming' occurred at a depth of < 1 m for a period > 3 s and was not included within Behaviour C discussed above. Increased VeDBA values were also observed during this behaviour.

Example behaviour

Between dive phases, the sharks would occasionally spend time swimming at the surface of the water, at depths of < 1 m (figure 14a). 'Surface swimming' occurred at a depth of < 1 m for > 3 s, during which time increased VeDBA values were observed in all individuals. During these periods, the rate of change of depth (figure 14b) had a mean of 2.09 $x10^{-5}$ m s^{-1} and remained within a much smaller range (between -0.05 and 0.05 m s^{-1}) compared to descent and ascent phases. However, the rate of change of depth was not constant and alternated between positive and negative values. Over these short periods, the counteractive movement of positive and negative rates of change of depth resulted in very minor changes of several centimetres in the shark's depth. It is also possible that some of the recorded fluctuations were a result of tag disturbance, especially if the sharks' fins protruded the surface of the water or wave action making the water above the tag deeper and shallower. The pitch angle mostly remained between -5° and 5° (figure 14c), in a manner similar to Behaviour C, and had a mean value of 0.6° (±2.3). Increased VeDBA (*g*) values were evident (mean 0.10 ±0.05 *g*) when swimming in depths of < 1 m (figure 14d). Although Behaviour C (horizontal swimming) was common at the surface, the rate of change of depth values overlapped little with those of Behaviour D, making surface swimming undetectable within the current Behaviour C algorithm.

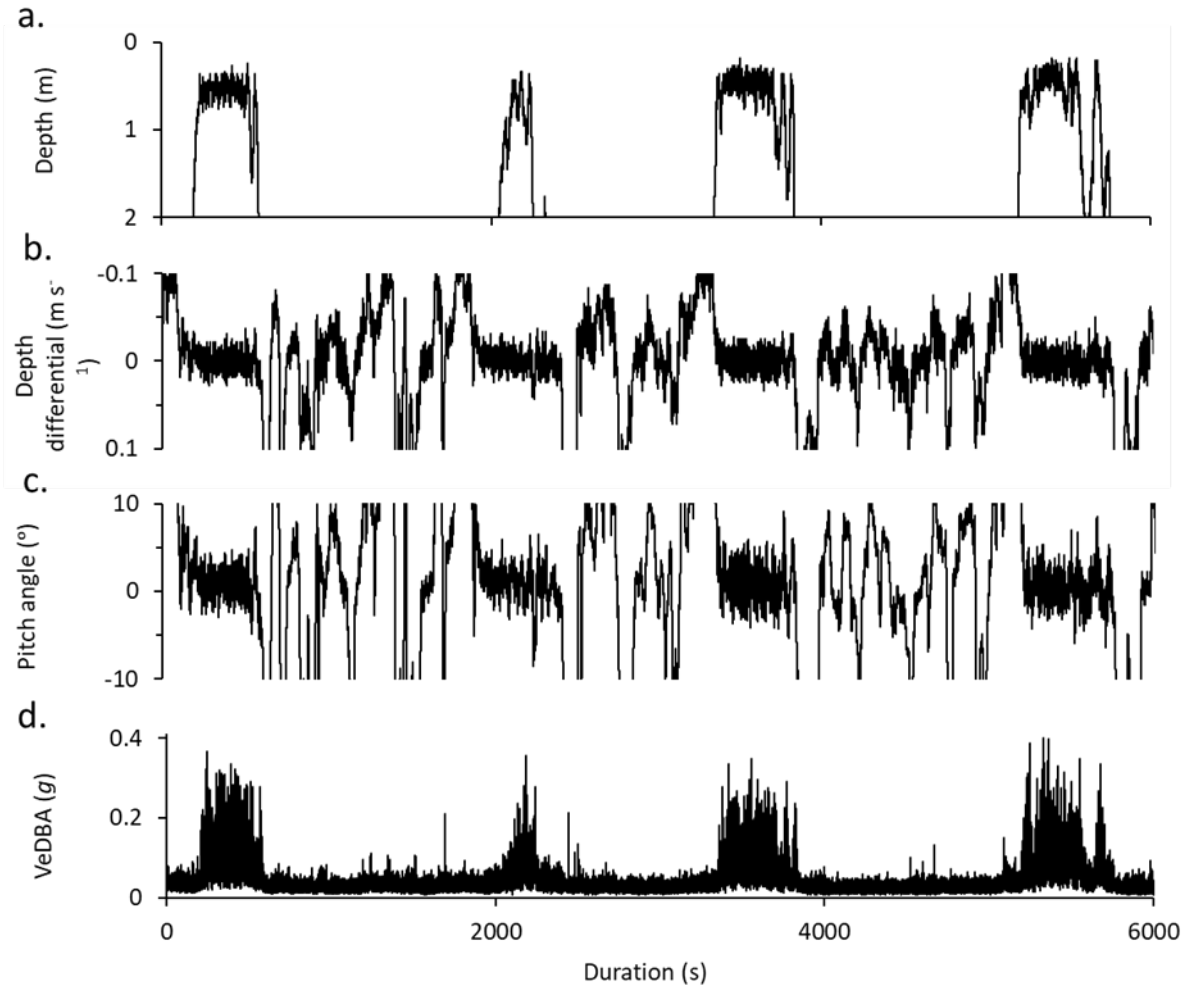

Figure 14. Time series plots illustrating the key features of Behaviour D within derived metrics, including a) depth (m) and b) rate of change of depth (m s^{-1}), c) pitch angle (°) and d) VeDBA (g). Metrics smoothed over 2 s.

Multiple examples of the behaviour within an individual

There was no multimodality shown by the frequency distributions of all metrics including a) rate of change of depth, b) smoothed pitch angle and c) smoothed VeDBA (figure 15). The most frequently occurring rate of change of depth values ranged between -0.002 and -0.001 m s^{-1} (mean -0.001 ±0.007 m s^{-1}). The smoothed pitch angle and the smoothed VeDBA also showed continuum distributions. The highest frequency of pitch angle values ranged between 1° and 2° (mean 1.9° ±2.7) and the highest frequency of smoothed VeDBA values ranged between 0.04 *g* and 0.05 *g* (mean 0.07 *g* ±0.04).

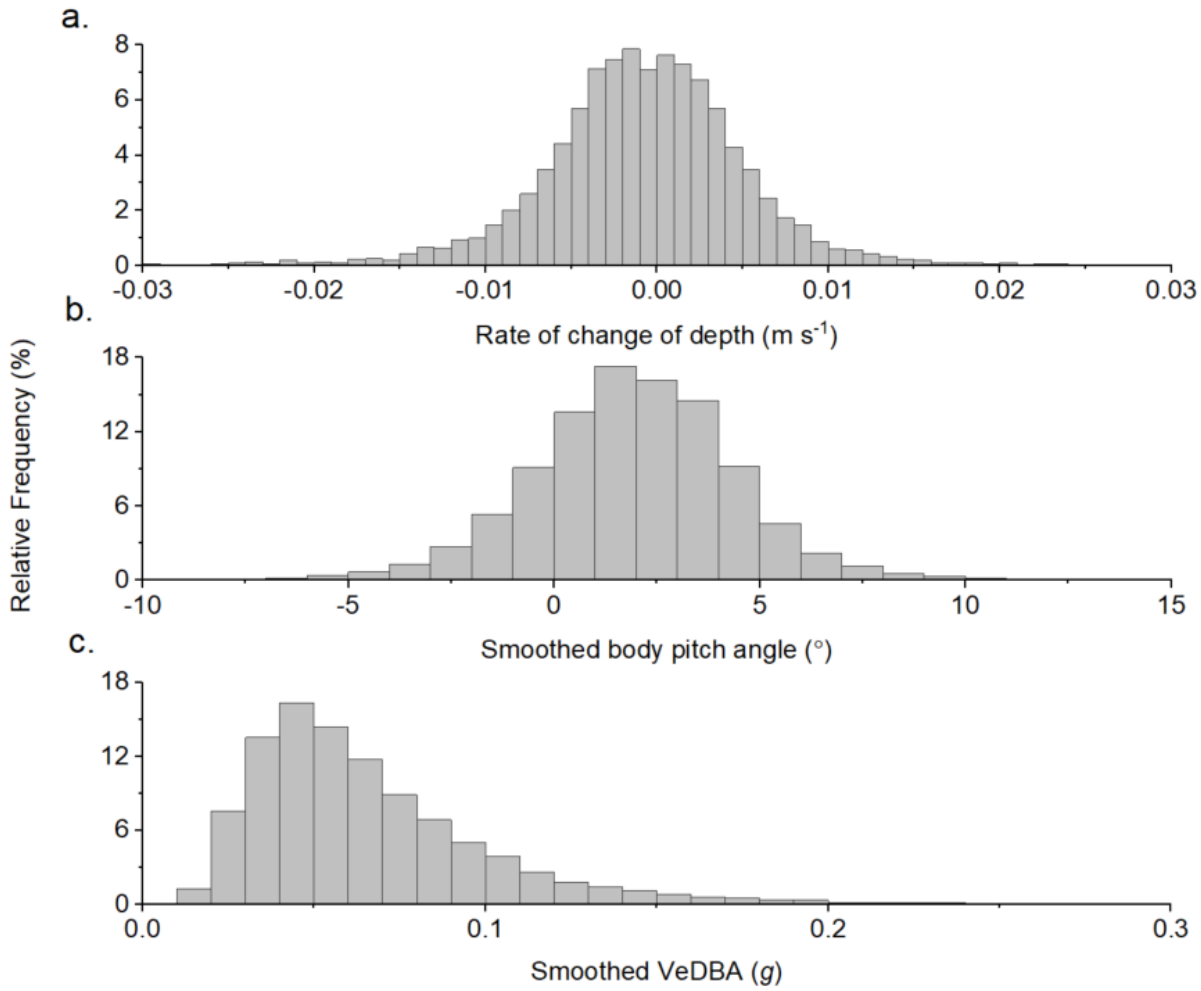

Figure 15. Frequency distributions of Behaviour D extracted from TS13's data. a) The rate of change of depth (m s^{-1}) data ranged from -0.058 to 0.057 m s^{-1}. b) Smoothed pitch angle (°) ranged from -31.6° to 21.3°. c) Smoothed VeDBA (g) data for TS13 during Behaviour D ranged between 0.007 g to 0.44 g.

Patterns across individuals

The algorithm for surface swimming detected the behaviour amongst the data of only six of the 10 sharks (figure 16). The majority of the VeDBA data for this activity fell between 0 and 0.15 *g* for all sharks, but all had a maximum value exceeding 0.4. In fact, TS19 produced a maximum VeDBA value of 0.91 *g*. TS19 also dedicated the highest proportion of time to swimming at the surface (37.5%), potentially providing more opportunity to produce higher VeDBA values whilst participating in this activity. For the rest of the sharks, proportion of time dedicated to Behaviour D varied. TS14, TS19 and TS24 each spent over 25% of their time at the water's surface, whilst TS13, TS15 and TS18 each spent less than 15% at the surface, with TS13 dedicating only 2.37% of recorded time to this activity. TS8, TS12, TS16 & TS17 spent no proportion of recorded time at the surface as no data was detected by the algorithm.

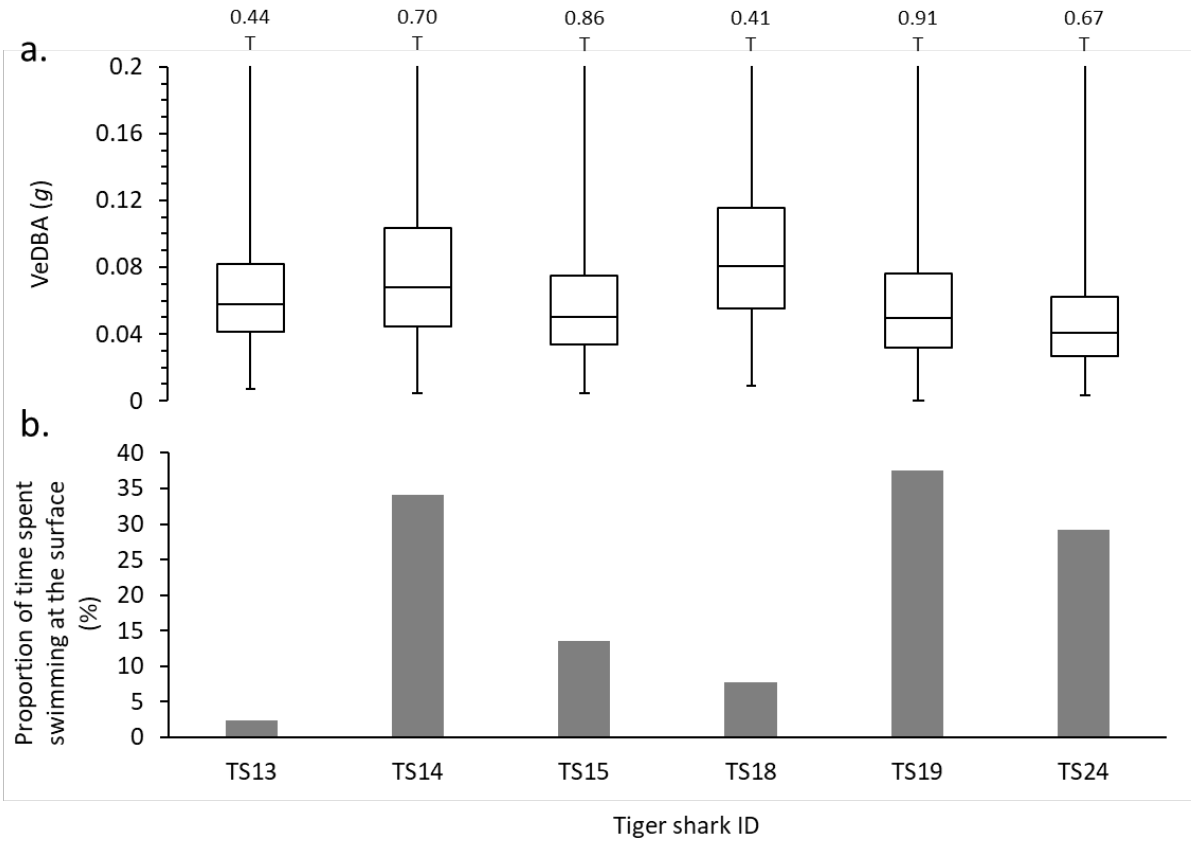

Figure 16. Comparisons of extracted a) smoothed VeDBA (g) data between sharks during Behaviour F (horizontal lines show medians, boxes quartiles and whiskers limits). b) compares the proportion of recorded time each shark dedicated to this behaviour.

Behaviour E – 'Undulatory Swimming'

Key metrics

Key numerical metrics could not be defined for this behaviour due to the varying nature between individuals and occurrences. However, the behaviour was visually readily identifiable by the sine wave-like pattern in the surge, depth and the rate of change of depth data. Thus, 'undulatory swimming' was defined as a regular oscillation around zero in the rate of change of depth channel.

Example behaviour

Three-dimensional dead-reckoning of this behaviour showed that this appeared as a repetition of descents and ascents, but with markedly smaller amplitudes than Behaviours A and B. Key features of Behaviour E, or undulatory swimming, are graphed in figure 17. Unlike complete dive movements (figure 18), the undulations in depth were smooth, consistent and lacked a 'bottom phase' between descents and ascents. Also, a relatively constant depth was

maintained overall. In the example given, Behaviour E was initiated at a depth of 15.3 m and terminated at a depth of 12.9 m and overall remained between 6.1 m and 15.4 m (mean 11.69 m ±1.6) throughout the activity, despite the undulations. The oscillations in the rate of change of depth values (figure 17b) created a sine-wave-like pattern that, in this example, remained between -0.1 and 0.1 m s^{-1} and had a mean value of -0.0008 ±0.036 m s^{-1}.

However, metrics varied between occurrences of this behaviour and between individuals, depending on the scale of the oscillations. This made it more difficult to define Behaviour E with set metric limits in order to construct an algorithm. Behaviour E was characterised by oscillations in the vertical [or depth] axis. A time series algorithm designed to detect and mark consecutive peaks 0 m s^{-1} and troughs <0 m s^{-1} in the rate of change of depth channel was tested. It successfully marked the peaks for the particular occurrence of the behaviour the algorithm was initially based upon, but not for other occurrences others with a differing wave period or amplitude. Following alterations to the algorithm to include these larger oscillations, upon testing the algorithm successfully marked the larger oscillations, however no longer marked the smaller oscillations. Defining limits for sinusoidal swimming and circling presented the same difficulties. This provides an area of development for this work in the future.

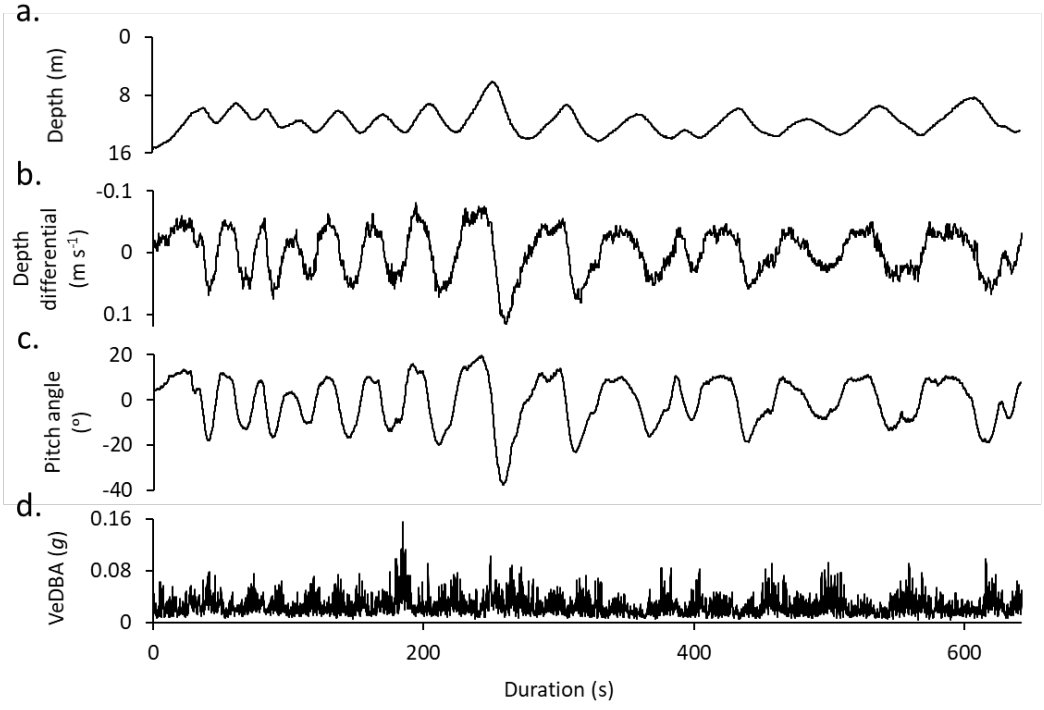

Figure 17. *Time series plots illustrating the key features of Behaviour E within derived metrics, including a) depth (m) and b) rate of change of depth (m s^{-1}), c) pitch angle (°) and c) VeDBA (g). Metrics smoothed over 2 s.*

As expected, the pitch angle (figure 17c) followed a near-identical visual pattern to the rate of change of depth, with values corresponding to steeper pitch angles. The pitch angle in this example had a mean value of -0.78° ±10.61° and mostly oscillated between -20° and 20° except for one deeper trough between 200 and 300 s. These are relatively shallow body pitch angles compared with the maximum pitch angles demonstrated in ascent (figure 3b) and descent (figure 6b). Despite continuous fluctuations in VeDBA (figure 17d) throughout this activity, there were distinctive periods of increased VeDBA during the ascent periods (mean 0.03 ±0.02 *g*).

Yo-yo Diving Behaviour

Expanding the time window over which behaviours were determined, it was possible to see that all sharks displayed vertical 'yo-yo'-like movements through the water column whereby the sharks would repetitively descend the water column and then ascend back to similar depth prior to the dive (cf. Nakamura *et al.,* 2011) (figure 18), although number of dives per hour and maximum depth per dive varied between individuals (figure 19). Complete dives were characterised by descent, bottom (though not always present) and ascent phases and other behaviours often occurred within these phases. For example, some of the sharks circled during descent or bottom phases or swam sinusoidally during any phase (see below). The three-dimensional dead-reckoning visualisation from TS13's tag data shown in figure 10 spans 4 h 50 min. During this time the depth ranged a maximum 93.08 m across 20 dives and more than 14 km of horizontal distance was travelled, with the total distance travelled likely much greater after vertical travel is considered.

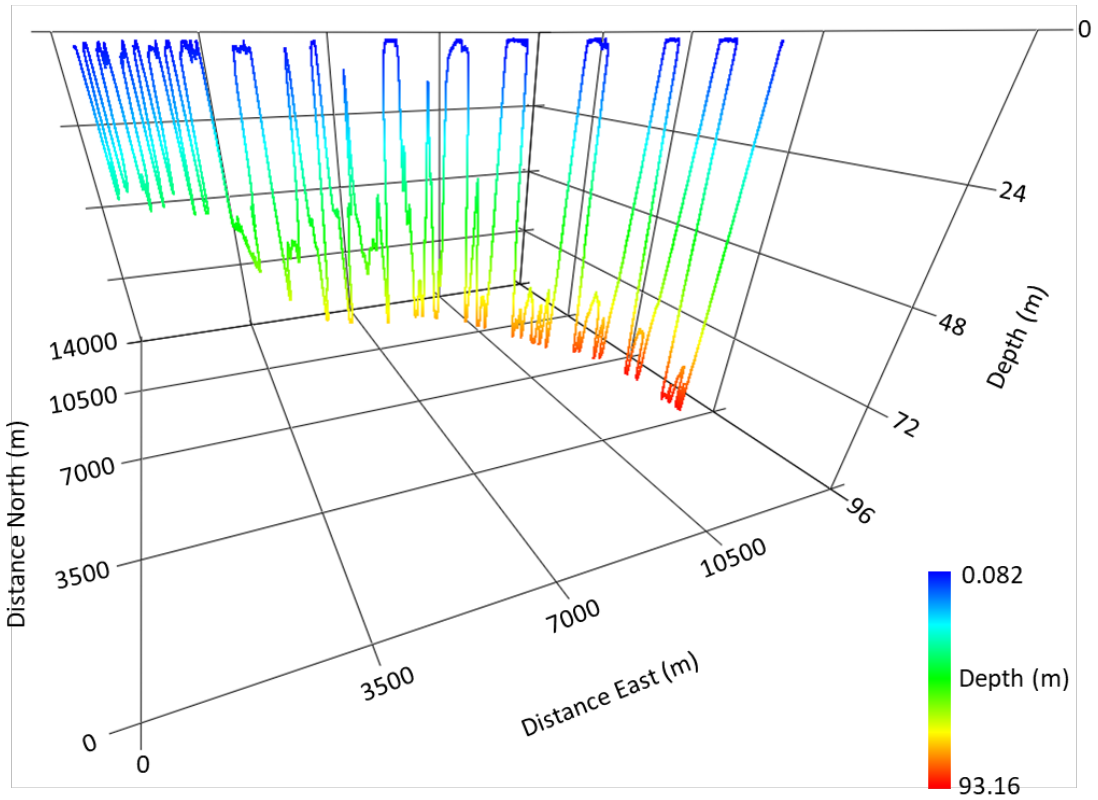

Figure 18. a) A three-dimensional dead-reckoning plot created in DDMT illustrates the yo-yo like diving behaviour comprised of Behaviours A and B, as well as bottom phases occasionally. Dead-reckoning is derived from the heading, speed and depth data channels over time (table 2).

The extracted depth data from Behaviour A reveals that most of sharks dived no deeper than 40 m at any time, except for TS13 and TS18, which reached depths exceeding 80 m (figure 19). TS18 reached a maximum depth of 93.81 m during a descent. TS13 and TS18 were the two sharks that also had the fastest rates of change of depth (figure 9).

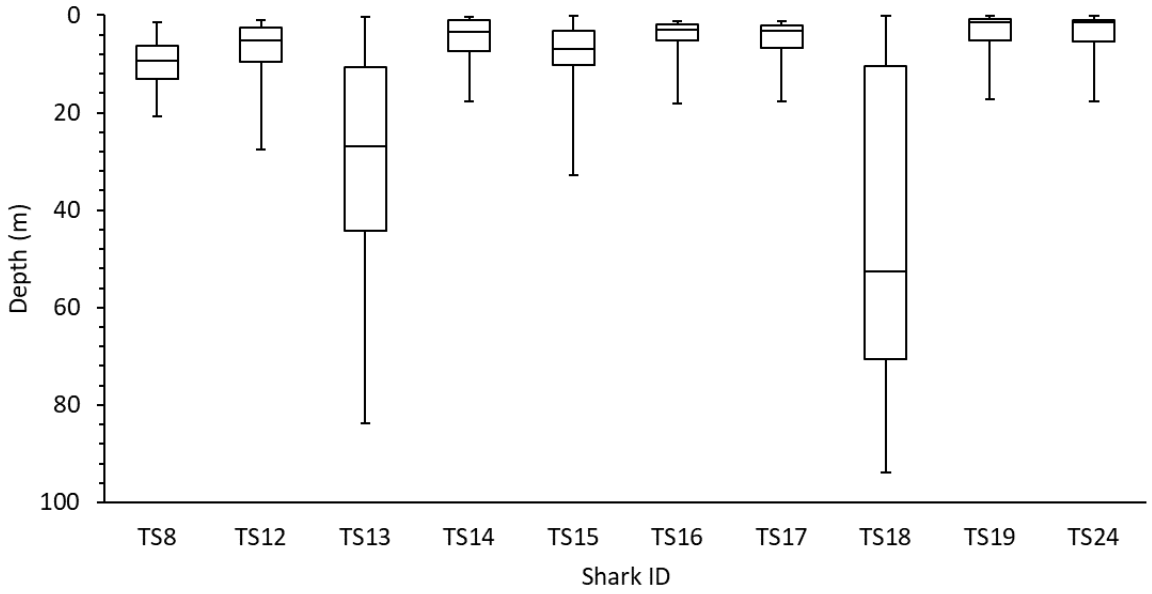

Figure 19. Comparisons of extracted depth data, m (smoothed over 2 s) between sharks during Behaviour A (horizontal lines show medians, boxes quartiles and whiskers limits).

BEHAVIOURS BASED ON HEADING

Behaviour F – 'Straight swimming'

Key metrics

'Straight swimming' was defined as periods of (forward) movement with a steady or slow-changing heading and no major directional changes based on the absolute rate of change of heading being $< 0.5^{o}$ s^{-1} for > 3 s.

Example behaviour

Due to the minor sinusoidal heading fluctuations (caused by tailbeats) present in the heading differential channel despite smoothing (over 80 events, 2 s), the rate of change of heading was not considered to be 0° s^{-1} during this activity. The data was not smoothed further to remain consistent and to avoid loss of information. However, upon inspection, the tailbeats rarely produced an absolute rate of change of heading value greater than 0.5° s^{-1}. Therefore, any period during which the magnetic heading was within -0.5 and 0.5° s^{-1} for three seconds or more was considered to be straight swimming.

The graphed example of Behaviour F spanned 42 seconds, in which time the absolute rate of change of heading was not constant but remained between 0.28 and 0.49° s^{-1}, with a mean value of 0.4° s^{-1} (±0.1) (figure 20a). As a result, the maximum range of the shark's heading was 8.5° during this behaviour, remaining between 179.5° and 188° (figure 20b). The mean magnetic heading was 183.3° (±1.5). Also, very little variation in magnetic field intensity was observed, with the magnetometer *x, y* and *z* axes remaining relatively constant (figure 20c). The magnetometer *y* axis, which recorded lateral movement in relation to the Earth's magnetic field, showed values remaining close to 0 mG (mean -0.11 mG ±0.02). This was another key indication that the direction of the sharks' swimming was steady.

Over a longer distance, any rate of change of heading greater than zero would have resulted in a significant difference in direction and position. However, due to the swimming mode of the sharks, a perfectly straight heading would be impossible to maintain unless they undertook long periods of gliding without the use of any tailbeats at all. The sharks only remained on straight courses for relatively short periods (figure 22c).

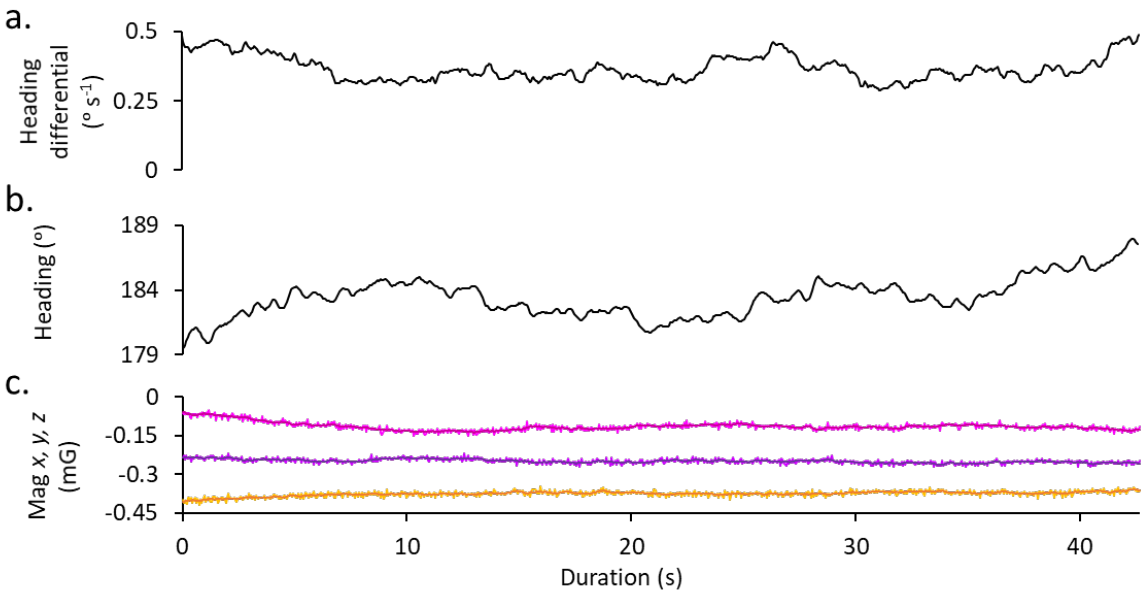

Figure 10. Time series plots illustrating the key features of Behaviour F within recorded and derived metrics, including a) rate of change of heading (° s^{-1}) and b) heading (°) and c) magnetic field intensity axes x (orange), y (pink), z (purple), (mG). Metrics smoothed over 2 s.

Multiple examples of the behaviour within an individual

There was no distinct multimodality within the magnetic headings at which straight swimming occurred. However, TS18 most frequently participated in straight swimming with a

magnetic heading between 176° and 178° (mean 170° ±13.95°). The frequency distribution of the *y* axis data recorded by the triaxial magnetometer (figure 21b) displayed a relatively unusual pattern. A significantly taller peak showed that the most frequently record magnetic field intensity values fell between the range of 0 and -0.01 mG (mean 0.05 ±0.07 mG). Another three peaks of increasing value but lessening frequency are also visible. However, again there is no distinct separation between these peaks to suggest clear, separate multimodality. Also, the frequency distributions of the other sharks' data either displayed a similar pattern to TS18 or displayed a single continuum of values. There was also a continuum in the frequency distribution of VeDBA values (figure 21c) recorded during Behaviour F by TS18 and the other sharks. The most frequently observed VeDBA values ranged between 0.010 and 0.011 *g* (mean 0.013 ±0.005 *g*). Thus, there was no distinct separation between the modes of acceleration engaged during this activity.

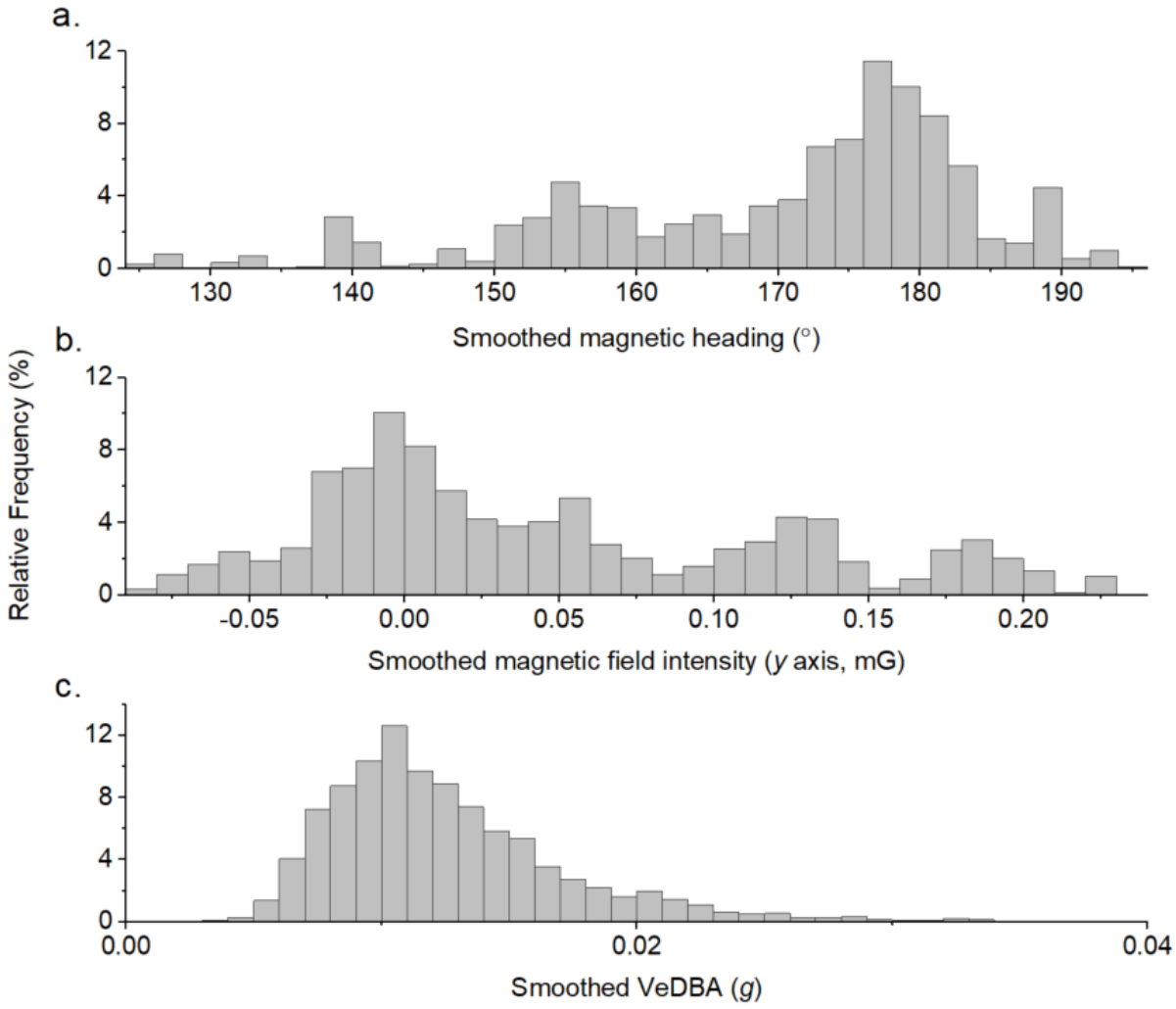

Figure 11. Frequency distributions of extracted data for TS18 during Behaviour F. a) Magnetic heading (°) data, b) magnetic intensity y axis (mG) and c) smoothed VeDBA (g). VeDBA

reached a maximum of 0.085 g, but values greater than 0.04 g were infrequent. Metrics smoothed over 2 s.

Patterns across individuals

The magnetic field intensity values, recorded along the magnetometry *y* axis, straddled 0 mG with both positive and negative values, except for TS16 and TS17 which had entirely positive values and TS24, which has entirely negative values. The graph also suggested that the values recorded by each sharks' tag were unlikely to be significantly different from one another, as the box and whisker plots for each shark broadly overlapped, despite some variation between individuals' values. The same was said for the smoothed VeDBA values plotted in figure 22b. It is evident that Behaviour F was very uncommon for these sharks, with all except TS12 dedicating less than 1% of the recorded time to swimming with a straight course (figure 22c).

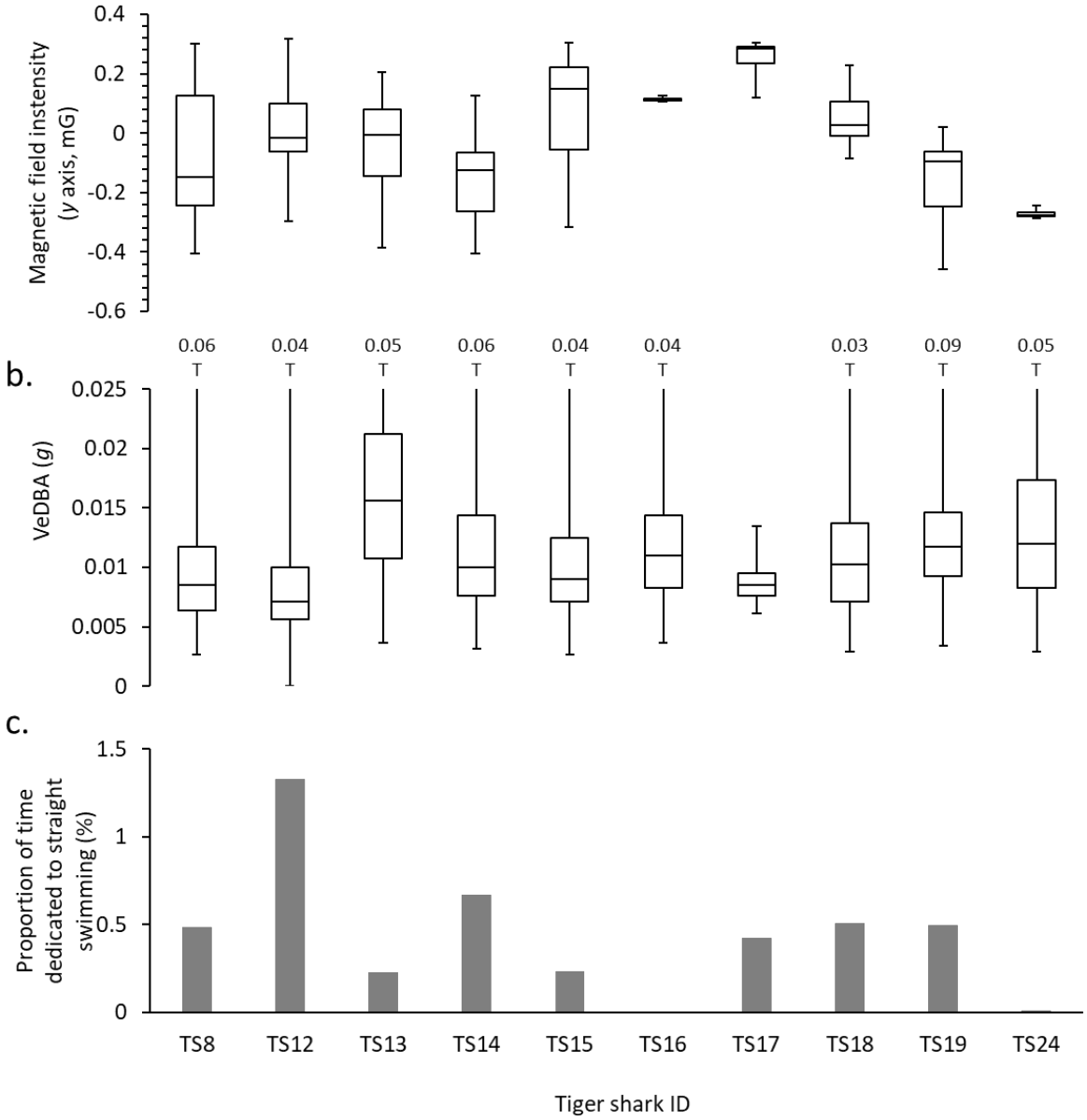

Figure 12. Comparisons of extracted a) magnetic field intensity y axis (mG) and b) smoothed VeDBA (g) data between sharks during Behaviour F (horizontal lines show medians, boxes quartiles and whiskers limits). c) compares the proportion of recorded time each shark dedicated to this behaviour. Metrics smoothed over 2 s.

Behaviour G – 'Burst power'

Key metrics

'Burst power' was defined by the absolute rate of change of VeDBA rapidly increasing above 0.03 g s^{-1}, for varied time periods.

Example behaviour

Some bursts were singular and short-lived, others lasted longer or were a series of bursts in close succession. Burst power periods were accompanied by an increased amplitude and decreased period in tailbeat curves. Behaviour G was characterised by sudden disorderly changes in most or all the recorded and derived data channels and occurred sporadically throughout the recorded time. The example event (figure 23) occurred over the course of approximately 50 seconds, but the seconds prior to and following the behaviour are included in the time series plot to provide context. Figure 23c shows the acceleration x (red), y (green) and z (blue) axes (raw channels represented by lighter colour hues, smoothed channels represented by darker hues). The increase in tailbeat frequency and magnitude shown in the raw acceleration y axis (light green) relative to prior and following activity suggested that the shark was engaging a sudden burst of power. This was also evident from the sudden increase in the absolute rate of change of VeDBA values observed during (figure 23a), which had a mean of 0.05 g s^{-1} (±0.02). VeDBA (figure 23b) showed a similar but less smoothed pattern.

In a manner similar to the acceleration axes, the magnetometer x (orange), y (pink) and z (purple) axes (figure 23d) recorded disorderly changes in the magnetic field intensity (mG) during this behaviour. The rapid, disorderly changes across all three acceleration and magnetometry axes indicated highly variable three-dimensional movement.

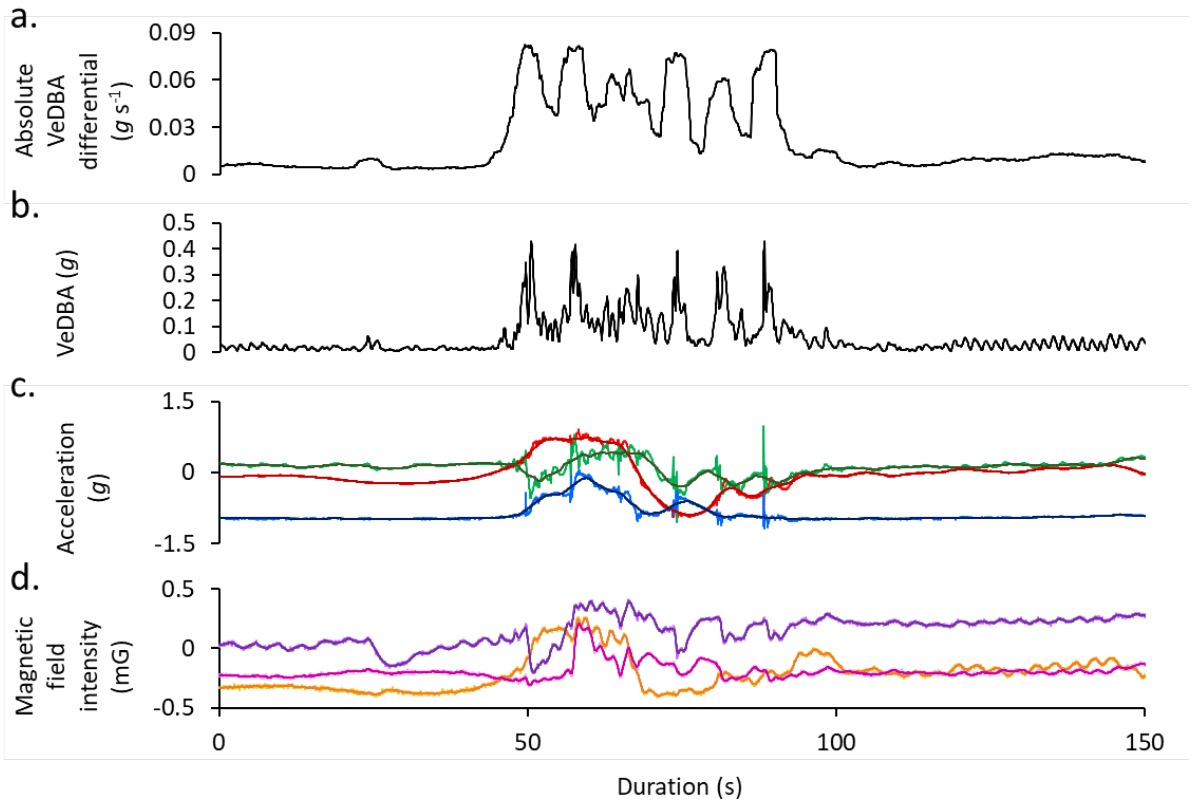

Figure 13. Time series plots illustrating the key features of Behaviour G within recorded and derived metrics, including a) absolute rate of change of VeDBA (g s^{-1}), b) VeDBA (g), c) acceleration (g) axes x (surge, red), y (sway, green), z (heave, blue) and d) magnetic field intensity axes x (orange), y (pink), z (purple), (mG). Raw channels in c) are represented by lighter colour hues, smoothed channels represented by darker colour hue. Metrics smoothed over 2 s. Note that the negative heave axis values indicated that this tag was fitted upside down and the recorded accelerometer and magnetometry data should be read accordingly.

Multiple examples of the behaviour within an individual

The metrics recorded during Behaviour G did not show multimodality, including absolute rate of change of VeDBA which showed a single steep-sided continuum from 0.03 *g* s^{-1} onwards. For TS19, the depths at which this behaviour occurred ranged between 0.1 m and 13.3 m (figure 24a) across all burst events performed but occurred most frequently between 0.4 m and 0.6 m (mean 0.96 m ±0.85), close to the water's surface. Whilst examining the frequency distributions for all metrics, a relatively unusual pattern was observed in the distribution of the magnetometer *y* axis. Figure 24b shows a smooth continuum distribution with a distinct peak between -0.59 mG to -0.6 mG. The frequency within the bins then decreased forming a trough, but then gradually increased and decreased again to form a smooth mounded shape. The most frequently recorded magnetic field intensity values in this second smooth peak ranged between -0.3 and -0.31 mG.

VeDBA values were relatively high compared with the other behaviours, reaching a maximum value of 0.42 *g* (figure 24c) and most frequently ranged between 0.04 *g* and 0.05 *g* (mean 0.08 *g* ±0.04), again showing a single continuum distribution.

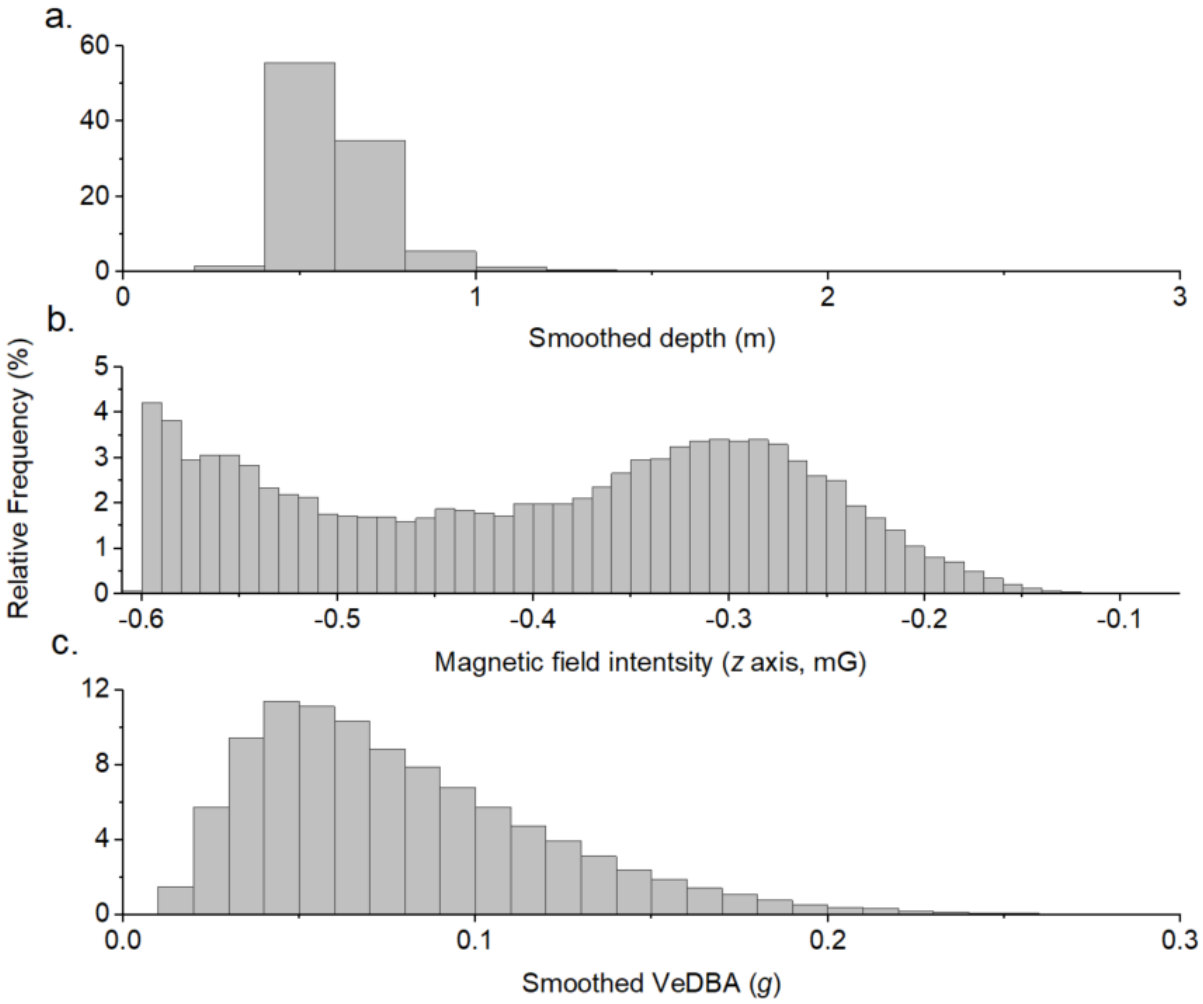

Figure 14. Frequency distributions of extracted data for TS19 during Behaviour G. a) Depth (m) data ranged between 0.1 and 13.3 m. b) Magnetic intensity z axis (mG) data. c) VeDBA (g) reached a maximum of 0.42 g. Metrics smoothed over 2 s.

Patterns across individuals

Most of the rate of change of VeDBA data (figure 25a) extracted for Behaviour G remained below 0.06 *g* s^{-1} for all sharks. Maximum rate of change of VeDBA values for all sharks exceeded this but remained below 0.36 *g* s^{-1}. This behaviour mostly occurred at shallow depths (< 3 m) for all sharks, except TS8 and TS13 (as shown by the interquartile ranges in figure 25b). However, TS13 and TS18 also expressed Behaviour G at depths greater than 75 m. Behaviour G was detected in less than 15% of the sharks' recorded time, except for TS14, which spent 23.8% swimming in a state of increased acceleration.

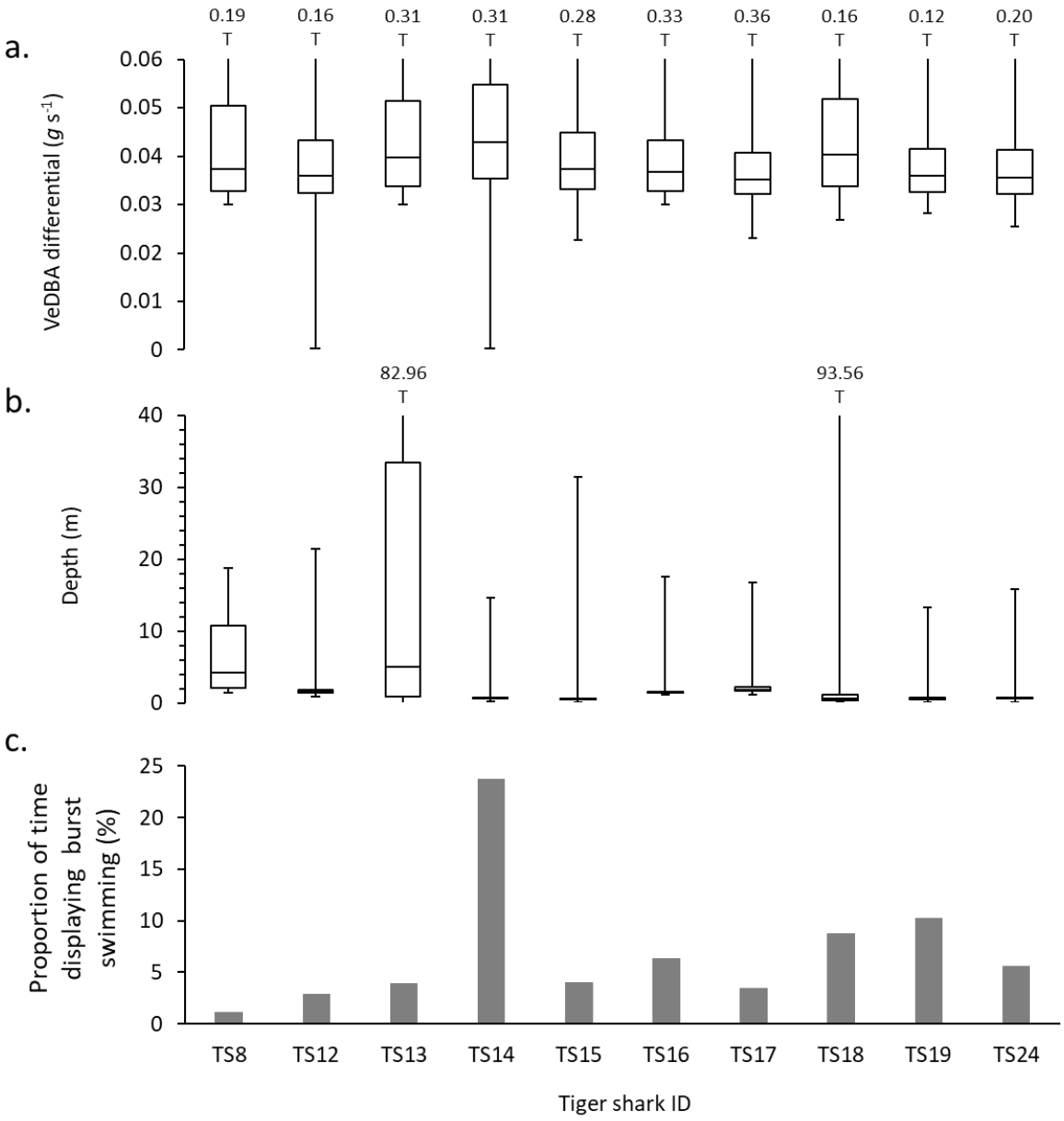

Figure 15. Comparisons of extracted a) rate of change of VeDBA (g s^{-1}) and b) depth (m) data between sharks during Behaviour G (horizontal lines show medians, boxes quartiles and whiskers limits). c) compares the proportion of recorded time each shark dedicated to this behaviour. Metrics smoothed over 2 s.

Behaviour H – 'Direction change'

Key metrics

'Direction change' was indicated by any instance in which the shark was not swimming with a straight heading described by Behaviour F. Direction change (or turn) had a rate of change of heading > 0.5° s^{-1} for > 3 s in the smoothed heading data (figure 27a).

Example behaviour

The tiger sharks spent very little time swimming with straight courses, as demonstrated in figure 21c and a birds-eye-view of this shark's dead-reckoning track (figure 26) illustrates a course with frequent changes in direction. This track spanned just over 48 minutes, in which time over 1.8 km horizontal distance was travelled and the shark's rate of change of heading (° s^{-1}) changed continuously (did not remain <0.5° s^{-1} for >3 s), implying a straight course (as defined by my algorithm) never occurred.

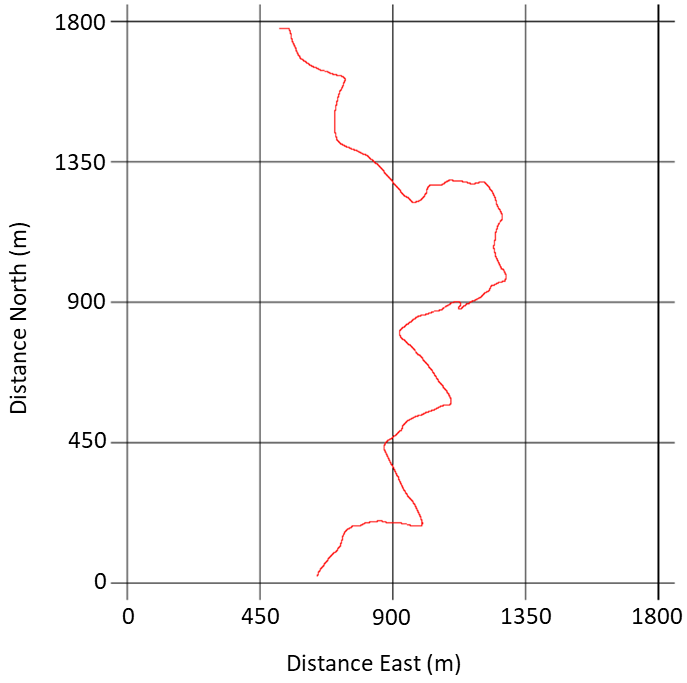

Figure 16 – A bird-eye-view dead-reckoning track of a shark swimming without a straight and steady heading at any time and continuously changing direction.

Figures 27b to 27d show the magnetic field intensity (mG), measured by the triaxial magnetometer *x*, *y* and *z* axes. Like the rate of change of heading, which they underpin, they displayed an unsteady pattern except for magnetometer axis *z,* which remained relatively constant at approximately -0.45 mG (mean -0.45 mG ±0.03). The lack of regularity in the

heading differential channel and magnetometry *x* and *y* axes suggested that the rates of lateral turning and turning angles varied between occurrences but were never greater than 5° s^{-1} in this example (mean 3.6° s^{-1} ±0.4).

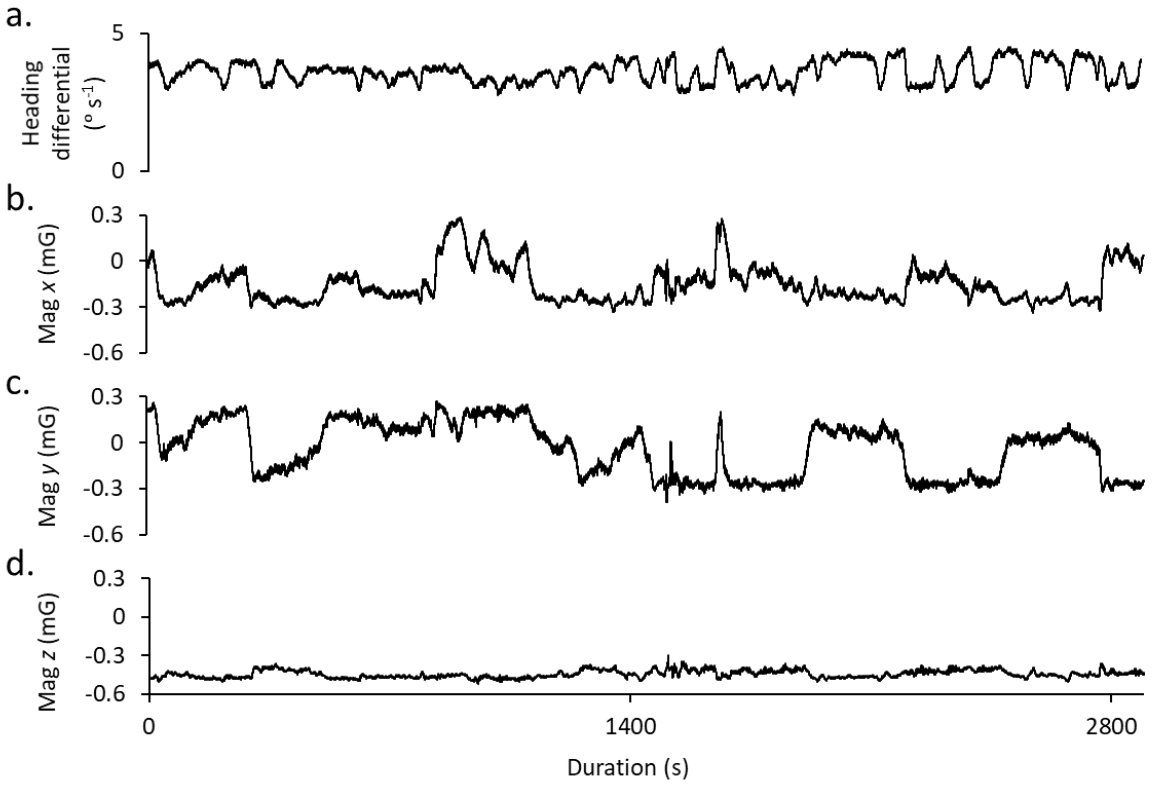

Figure 17. Time series plots illustrating the key features of Behaviour H within recorded and derived metrics, including a) rate of change of heading (° s^{-1}), as well as b) magnetic field intensity axis x (mG), c) axis y (mG) and c) axis z (mG). Metrics smoothed over 2 s.

Multiple examples of the behaviour within an individual

In an attempt to determine whether the sharks had distinct modes of turning rate (e.g. fast, slow), the frequency distributions of the absolute rate of change of heading data were assessed. However, steady continuum distributions were expressed, as seen in the data of TS16 in figure 28. For TS16, absolute rates of change of heading most frequently ranged between 2 and 3° s^{-1} (mean 3.4° s^{-1} ±4.0). A relatively unusual pattern was observed in the smoothed magnetic heading data for this shark, with three conjoined peaks appearing (figure 28b). Although they were not distinctly separated from one another, the bin values ranged between 300° and 305°, 055° and 060° and finally, 170° and 175° (in order of frequency). The mean magnetic heading was 181.6° (±105.7). The frequency distribution of smoothed roll angle demonstrated that this behaviour could also be cascaded into left and right turns, because the

body roll angle changed as the sharks leaned into a turn. Left or anticlockwise turns produced negative roll angles, whilst right or clockwise turns produced positive roll angles. Figure 28c shows a peak in the positive smoothed body roll angle values (most frequently expressed angles ranged between -9° and -10°) and a peak in the negative smoothed body roll angle values (most frequently expressed values ranged between 5° and 6°). This could also be shown using the standard heading differential instead of the absolute heading, with left or anticlockwise turns producing positive differential values and right or clockwise turns producing negative values.

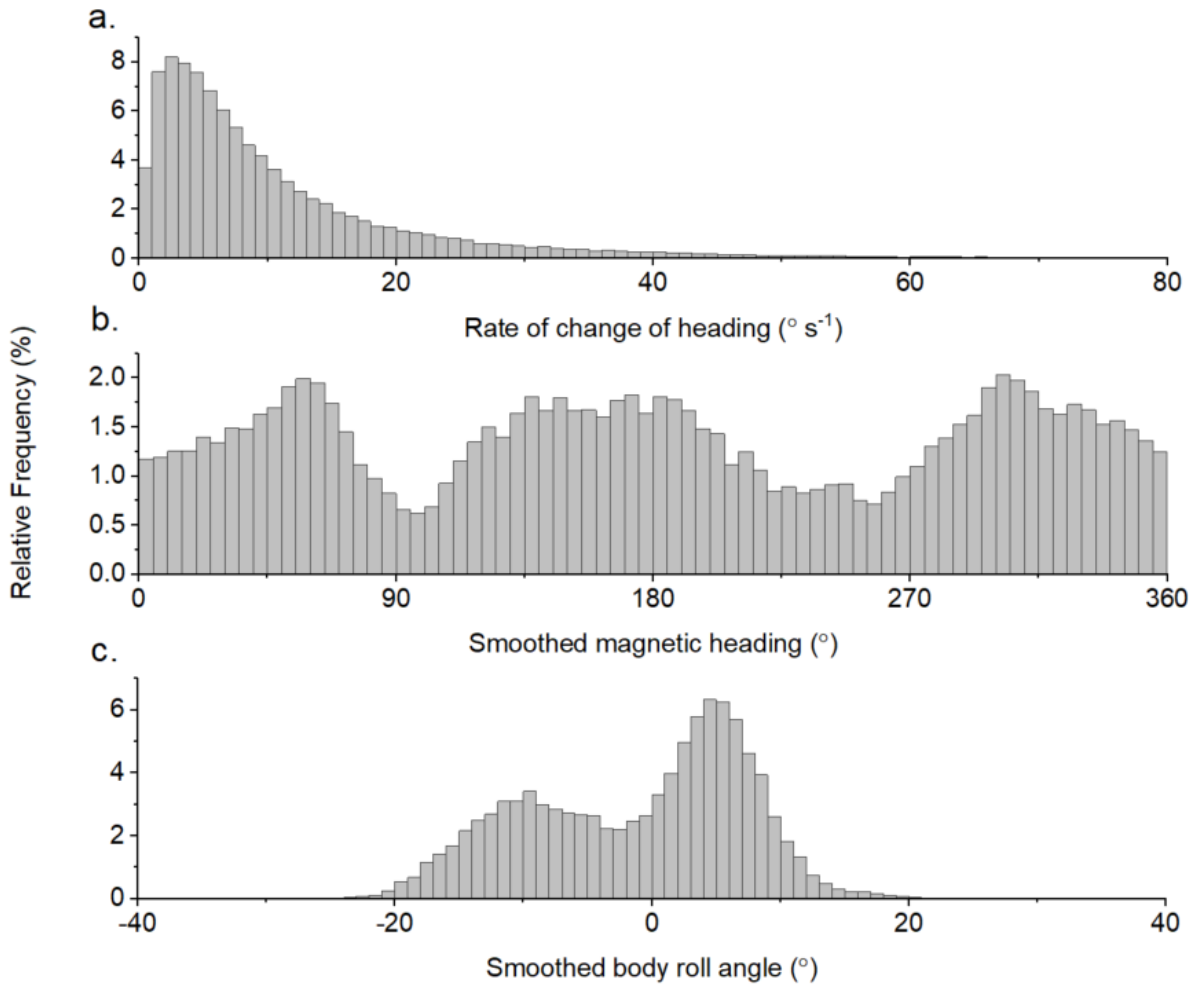

Figure 18. Frequency distributions of extracted data for TS16 during Behaviour H. a) Rate of change of heading (° s^{-1}) has values as high as 179.8° s^{-1}. b) Magnetic heading (°). c) Body roll angle ranged between -68.9° and 64.7° but rarely exceeded a roll of 20° either side. Metrics smoothed over 2 s.

Patterns across individuals

The extracted Behaviour H data identified that the rate of change of heading (figure 29a) mostly remained below 5° s^{-1} and always remained below 50° s^{-1} for all sharks except TS17, which had a maximum rate of change of heading value of 179.8° s^{-1}. The smoothed

VeDBA data mostly remained below 0.1 *g*, although all sharks exceeded this value (as particularly shown by the upper extreme quartiles in figure 29b). Figure 22c shows that the sharks spent very little time with straight headings, the rest of their time was spent continually changing heading. The faster rates of change of heading seen in figure 28a implied faster turns. However, the distributions of this metric (example shown in figure 28a) suggest these higher values were an infrequent occurrence for all sharks.

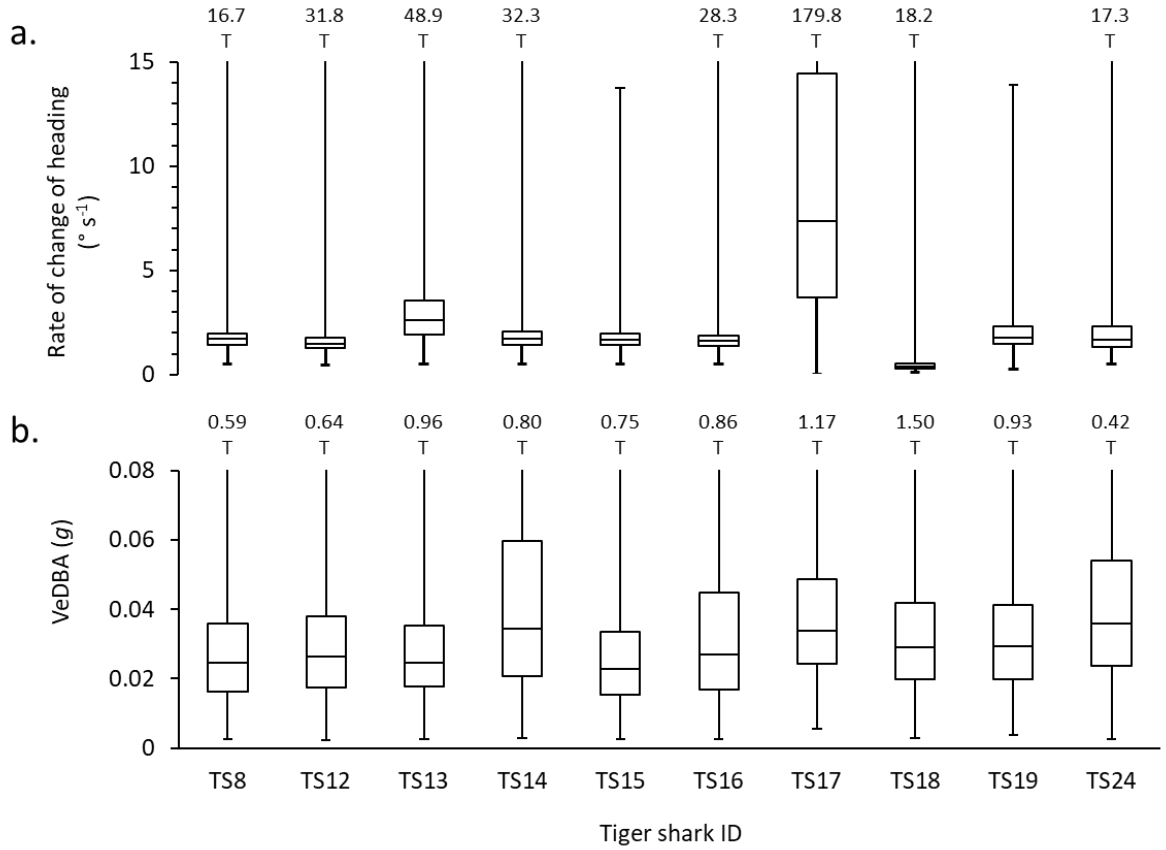

Figure 19. Comparisons of extracted a) rate of change of heading (° s^{-1}) and b) VeDBA (g) data between sharks during Behaviour H (horizontal lines show medians, boxes quartiles and whiskers limits). Metrics smoothed over 2 s. No ethogram for Behaviour H is presented as time dedicated to this behaviour is the recorded time remaining after Behaviour F had been removed (figure 22c).

Behaviour I – 'Circling'

Key metrics

'Circling' was characterised by regular oscillation in all three magnetometer axes and forward motion with systematic change across the full 360° magnetic heading, in either clockwise or anticlockwise direction. Numerical metric limits were not defined due to the variation in occurrences between individuals and instances. Variation in the depth differential

was also sometimes observed during this behaviour between occurrences and individuals. Some occurrences showed no change in depth (in some instances, the rate of change of depth revealed oscillatory fluctuations), whilst others demonstrated a continuous descent or ascent.

Example behaviour

'Circling' was observed at least once in six out of the 10 sharks' tag data. A birds-eye-view of the dead-reckoning track of TS13 shows that she completed eight full clockwise circular movements over a span approximately nine minutes and 23 seconds (figure 30). Figure 31 gives a three-dimensional view of the dead-reckoning track, which illustrates that TS13's depth steadily decreased from 25.16 m to 52.28 m whilst exhibiting this behaviour. However, this was not necessarily the case for all instances of this behaviour. The mean rate of change of depth during this example activity was 0.01 m s^{-1} (±0.01) and the mean smoothed body pitch angle was 7.7° (±7.1).

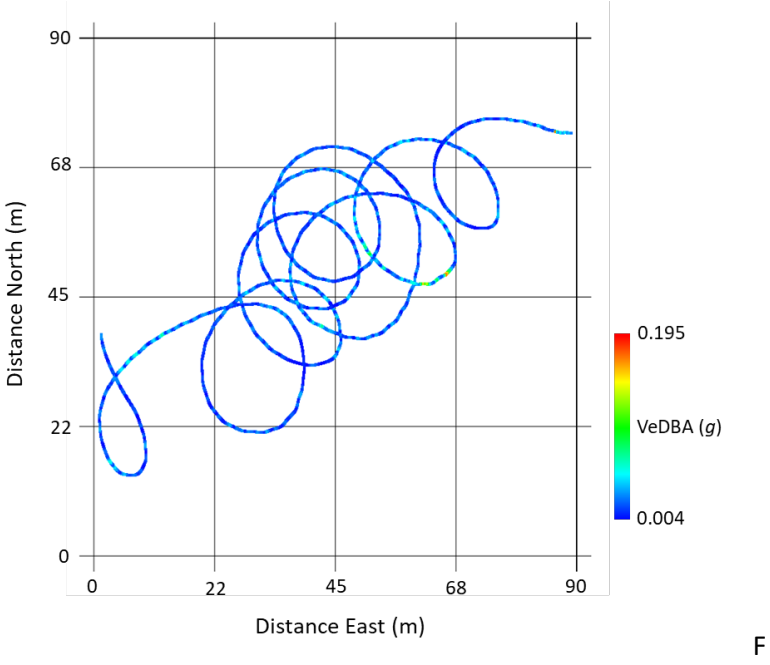

Figure 20. A birds-eye-view dead-reckoning plot from TS13 created in DDMT illustrates the pattern of movement of Behaviour I.

The VeDBA values (represented by the track colour and explained by the colourmap key) remained relatively low and had a narrower range and smaller maximum value than seen when all descents behaviours were combined within a frequency distribution in figure 4c. The mean VeDBA during the example of Behaviour I in figure 31 was 0.023 ±0.014 *g,* whereas the mean VeDBA from TS13's combined descent data (Behaviour A) was 0.031 ±0.029 *g.*

Although these figures overlap somewhat, it suggests that less acceleration was utilised during Behaviour I, than other circumstances of descent.

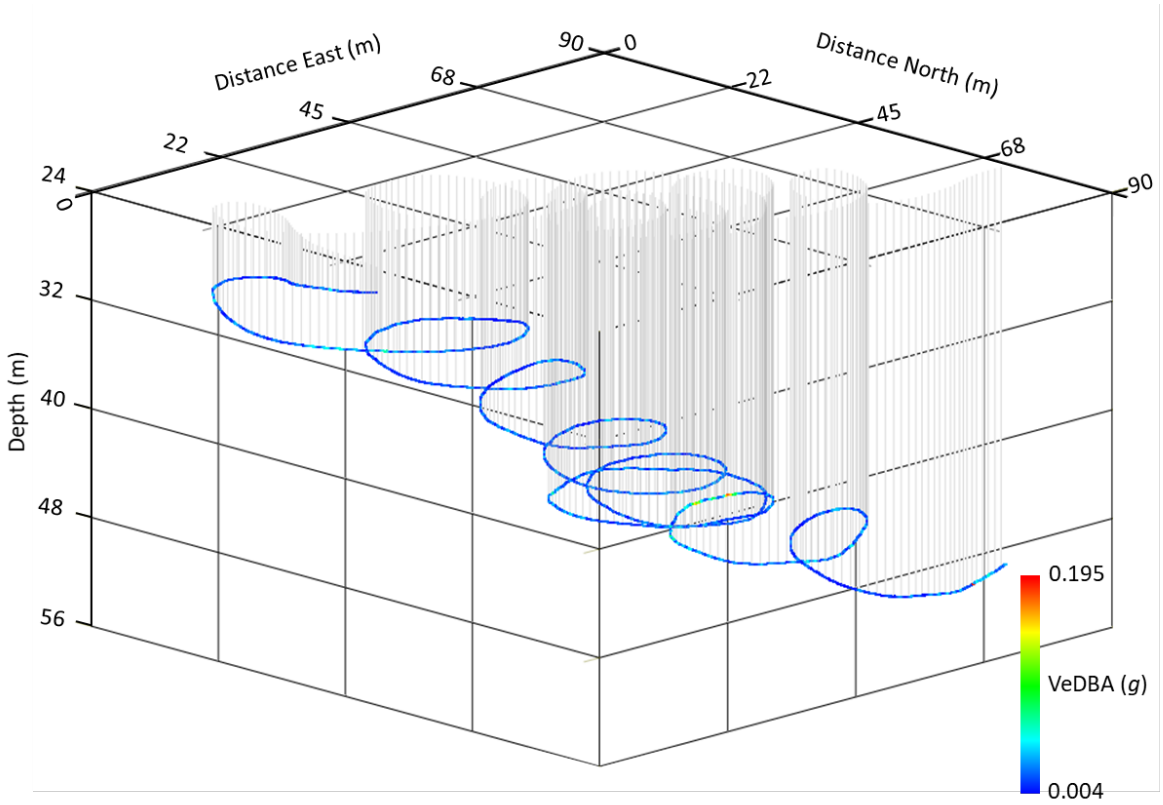

Figure 21. A three-dimensional dead-reckoning track of the downward-circling movement of Behaviour I from the data of TS13.

Figure 32 displays time series plots of a similar but separate Behaviour I event to that shown in figures 30 and 31, but again from TS13. This behaviour spanned 188 s, during which time TS13 performed 11 anticlockwise complete circles. Without looking at the dead-reckoning track, the sine-wave patterns are evident in all three magnetometry axes (figure 32a) and are the most distinct feature within the data. A distinct pattern is not present in the acceleration axes associated with data recorded by the triaxial accelerometer for this behaviour (figure 32b). The smoothed surge (acc *x*) axis remained mostly negative between 0 and -0.3 *g*, and occasionally rose into positive values. This corresponds to the body being angled slightly downward, with a mostly negative body pitch angle (figure 33e) to assist the gradual descent seen in figure 33d. The smoothed sway (acc y) axis showed a similar range and fluctuation of acceleration to the surge axis. The minor fluctuations may have been caused by slight adjustments to movement using tailbeats to maintain the behaviour. The mostly negative values

suggest that TS13 was banking to one side into the turn, during this activity. The heave (acc *z*) axis experienced very little change and showed that the shark was not completely level, which corresponds to the shark banking slightly into the turns.

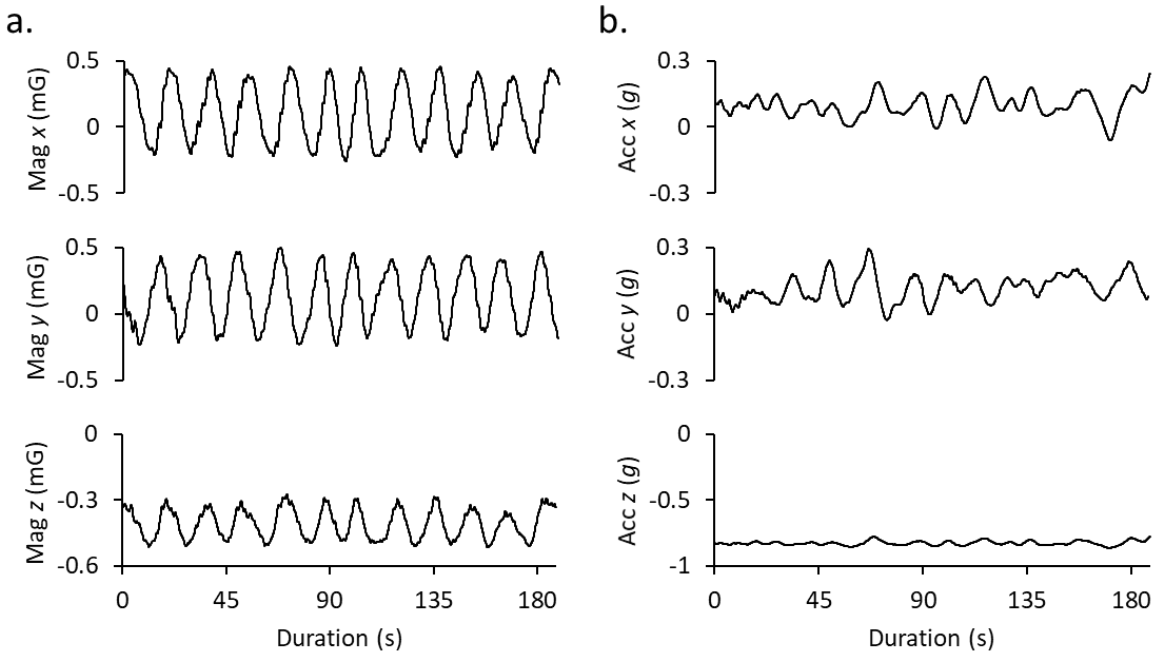

Figure 22. Time series plots illustrating the key features of Behaviour I within recorded metrics, including a) magnetic field intensity axes x, y and z, b) acceleration axes x (surge), y (sway) and z (heave) from the data of TS13. Metrics smoothed over 2 s. This tag was fitted upside down and, indicated by the inverted acceleration data is inverted and appears along the opposite axis. An acceleration z axis value close to -1 g would imply that TS13 was almost completely upside. This is unlikely as tiger sharks can experience a state of tonic immobility when inverted in this way (Holland et al., 1999; Kessel & Hussey, 2015). The acceleration data is interpreted as though it has been inverted onto the opposite axis.

Behaviour I is immediately evident in the magnetic heading data (figure 33a). In this example, the derived heading data shows that TS13 was circling in an anti-clockwise direction. Over time, the heading passed through to 359° from 000°, an indication that the shark's heading crossed magnetic North. The derived values then began to decrease back to 000° and the cycle would repeat. The rates of change of heading (figure 33c; mean -4.3° s^{-1} ±1.3) and smoothed body roll angles (figure 33f; mean -7.9° ±5.3) were mostly negative, due to the anticlockwise nature of the circles. In this case, faster rates of change of heading were observed when TS13's heading approached approximately 180°. This indicated that some sections of the circles were turned at faster rates than others. Although the VeDBA remained fairly constant (figure 33b; mean 0.05 *g* ±0.02), peaks were observed at similar intervals to the increases in the rate of change of heading. This suggests that TS13 was employing more dynamic acceleration,

possibly to turn that section of the circle more quickly. The depth slowly increased throughout this activity (figure 33d; mean rate of change of depth of 0.008 m s^{-1} ±0.008), which corresponds to the mostly negative (smoothed) body pitch angle (figure 33e; mean -6.7° ±4.4).

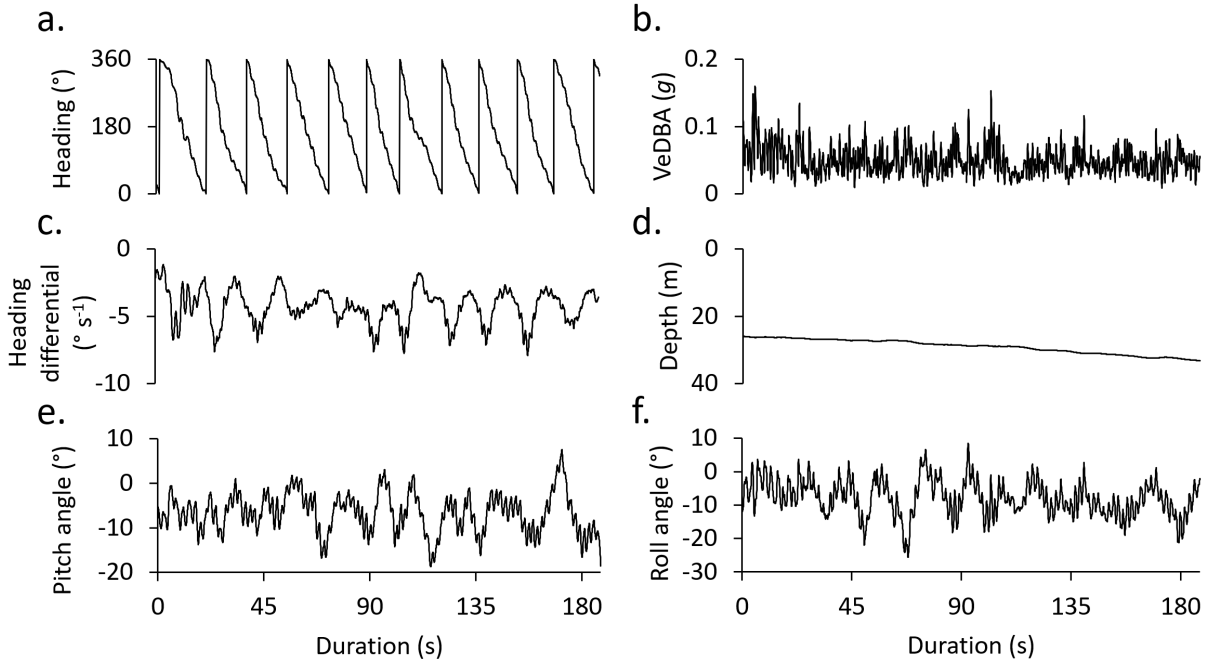

Figure 23 - Time series plots illustrating the key features of Behaviour I within derived metrics, including a) magnetic heading (°), b) VeDBA (g) c) rate of change of heading (° s^{-1}), d) depth (m), e) body pitch angle (°) and f) body roll angle (°). Metrics smoothed over 2 s.

Patterns across individuals

Information on patterns across individuals is not provided as an accurate search algorithm was not constructed within the current time, similarly to Behaviours E and I. This leaves open the opportunity for further development in the future.

Behaviour J – 'Sinusoidal swimming'

Key metrics

'Sinusoidal swimming' was characterised by regular oscillation around zero in the heading differential channel, although greater than the minor oscillations caused by tailbeats. Numerical metric limits were not defined due to the variation in the metrics of different occurrences of this behaviour.

Example behaviour

Behaviour J was picked up by the algorithm constructed for Behaviour H and included in the subsequent extracted data as rate of change of heading being greater than 0.5° s^{-1}. However, it is important to note that although this behaviour does involve constant directional change, it was much more uniform and often smoother than other general changes in direction. It presented a sine-wave-like pattern in several data channels, including the sway axis (figure 34). The sine-wave patterns occurred on a greater scale than the patterns caused by the sharks' tailbeats, which are still partially evident in the smoothed magnetic heading channel (figure 34b) and smoothed body roll angle (figure 34c). The characteristic sine wave patterns of Behaviour J are also clear in the smoothed sway (acc *y*) axis (figure 34b) and the magnetometer *y* axis data (figure 34e).

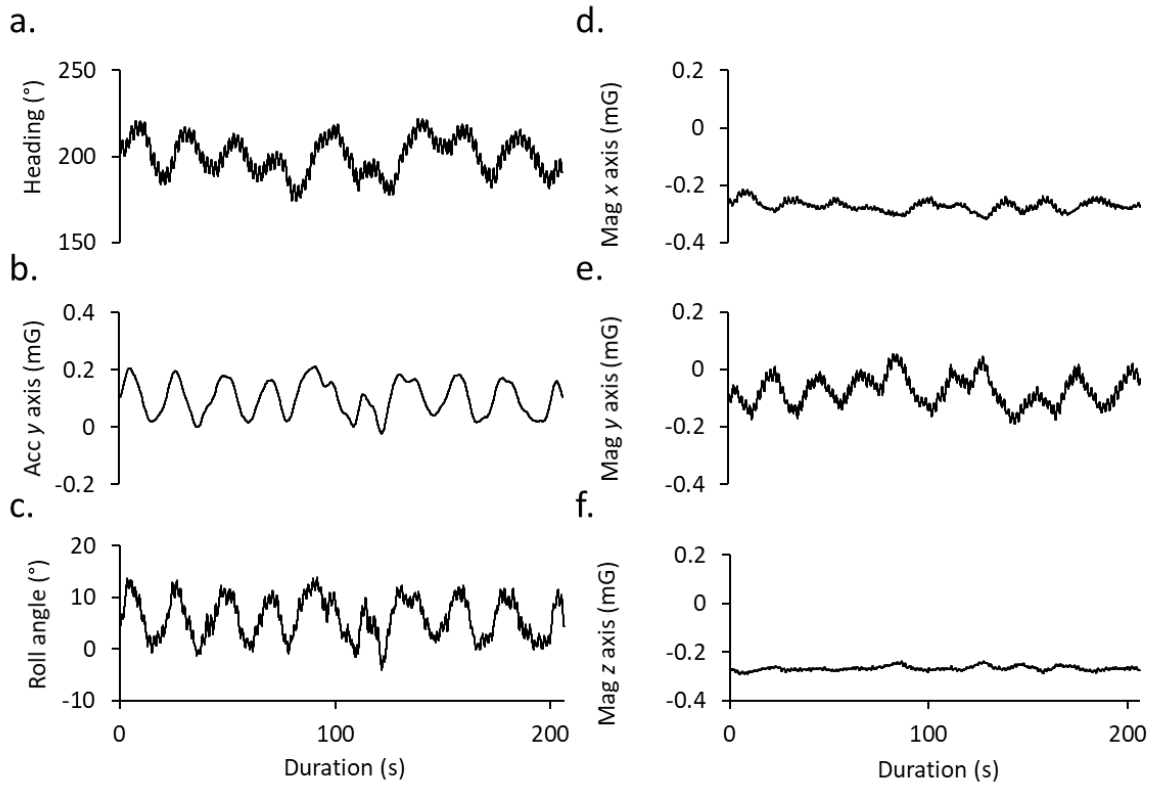

*Figure 24. Time series plots illustrating the key features of Behaviour J within recorded and derived metrics, including a) magnetic heading (°), b) sway (y) acceleration (*g*) c) body roll angle (°), d) magnetic field intensity x axis (mG), e) magnetic field intensity y axis (mG) and f) magnetic field intensity z axis (mG). Metrics smoothed over 2 s, except for a).*

Behaviour J was observed in all the sharks' tag data. The example graphed in figure 34 spanned 206.25 seconds, the wavelength of magnetic heading was approximately 20 s and the amplitude was approximately 40°. However, the length of other occurrences of this behaviour varied, as did the amplitude and wavelength of the sine waves produced in the recorded and derived data between occurrences and individuals. This made it particularly difficult to set defined limits within the data to construct an algorithm that would successfully extract all Behaviour J occurrences. Within the current time, I was unsuccessful in constructing such an algorithm.

BEHAVIOUR SUMMARIES

All identified behaviours are summarised below (table 3).

Table 3. The behaviours of G. cuvier identified from CATS tag data using DDMT software, mostly described using quantifiable metrics that allow behaviours to be detected in other tag data using algorithms input into DDMT's BB.

Behaviour	Key features
A	**'Descent'** of the water column was manifest by a continuous increase in depth and pressure. Rate of change of depth was > 0 m s^{-1} for > 3 s. Pitch angle was also commonly < -5°. Frequency distribution plots showed a continuum in the rate at which these sharks descended, instead of uni- or multi-modality. Descent varied between powered or glided although both could occur within the same descent. A steeper negative pitch angle (°) was accompanied by a faster rate of change of depth, suggesting a relationship between the two metrics. Descent could occur simultaneously alongside Behaviours F, G, H, I & J.
B	**'Ascent'** of the water column was manifest by a continuous decrease in depth and pressure. The rate of change of depth was < 0 m s^{-1} for > 3 s and the pitch was mostly > 5°. Frequency distribution plots showed a continuum of modality. Ascent could occur simultaneously alongside Behaviours F, G, H, I & J.
C	**'Horizontal swimming'** was defined when the rate of change of depth was equal to 0 m s^{-1} for > 3 s. Pitch usually ranged between -5° < pitch < 5°. Horizontal swimming could occur within Behaviours D, F, G, H, I & J.
D	'**Surface swimming**' was defined to have occurred at a depth of < 1 m for > 3 s, during which time, increased VeDBA values were observed in all individuals. Surface swimming could occur within Behaviours A, B, C, E, F, G, H & J. Sharks were not seen participating in Behaviour I at the surface.
E	'**Undulatory swimming**' was defined as a regular oscillation around zero in the rate of change of depth channel. Three-dimensional dead-reckoning of this behaviour showed this as a repetition of descents and ascents, smaller in scale than 'deeper' dives.
F	'**Straight swimming**' was defined when there were periods of forward movement with a steady or slow-changing heading and no major directional changes (an absolute rate of change of heading of < 0.5° s^{-1} for > 3 s). Due to the minor sinusoidal heading fluctuations (caused by tailbeats) present in the heading differential channel despite smoothing (80 events, 2 s), the rate of change of heading was not considered to be 0° s^{-1} during this activity. Straight swimming could occur within Behaviours A, B, C, D & E.
G	'**Burst power**' was defined by the rate of change of VeDBA rapidly increasing above 0.03 *g* s^{-1}, for varied time periods. Some bursts were singular and short-lived, others lasted longer or were a series of bursts in close succession. Burst power periods were accompanied by an increased amplitude and decreased period in tailbeat curves. Burst power events could occur during Behaviours A, B, C, D & H.
H	'**Direction change**' was indicated by any instance in which the shark was not swimming with a straight heading described by behaviour F. Direction change (or turn) had a rate of change of heading > 0.5° s^{-1} for > 3 s in the smoothed heading data. Directional change could occur during all behaviours, except for Behaviour F.

I	'**Circling**' was characterised by regular oscillation in all three magnetometer axes and forward motion with systematic change across the full 360° magnetic heading. Variation in the depth differential was also sometimes observed during this behaviour between occurrences and individuals. Could occur during Behaviours A, B,
J	'**Sinusoidal swimming**' was characterised by regular oscillation around zero in the heading differential channel, although greater than the minor oscillations caused by tailbeats. During some occurrences, there was minimal change to depth but Behaviour I was also observed occurring alongside Behaviours A, B & D.

After presentation, the recognised behaviours are also labelled alphabetically in a decision tree, constructed using the descriptive metric limits set within the algorithms for defining the behaviours. For the purpose of this simplified decision tree, all behaviours are described as if they occur in isolation, although two or more could also occur simultaneously (table 3).

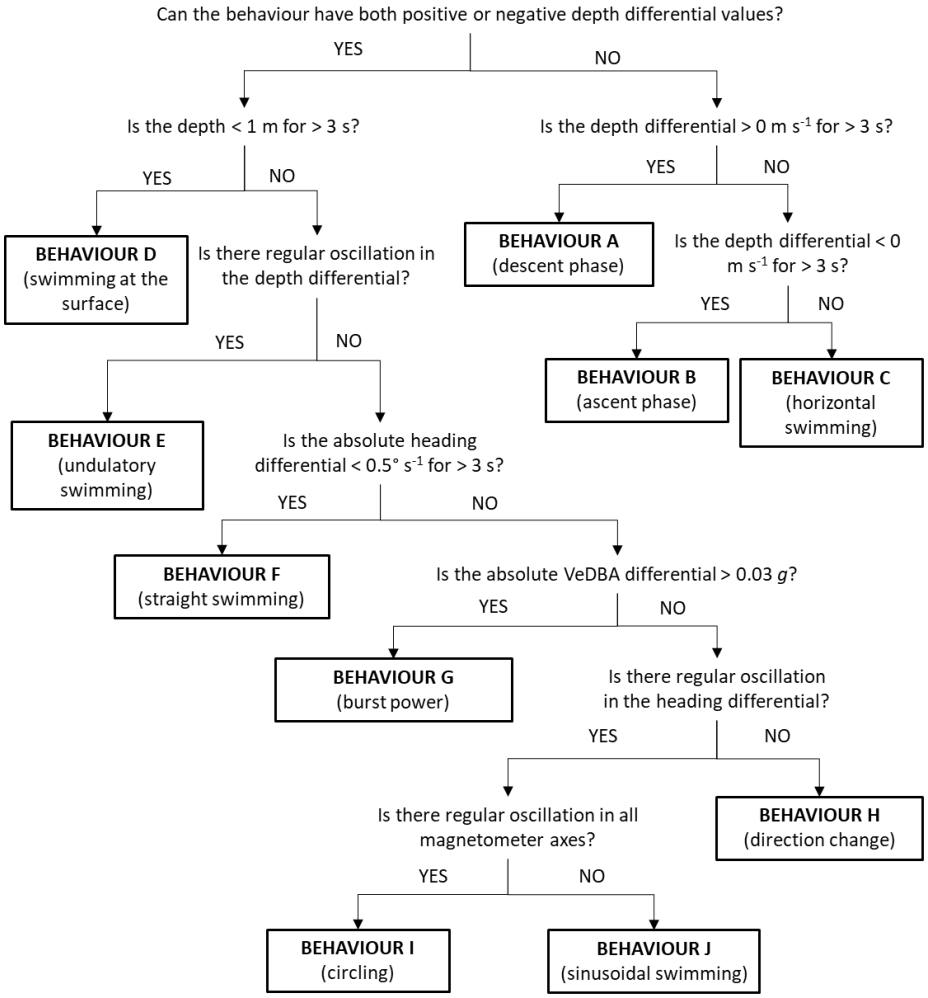

Figure 25. A decision tree differentiates the identified behavioural categories based on the key derived metric limits that quantify and define them.

DISCUSSION

The use of biologging tags and the inspection of the high-resolution data they record is akin to observing the movement and behaviour of free-roaming animals in their natural environment. However, the influence that observer presence or captive habitat conditions may have on the normal performance of any animal is removed. This technique of recording behaviour from the animal's perspective also removes our own visual bias, as well as any bias towards behaviours that are caused by baiting or more commonly occur at the surface or (Heithaus *et al.,* 2002) by measuring metrics inaccessible by visual observation (Ropert-Coudert & Wilson, 2005; Ellwood, Wilson & Addison, 2007).

Despite the use of multichannel biologging tags being the norm for the study of animal biotelemetry today (Ropert-Coudert & Wilson, 2005), to the best of my knowledge this is the first piece of work attempting to identify the behaviour of tiger sharks solely from human inspection and interpretation of animal-attached tag data, without using field observations or camera footage as a reference to confirm or the aid of ML. While seemingly complex, the process of inspection of multi-sensor data is, in essence, no different from what people do when they watch an animal in the field and classify behaviours – typically concentrating on patterns in body part movement and travel through space. Thus, the process I have adopted is essentially no different from that adopted for classifying behaviour over decades (e.g. Tinbergen, 1960). I note that ML has been successfully used to detect and categorise patterns in accelerometer data to separate animal behaviours in numerous studies (e.g. Sakamoto *et al.,* 2009). However, supervised ML requires training data of behaviours already described using data derived from observed animals wearing tags (Nathan *et al.,* 2012), which is obviously problematic for identifying behaviours that are difficult or impossible to observe naturally (Wang *et al.,* 2019). Whilst unsupervised ML can detect and categorise patterns in the data of potentially unseen behaviours without the aid of training data (Valetta *et al.,* 2017), the algorithms cannot interpret these categories and explain them in behavioural terms. This requires human interpretation of the data to understand and communicate what the animal is doing.

Humans possess the capacity to detect highly complex regular and irregular visual patterns (Zeki *et al.,* 2008) and are therefore more than capable of detecting patterns within triaxial accelerometer data. This work aimed to 'cut out the middleman' and identify and categorise movement patterns in acceleration data, without the aid of ML. It was successful in that 10 behaviours were identified and described *via* human understanding and interpretation of triaxial accelerometer data based on visualizations. Furthermore, defined numerical limits

within recorded and derived metrics were set for some of the behaviours, which allowed the construction of algorithms using BB to sift the data and extract repetitions of the behaviours. Although algorithms were not constructed for some of the more complex behaviours within the available time frame, it is certainly possible. For the behaviours for which BB algorithms constructed, data was extracted and used to produce ethograms and frequency distributions to assess time allocation for each behaviour and modality of metrics within them. Below, I describe what the data suggests the sharks are doing during each behaviour and their potential functions in a natural setting.

Behaviours A, B, E & J

During descents, the downward angled posture of the sharks produced negative surge values and thus, DDMT derived mostly negative body pitch angles from this data. Consequently, there was a sustained (longer than 3 s) increase in depth, which made descents easily identifiable by searching for periods in the data with rates of change of depth greater than 0 m s^{-1} (figure 3c). The direct opposite was observed for Behaviour B (ascent). Surge acceleration values were positive, as were the body pitch angles and a sustained decrease in depth occurred. Therefore, to identify ascent periods, rate of change of depth values less than 0 m s^{-1} occurring consecutively for longer than 3 s were searched for, marked and extracted. Only periods sustained for longer than 3 s were accepted to avoid the inclusion of data recorded due to noise or tag disturbance. The peaks in VeDBA (figure 3b) suggested the sharks occasionally used power to assist the descent, instead of solely gliding to reserve energy as would be expected (Gleiss, Norman & Wilson, 2011). In figure 10, the higher frequency and greater amplitude of tailbeats during ascents than descents implied that the shark was employing greater dynamic acceleration more quickly, probably to counteract its negative buoyancy and rise through the water column.

The continuum of data within the distributions for all the sharks' data implied that there was no clear distinction between gliding and powered modes during both descents (figure 4) and ascents (figure 7). However, without the ability to extract the finely resolved behaviours, it would have been possible to extract larger periods of data and assess the frequency distributions to assess what modes were present. All rate of change of depth (figure 26a) and body pitch angle (figure 26b) data were extracted from TS8. The frequency distributions show a clear divide between two modes around zero within these metrics, identifying bi-modality

within them and demonstrating why they were separated into two separate behaviours in this work (up and down, essentially).

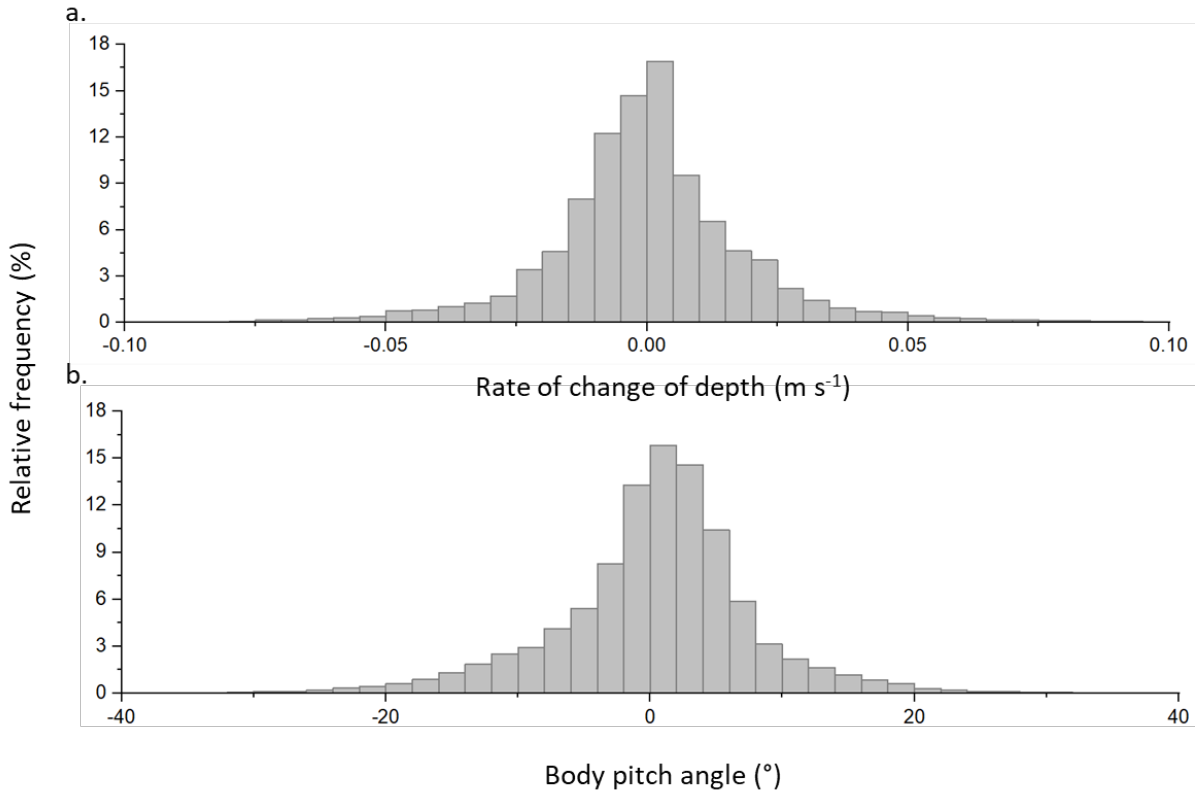

Figure 26. a) The rate of change of depth (smoothed over 2 s) data extracted from the entire data file of TS8. Extreme values were cut off at -0.1 and 0.1 m s^{-1} due to much lower relative frequencies but reached a minimum value of -0.19 m s^{-1} and a maximum of 0.22 m s^{-1}. Negative values represent a decrease in depth and positive values represent an increase. b) Body pitch angle (smoothed over 2 s) data extracted from the entire data file of TS8. Extreme values were cut off at -40° and 40° due to much lower relative frequencies but reached a minimum value of -55.6° and a maximum of 77.2°[1]. Negative values represent downward pointing postures and positive values represent upwards pointing postures.

Furthermore, this is a relatively small sample of data from only 10 individuals and without being able to easily separate other behaviours that involve descent, such as circling descent or undulatory swimming, it is currently not given the extent to which these different behaviours within descent contribute differentially to the continuum distribution. There was certainly variation in the rates of change of depth used by individuals (figures 5a and 8a), for whatever reasons (presumably a result of environmental context (Bestley *et al.,* 2013)). All sharks spent a large proportion of time descending and ascending through the water column executing the yo-yo diving behaviour (see Nakamura *et al.,* 2011) and very little time at a maintained depth (figures 5b and 8b), possible reasons for which are discussed below.

Energy management and conservation are critical to survival (Roth II, Rattenbourg, & Pravosudov, 2010) and therefore, to reproductive success (Pianka, 1976). It was suspected that the sharks would utilise their negative buoyancy to glide during descents, as seen in whale sharks, *Rhincodon typus* (Gleiss, Norman & Wilson, 2011), to minimise energetic costs of travel. Weihs (1973) predicted that energy conservation of up to 50% was possible by negatively buoyant fish oscillating between gliding descents and powered strokes to ascend back to their original depth. However, the sharks in this work were regularly observed using power strokes during descent phases manifest by uniform peaks and troughs in the sway axis indicating regular tailbeats. Heithaus *et al.* (2002) also observed tiger sharks powering during descents using animal attached 'Crittercam' video recordings and Nakamura *et al.* (2011) found only 50% of studied sharks glided during descents, which accounted for <18% of total descent time.

Mean smoothed VeDBA values were expected to be lower during descents than ascents if the sharks had in fact glided during descents and required less dynamic acceleration. However, they were found not to be significantly different (see results). This fact, alongside the presence of powered strokes in the sway axis during both descents and ascents, suggests that similar acceleration levels were utilised for both behaviours on average.

In tandem with this, the mean body pitch angle during descents was –7.1° (±8.3), and the steepest recorded descent angle was -87.8° (TS13). The mean body pitch angle during ascents was 6.1° (±6.1), and the steepest recorded descent angle was 85.7° (also TS13). Although the mean descent values are relatively shallow, much steeper values were expressed by all sharks. This is not consistent with shallow pitch angles expressed by other species of negatively buoyant fish utilising powerless descent to increase energetic efficiency (Kawabe *et al.,* 2004). Whale sharks adhere quite rigorously to a gliding descent, powered ascent regime, with corresponding VeDBA data (Gleiss, Norman & Wilson, 2011), which is symptomatic of animals operating on a tight energy budget feeding on essentially immobile prey (plankton (Gleiss *et al.,* 2013)). Tiger sharks must catch large, fast and agile prey (Drymon *et al*., 2019; Simpfendorfer, Goodreid & McAuley, 2001; Dicken *et al.,* 2017), thus requiring them to have a strategy that allows them to move rapidly in a 3D space. Therefore, they would be expected to have a much more dynamic, and less energetically optimal, movement strategy than plankton feeders.

Chum salmon were found to be negatively buoyant during vertical movements through the water column, despite the presence of a swim bladder (absent in elasmobranchs) (Tanaka, Takagi & Naito, 2001). Accelerometer data showed that the salmon descended faster, at much steeper angles than when they ascended and tailbeat frequency and amplitude was higher during ascents, suggesting more energy was spent during ascent phases. The purpose of the salmons' diurnal vertical movements during migration to spawning grounds was attributed to differences in geography, hydrographic features, physical condition or reproductive strategy (Tanaka, Takagi & Naito, 2001). Although the pitch angle gradients appear relatively similar between descents and ascents for the tiger sharks (unlike the chum salmon), figure 10 suggests that tailbeats were faster and more intense during ascents than descents like the chum salmon.

When inspecting the data of all 10 sharks, it was clear that *G. cuvier* frequently descend and ascend repetitively, creating what has been coined 'yo-yo vertical movement' (Nakamura *et al.,* 2011). Behaviour E (undulatory swimming) also consisted of uniformly alternating vertical movements. Although this behaviour was detected by the algorithms constructed to extract Behaviours A and B, it has also been described as a separate behaviour (Gleiss *et al*., 2011). This is because the data exhibited much smoother and smaller scale oscillations in depth that could occur during any phase of the deeper dives observed, as well as during horizontal movements. This distinction between deeper dives and oscillations with smaller amplitudes was also observed by Holland *et al.* (1999) with Gleiss *et al.* (2011) pointing out that movement using small vertical oscillations is an energetically efficient mode of locomotion in fluid media.

Behaviour J (sinusoidal swimming) presented a similar oscillating pattern as Behaviour E however, the oscillations occurred in the sway axis, rather than the surge. In other words, the sharks were also exhibiting a regularly oscillating lateral movement, on a larger scale than that produced by tailbeats. Such lateral oscillations are more difficult to explain than vertical oscillations because there is no energetic advantage to them. Rather, straight-line swimming is the most energetically efficient (Wilson *et al.,* 2013) and so, the costs of these oscillating three-dimensional movements must offset the benefits of energetics savings. I suggest that the particular pattern might be due to 'trail following', whereby animals follow a scent whilst moving laterally (and vertically in a three-dimensional environment) up an odour plume to hone in on the source (Vickers, 2000). Certainly, sharks have particularly sensitive smell receptors (Yopak, Lisney & Collin, 2015) and odour following has been documented widely in them (e.g. Tucker *et al.,* 2019; Gardiner & Atema, 2007; 2010).

Overall, it is perhaps relevant Nakamura *et al.* (2011) concluded that energy conservation was unlikely to be the primary objective of this 'yo-yo' swimming pattern, but rather a method for expanding the searched area throughout water column for potential prey. Although there are other proposed theories, such as behavioural thermoregulation and navigation (Carey, Scharold & Kalmijn, 1990; Klimely, 1993), tiger sharks are generalist and opportunistic feeders that exploit easily captured prey within their current habitat (Lowe *et al.,* 1996). When foraging in deeper waters across distances of a few to hundreds of kilometres, marine predators are less likely to rely on sensory information from proximal cues (e.g. vision) and become more probabilistic hunters that depend on an optimal search strategy to maximise prey encounters (Sims *et al.,* 2008). Some of these movements have been classified as Lévy walks (Shlesinger, Zaslavsky & Klafter, 1993). Thus, these swimming modes combined potentially represent a three-dimensional foraging strategy to increase the likelihood of detecting visual and olfactory cues to maximise encounter rates with sparsely distributed prey whilst travelling throughout the water column (Carey, Scharold & Kalmijn, 1990; Bres, 1993; Nakamura 2011; Sims *et al.,* 2008; Sims, 2010). This suggests that the potential gain of increased prey encounter rates outweigh the energetic 'inefficiency' of these swimming modes.

Behaviour C – Swimming at a maintained depth

The algorithm constructed for this behaviour only detected a very small proportion amongst only two of the sharks' tag data (figure 16b). The tiger sharks evidently spent a large proportion of time making horizontal movements through the water column during their descents and ascents and so swimming at a maintained depth was likely to be less common. It could also be due to tag disturbance making a depth differential reading of 0 m s^{-1} less likely, in which case an adjustment to the algorithms would be required. Despite this, tiger sharks do appear to spend periods of time swimming at relatively horizontal invariable depths at times (e.g. swimming along the seabed or at the surface) and I propose that the algorithm used here was too exact by searching for sustained periods where rate of change of depth remained at 0 m s^{-1}.

The reason for such an exact figure was to prevent overlap with Behaviours A and B, however it does not allow for possible disturbance to the tag despite a relatively unchanged depth. For example, figure 14a shows one of the sharks swimming at a relatively constant depth at the surface, but with many minor fluctuations in depth. This is likely a result of swimming in a fluid medium, in a high drag area with increased wave amplitude, which is registered by the depth sensor. Periods where this is speculated to have occurred were not detected by the

current algorithm. Future development of this work would investigate construction of an algorithm that accounts for minor depth fluctuations occurring during periods of relatively unchanged depth, without overlapping with descent and ascent behaviours.

Behaviour D – Swimming at the surface

The smoothed VeDBA rose above 0.03 *g* whilst swimming at depths of <1 m. Andzrejaczek *et al.* (2019) had similar findings of increased ODBA values when tiger sharks swam at the surface and attributed the increased acceleration values to wave action (ODBA and VeDBA can be considered synonymous (Wilson et al. 2020)). Yoda *et al.* (1999) found that it was energetically cheaper for Adélie penguins to dive deeper than necessary between breaths, than to swim close to the surface due to increased surface drag forces caused by wind, waves and currents. Thus, it is possible that the tiger sharks required increased dynamic acceleration to overcome greater friction forces whilst swimming within the high-drag layer, hence the greater smoothed VeDBA values expressed at the surface. If the increased VeDBA associated with surface swimming is a genuine manifestation of effort (Gleiss *et al.,* 2010) rather than an artifact due to wave motion affecting the tag stability (cf. Wilson *et al.* 2020; Lear, Gleiss & Whitney, 2018) then, as with the apparently non energetically optimal yo-yo diving, the question is why sharks should swim so close to the surface anyway.

Only six of the 10 sharks displayed periods of swimming at the surface. Three of these sharks spent relatively little time (< 15%) swimming at the surface compared to the other three (> 25%), possibly because it is more energetically taxing due to the increased drag forces (Yoda *et al.,* 1999). Also, swimming at the surface would reduce their ability to visually detect silhouettes of air-breathing prey (e.g. sea turtles), as well as the effectiveness of their camouflage to prey positioned above them (Heithaus *et al.,* 2002). However, tiger sharks are opportunistic predators (Lowe *et al.,* 1996) feeding on benthic, as well as pelagic and surface prey. Their white ventral colouration in beneficial when hunting prey that is beneath them (i.e. pelagic or benthic) as it reduces silhouette produced by downwards sunlight (Heithaus *et al.,* 2002) and so, positioning to reduce the likelihood of being detected by benthic prey may force them towards the surface. Also, stomach contents have frequently revealed the consumption of seabirds (Drymon *et al.,* 2019), as well as visual accounts of tiger sharks actively hunting seabirds at the surface of the water at several different locations globally (Meyer, Papastamatiou & Holland, 2010; see *South Pacific*, 2009 for example). Furthermore, they are known to be facultative scavengers, feeding on floating whale carcasses for example (Clua *et*

al., 2013). Therefore, it is possible that the tiger sharks were swimming to the surface to scavenge on floating animal carcasses or to capture potential prey floating on or breathing at the surface and the energetic gains accrued from this strategy outweigh the increased movement costs.

Behaviour F (straight course swimming) & Behaviour H (directional change)

Several species of shark including scalloped hammerhead sharks, *Sphyrna lewini* (Klimely, 1993) and tiger sharks (Holland *et al.,* 1999) have been described to swim with highly directional or straight-line horizontal courses. For example, using acoustic GPS tracking tags, Holland *et al.* (1999) recorded three sharks making very similar direct tracks to the same location following release. However, the sharks observed in this work spent relatively little time swimming with straight paths (figure 23c), despite it being the most energetically efficient form of horizontal travel (Wilson *et al.,* 2013). Heithaus *et al.* (2007) suggested that sharks travelling between home ranges would exhibit straight course swimming, whilst sharks restricting their movement within a home range would demonstrate less straight-line movement. Perhaps during the period the tags (mean 20 h 34 min, range 13 h 48 min to 48 h 44 min) were attached to the sharks, they had restricted their movements to a particular home range within Ningaloo Reef and thus displayed less straight-line courses.

Furthermore, although Holland *et al.* (1999) described tiger sharks' movements as highly directional in offshore waters, they also observed frequent turning and looping in the tracks of tiger sharks whilst they were in shallow waters of <300 m. None of the sharks observed in this work exceeded depths of 100 m during the time the tag was attached, which could explain why their dead reckoned tracks were highly tortuous and lacked longer periods of straight course swimming. This tortuous swimming behaviour has been observed prior to, and is associated with, prey investigation by tiger sharks (Andrejaczek *et al.,* 2019; Heithaus *et al.,* 2007; Sims *et al.,* 2008). Thus, perhaps high tortuosity horizontal travel patterns contribute to prey capture success and offset the energetic costs of turning (Andrejaczek *et al.,* 2019), compared with straight-line swimming (Wilson *et al.,* 2013). Furthermore, studies that have reported longer periods of straight-line swimming and less tortuous tracks used GPS tracking tags that recorded over periods of weeks rather than days and declared that position fixes lacked temporal resolution (Holland *et al.,* 1999; Heithaus *et al.,* 2007). Therefore, they were more likely to observe long distance tracks between home ranges that required straight line swimming and detailed smaller scale tortuous tracks may have been less obvious.

Behaviour G – Burst swimming event

Burst swimming events were obvious amongst the data as sporadic periods in which all or most data channels recorded extreme values unlike those that were recorded immediately before or afterwards. As seen in figure 24, the rate of change of VeDBA rapidly increased, caused by increased tailbeat frequency and amplitude (visible in the raw sway axis). The raw and smoothed sway axes show the shark was swimming a course with relatively little lateral movement and almost undetectable tailbeats before the event. Then suddenly, some large lateral movements occur throughout the ~50 s event. Rapid postural changes are also seen in the surge and heave axes, as well in the three magnetometer axes.

Large tiger sharks, such as those studied here (266 to 380 cm TL), are unlikely to experience predation risk or interspecific competition (Heithaus, *et al.,* 2002). However, intraspecific competition resulting in spatial segregation of males within different size classes (Heithaus, 2001) or sexual segregation (male avoidance by females; Sims, 2003; Meyer *et al.,* 2014), could result in avoidance behaviour if conspecifics were to encounter each other. Thus, it is possible that these sporadic periods of increased dynamic acceleration and changes in swimming direction are a result of avoidance action taken by the sharks upon encountering a conspecific.

Another cause for burst swimming events could be prey investigations and/or capture. Andrzejaczek *et al.* (2019) observed burst, stalking and/or turning behaviours immediately preceding investigations of prey. Additionally, tiger sharks rarely engaged in prolonged high-speed chases due to limited manoeuvrability compared with highly vigilant prey (Heithaus *et al.,* 2002), which would explain why burst events observed in this data were brief. Nakamura *et al.* (2017) also observed bursts by tiger sharks in the presence of potential prey such as unicornfish, *Naso spp*. However, they also demonstrated that not all burst events were apparently related to the presence of prey using video footage in conjunction with acceleration data.

Behaviour I – Circling

This behaviour was evident from oscillation patterns in all the magnetometer axes and derived heading data, which also indicated whether the circular motions were clockwise or anticlockwise. In almost all occurrences, there was a gradual increase in depth during this circling behaviour, which was performed by six of the 10 sharks observed in this work although, frequency of occurrences varied between individuals. In a manner similar to

Behaviours E & J, due to variance in the oscillatory nature of the data channels, it was difficult to set defined limits that successfully detected all occurrences of this behaviour. Thus, an algorithm to detect this behaviour has not yet been constructed. However, its legitimacy as a behaviour is undoubted as it has been described in previous literature using other methods (Andrzejeczak *et al.,* 2018; Narazaki *et al.,* 2021).

Despite being ram ventilators and therefore obligate swimmers, it is unlikely that tiger sharks and other species alike have evolved to no longer require sleep (Kelly *et al.,* 2019), due to their extensive cognitive capabilities (Lisney *et al.,* 2012; Hart, Lisney & Collin*,* 2006). Furthermore, the evolutionary persistence of sleep across the animal kingdom (Rihel, 2020) and evidence for sleep-like behaviours in other, albeit buccal ventilating, shark species (Randall, 1977; Kelly *et al.,* 2020) make it unlikely for ram ventilating shark species to have entirely lost the need for it. Additionally, cyclic diel vertical migrations have been considered as evidence for endogenous circadian rhythm in several obligate swimmer species (see Kelly *et al*., 2019; Myrberg & Gruber, 1974). It is hypothesised that ram ventilating sharks such as tiger sharks sleep unihemispherically (Kelly *et al.,* 2019; Grainger *et al.,* 2022), whereby one hemisphere of the brain remains active whilst the other participates in non-rapid eye movement (REM) rest. It enables the eye neurologically linked to the awake side of the brain to remain open and monitor the individuals' surroundings (Lyamin *et al.,* 2002), whilst maintaining continuous swimming. Most cetaceans (Kelly *et al.,* 2019) and some other marine mammals sleep this way (Lyamin, Mukhametov & Seigel, 2004; Lyamin *et al.,* 2008; 2016). Within birds too, great frigatebirds, *Fregata minor,* have been observed soaring on rising air currents in a circling motion whilst engaged in unihemispherical asymmetric non-REM sleep with a single eye open. Depending on which side of the brain is asleep and which is awake, the birds have their open eye leaning in towards the turn and the asleep eye facing outwards (Rattenbourg *et al.,* 2016), possibly to avoid birds soaring in the same air mass. However, this behaviour could only be maintained for relatively short periods (<1 h per night; Rattenbourg *et al.,* 2019).

These tiger sharks were noted to be circling for relatively short periods (typically between 3-10 min) and in several cases their depth gradually increased throughout the behaviour. It may also be relevant to this that Ritter (2020) described a bull shark, *Carcharhinus leucas,* that drifted 'without control from tailbeats or fin movements' sinking at a steady rate of 0.1 m s^{-1} for a period of 120 s. Perhaps, when the tiger sharks were participating in these circling motions, they were exhibiting unihemispherical sleep. Instead of maintaining or increasing altitude on warm air masses like the figatebirds (Rattenbourg *et al.,* 2016), they were gradually

descending like the bull shark (Ritter, 2020) due to their negative buoyancy (Andrzejaczek *et al.,* 2019). However, it is impossible to say for sure whether this was the case from this data as the tags could not sense eye state, nor were they equipped with an electroencephalogram (EEG) to record electrical activity within the brain. Alternatively, circling behaviours occurring during the day at a maintained depth have been associated with foraging behaviours in tiger sharks (Narazaki *et al.,* 2021) and sandbar sharks, *Carcharhinus plumbeus* (Andrzejaczek *et al.,* 2018). It is also perhaps relevant that Meyer *et al.* (2018) used a shark-mounted video camera to document a male tiger shark approaching a female using circling motions for courtship.

Limitations

It is essential to acknowledge the limitations presented in this work, so that they can be improved upon in future research. Firstly, catch and release procedures come with risks to both animals and researchers (Gleiss *et al.,* 2009). No major deleterious effects on the sharks during capture and release were described by Andzrejeczak *et al.* (2019). However, due to tiger sharks being obligate ram ventilators and requiring a constant flow of oxygenated water over their gills (Tomita *et al.,* 2018), there is a risk of fatal suffocation when fastened alongside a stationary vessel (Kawatsu *et al.,* 2010). Gallagher *et al.* (2014) ranked tiger sharks as low risk from suffering reflex impairment, physiological stress responses and mortality following capture and release relative to four other studied shark species. However, they suggested that additional research was required. Drumlines equipped with baited hooks (used to capture the tiger sharks in this study) have resulted in mortality of sharks and non-target species when not checked frequently (Gribble, McPherson & Lane, 1998). However, the drumlines used in this study were checked hourly and no mortalities occurred. Nonetheless, some sharks had wrapped themselves amongst the lines and occasionally, hooks were broken when attempting to remove them from the sharks' jaws. Gleiss *et al.* (2009) successfully tagged 11 whale sharks (*Rhincodon typus*) without capture and restraint by swimming alongside the animals, although, this species is larger and considered less dangerous than tiger sharks.

Secondly, external animal-attached tags can have deleterious effects on animals, including abnormal behaviour and increased energy expenditure (Wilson, Shepard & Liebsch, 2008; Wilson & McMahon, 2006; Ellwood, Wilson & Addison, 2007). It is unknown to what degree (if at all) the tiger sharks' behaviours were altered by the CATS tags in this study, as determining this can be complex (Wilson & McMahon, 2006). Most of the data files began with chaotic changes in the recorded data channels, lasting no longer than a few minutes. These recordings may have occurred during tag attachment or be a result of fleeing or aberrant

behaviour following the release of the sharks. Ideally, tagging procedures would have minimal effect on the animal and its behaviour and further investigation into less perturbing techniques for both animals and researchers is recommended (Wilson & McMahon, 2006).

No magnetometer calibrations were made for the tags prior to deployment. Garde *et al.* (2022) demonstrated how tag type, placement, and calibrations (or lack thereof) affected the acceleration signal, which resulted in calculated DBA values varying up to 25%. Calibrations for the tags used in this study were subsequently made by eye in DDMT to correct any offset, however this made room for human error even though DDMT is a bespoke software originally designed to inspect data recorded via DD tags (Wildbyte Technologies, http://www.wildbytetechnologies.com/). The data used in this study was recorded using CATS tags (Customised Animal Tracking Solutions, https://www.cats.is/products/cats-diary/) and alterations were required to correct faulty imported calculations in the heading channel, possibly caused by the lack of magnetometry calibrations. As a result, accuracy of the derived metrics calculated in DDMT from the provided data cannot be fully guaranteed. Furthermore, some of the tags had been fitted upside down and the data of some recorded channels (e.g. acceleration axes) and derived channels had to be subsequently inverted. Kawatsu *et al.* (2010) discussed the discrepancies in pitch angle data when accelerometer attachment angles are not suitably calibrated. Sequeira *et al.* (2021) highlighted the importance of data compatibility, and so a standardisation of procedures for deployment and calibration, and tag characteristics could be adopted. For example, Wilson *et al.* (2020) recommended tags be placed onto the animal's main mass (i.e. the body trunk) and that position should remain constant between individuals. Fortunately, all tags used in this study were placed in a similar location at the base of each shark's dorsal fin (Andrzejaczek *et al.,* 2019). Despite the concerns with magnetometer and attachment calibrations (human error), the tags' small size relative to the size of the sharks results in small device induced error (DIE) and higher tag accuracy (Ellwood, Wilson & Addison, 2007), implying that the data recorded by the tag can be reasonably 'trusted'.

The tags used in this study recorded at a frequency of 20 Hz, however, Broell *et al.* (2013) recommended frequencies greater than 30 Hz, as detection probability for feeding and escape activities decreased by 50% when reduced from 100 Hz to <10 Hz during a study on great sculpin (*Myoxocephalus polyacanthoceaphalus*). However, great sculpins are significantly smaller in size than tiger sharks and have movements that are typified by higher frequency waveforms, thereby requiring higher sampling frequencies for sufficient resolution. Furthermore, increased sampling frequencies across multiple channels significantly reduces

available recording time (Wilson, Shepard & Liebsch, 2008). Qasem *et al.* (2012) also challenged the validity of using VeDBA for the investigation of short time-scale movements due to a loss of detail, later work has found it suitable (Wilson *et al.,* 2020).

There is currently no environmental context to accompany the behaviours observed within the data from the CATS tags. Knowledge of the environmental context in which behaviours occur is key to understanding animal-environment interactions and a species' responsiveness to environmental change (Bestley *et al.,* 2013). It also infers links between the biomechanical, behavioural, and ecological processes that influence variations in the behaviours of individuals and determines behavioural modality (Nathan *et al.,* 2012). For example, the occurrence of spawning behaviours performed by female chum salmon, *O. keta,* was significantly affected by turbidity influenced by runoff water following a storm (Tsuda *et al.,* 2006) and substrate type influenced mating display multimodality in male wolf spiders (Gordon & Uetz, 2011). The dead-reckoning track could be aligned with the deployment and retrieval GPS coordinates, to provide locations for which individual behaviours occurred. Known locations could provide information about the underwater environment, as well as local weather and sea conditions at that time, for example (Fedak, 2004). This, combined with recorded parameters, such as light intensity, depth and temperature could provide deeper insight into which conditions influence certain behavioural modes.

Against this, however, the sharks will have experienced drift due to currents of varying speed and direction, a factor that cannot be directly measured by the tag. Therefore, the accuracy of the position given by the dead-reckoning will likely decrease over time (Wilson, Shepard & Liebsch, 2008). GPS technology can be applied to tags (Nathan *et al.,* 2012) to provide relatively accurate and precise spatio-temporal data, although such technology does come with its own faults, including high current drain and being unusable beneath salt-water (reviewed by Hebblewhite & Haydon, 2010). Estimates of latitude and longitude have previously been made using ambient light levels, depth and sea surface temperatures from archival tag data (Wilson *et al.,* 2007) but these are a crude substitute for GPS accuracy. Gunner *et al.* (2021) have proposed a method for correcting the cumulative drift errors associated with dead reckoning of terrestrial, aquatic and aerial biotelemetry data from triaxial accelerometer tags. Verified Position Correction (VPC) is possible *via* an R package called *Gundog.Tracks* that uses periodic ground-truthing with aligned location data (see Gunner *et al.* 2021 for details).

Finally, the scope of behaviours described in this study was limited by a relatively small sample size. Data from only 10 individuals of a single species were analysed, all of which were tagged in the same location during a similar period. Seasonal and spatial shifts in tiger shark behaviour have been observed and can also be influenced by sex and size/age (Lowe *et al.,* 1996). Therefore, behaviours displayed by animals of different species or occupying different environments or ecosystems may also differ greatly and so, it is unlikely that these algorithms could be applied so widely. Nonetheless, they may be applicable to other *Selachii* or teleost species of similar swimming modes, assuming similar behaviours are displayed. Undoubtedly, this approach of identifying and defining behaviours could be applied to a much wider scope of species in the future.

CONCLUSIONS

The behaviours described in this work were successfully identified remotely using triaxial accelerometer and magnetometer tag technology and the DDMT software, despite my limited prior knowledge of their function and appearance amongst acceleration data. However, using my understanding of acceleration data, I was able to detect patterns amongst the recorded and derived channels and interpret them. There is extensive literature already describing these identified behaviours (see discussion) *via* video footage or *in-situ* visual observation, which provides evidence to suggest that it this is a viable method for identifying and observing the movements and behaviours of free-roaming animals in their natural environment.

It is also evident that algorithms can be constructed by hand using BB (within DDMT), without the aid of ML. Although algorithms were not constructed for some of the more complex behaviours within the time-frame, it would undoubtedly be possible once more familiarity with the DDMT software is achieved. The frequency distributions produced from the behaviours that were successfully extracted using the constructed algorithms suggest that modality within the metrics of the tiger sharks' behaviours described occur as more of a continuum, rather than distinctly separate modes. However, the overlap between behavioural occurrences could potentially be cascaded with further investigation. It cannot be confirmed or denied whether distinct modalities occur within Behaviours F, I & J at this time.

Future development of this work could be firstly directed towards ensuring the accuracy of the current algorithms, as well as developing algorithms for the behaviours that were not successfully extracted from the data and then assessing the modality of metrics within them.

Furthermore, investigation into the diurnal modalities and times at which certain behaviours occurred most frequently could be considered.

Overall then, simple visual inspection of patterns in acceleration, magnetic field intensity and pressure data and their derivatives appears to be a viable method for detecting, interpreting and identifying behaviours in species that are difficult or impossible to observe. I suggest that this approach could be applied to numerous other species and used for a suite of other behavioural investigation applications.

APPENDICES

Appendix I – Inverted Tags and Acceleration Data

During data inspection of periods when the sharks were swimming at the surface, it was noticed that the tags were probably fitted upside-down due to the negative values close to -1 *g* in the heave (acceleration *z*) axis. This implied that the sharks would have been upside down at the surface, which seemed unlikely. Furthermore, the values of all three acceleration axes should sum to 1 *g,* but the VeSBA (Vector of Static Body Acceleration) was reading values less than this. However, the surge (acceleration *x*) axis and pitch angles remained close to zero when the depth was unchanging, which verified that the tags were level along the longitudinal axis. However, because the tags' magnetometer axes had not been fully calibrated and the heading calculations made by the tag were not fully compatible with DDMT software, corrections were made for this in DDMT. When corrections for the inverted acceleration data were attempted, it altered the offsets for the magnetometer axes. Reasons for this were unclear, however, it may have been because the DDMT software was originally made for a different type of tag, known as the Daily Diary. Therefore, it was decided to leave the acceleration data inverted, but make the reader aware. This issue highlights the importance of tag calibration prior to deployment onto a subject, as well being fitted in the correct orientation. The topic of calibration and its' importance is discussed in detail by Garde *et al.* (in press).

Appendix II – DDMT BB/TS Algorithms

Behaviour	BB and TS algorithms
A	'If (Diff_Chan(Pressure (R=5)) > 0) then Mark Events' -> 'Element (1): ABS Diff Depth > 0, present for 60 events, %time 100, with next expression starting from range 100, flexibility after of 10'
B	'If (Diff_Chan(Pressure (R=5)) < 0) then Mark Events' -> 'Element (1): ABS Diff Depth < 0, present for 60 events, %time 100, with next expression starting from range 100, flexibility after of 10'
C	'If (Diff_Chan(Pressure (R=5)) = 0) then Mark Events' -> 'Element (1): ABS Diff Depth = 0, present for 60 events, %time 100, with next expression starting from range 100, flexibility after of 10'
D	'If (Pressure (R=5) < 1) then Mark Events' -> 'Element (1): Depth < 1\, present for 60 events, %time 100, with next expression starting from range 100, flexibility after of 10'
E	N/A
F	'If (ABS (Diff_Chan(Heading (R=5)) < 0.5)) then Mark Events' -> 'Element (1): ABS Diff Head < 0.5, present for 60 events, %time 100, with next expression starting from range 100, flexibility after of 10'
G	'If (ABS (Diff_Chan(VeDBA (R=5)) > 0.03)) then Mark Events'
H	'If (ABS (Diff_Chan(Heading (R=5)) > 0.5)) then Mark Events' -> 'Element (1): ABS Diff Head < 0.5, present for 60 events, %time 100, with next expression starting from range 100, flexibility after of 10'
I	N/A
J	N/A

Appendix III – Tiger shark tagging metadata (reduced)

	Length (cm)				Tag deployment + release				Tag detatchment	
Shark ID	**PCL**	**FL**	**STL**	**Girth**	**Date**	**Time**	**Latitude**	**Longitude**	**Date**	**Time**
TS8	260	283	321	159	28/04/2017	12:01	23.00.802	113.48.148	29/04/2017	05:15
TS12	301	332	380	181	30/04/2017	13:50	23.00.776	113.48.151	01/05/2017	03:38
TS13	215	229	277	119	30/04/2017	14:37	23.00.944	113.48.145	01/05/2017	10:52
TS14	267	299	351	167	30/04/2017	15:13	23.00.602	113.45.067	01/05/2017	08:45
TS15	270	298	329	161	02/05/2017	12:19	23.00.945	113.47.861	04/05/2017	13:03
TS16	202	223	268	108	03/05/2017	09:19	23.00.627	113.48.012	04/05/2017	02:48
TS17	297	323	373	171	03/05/2017	09:35	23.00.638	113.47.997	04/05/2017	01:12
TS18	270	300	330		07/05/2017	10:31	23.01.174	113.47.993	08/05/2017	02:37
TS19	224	252	299	140	07/05/2017	13:40	23.00.965	113.48.058	08/05/2017	04:50
TS24	300	330	373	171	14/05/2017	12:08	23.00.757	113.48.154	15/05/2017	11:51

CITED REFERENCES

Andrzejaczek, S., Gleiss, A. C., Lear, K. O., Pattiaratchi, C. B., Chapple, T. K., & Meekan, M. G. (2019). Biologging tags reveal links between fine-scale horizontal and vertical movement behaviours in tiger sharks (*Galeocerdo cuvier*). *Frontiers in Marine Science, 6,* 229. DOI: 10.3389/fmars.2019.00229

Andrzejaczek, S., Gleiss, A. C., Pattiaratchi, C. B., & Meekan, M. G. (2018). First insights into the fine-scale movements of the sandbar shark, *Carcharhinus plumbeus*. *Frontiers in Marine Science, 5*, 483. DOI: 10.3389/fmars.2018.00483

Bestley, S., Jonsen, I. D., Hindell, M. A., Guinet, C., & Charrassin, J-B. (2013). Integrative modelling of animal movement: incorporating in situ habitat and behavioural information for a migratory marine predator. *Proceedings of the Royal Society B: Biological Sciences, 280(1750)*, 20122262. DOI: 10.1098/rspb.2012.2262

Bidder, O., Soresina, M., Shepard, E. L. C., Halsey, L. G., Quintana, F., Gómez-Laich, A. and Wilson, R. P. (2012). The need for speed: testing acceleration for estimating animal travel rates in terrestrial dead-reckoning systems. *Zoology, 115*(1), pp.58-64. DOI: 10.1016/j.zool.2011.09.003

Block, B. A., Jonsen, I. D., Jorgensen, S. J., Winship, A. J., Shaffer, S. A., Bograd, S. J., Hazen, E. L., Foley, D. G., Breed, G. A., Harrison, A. -L., Ganong, J. E., Swithenbank, A., Castleton, M., Dewar, H., Mate, B. R., Shillinger, G. L., Schaefer, K. M., Benson, S. R., Weise, M. J., Henry, R. W., & Costa, D. P. (2011). Tracking apex marine predator movements in a dynamic ocean. *Nature, 475(7354)*, 86-90. DOI: 10.1038/nature10082

Bres, M. (1993). The behaviour of sharks. *Reviews in Fish Biology and Fisheries*, *3*(2), 133-159. DOI: 10.1007/bf00045229

Broell, F., Noda, T., Wright, S., Domenici, P., Steffensen, J. F., Auclair, J-P., & Taggart, C. T. (2013). Accelerometer tags: detecting and identifying activities in fish and the effect of sampling frequency. *Journal of Experimental Biology, 216(7),* 1255-1264. DOI: 10.1242/jeb.088336

Brown, D., Kays, R., Wikelski, M., Wilson, R. P., & Klimley, A. (2013). Observing the unwatchable through acceleration logging of animal behaviour. *Animal Biotelemetry, 1(1)*, 20. DOI: 10.1186/2050-3385-1-20

Brown, J. S., Laundre, J. W., & Gurung, M. (1999). The Ecology of Fear: Optimal Foraging, Game Theory, and Trophic Interactions. *Journal of Mammalogy*, *80*(2), 385-399. DOI: 10.2307/1383287

Butchart, S. H. M., Walpole, M., Collen, B., Van Strien, A., Scharlemann, J. P. W., Almond, R. E. A., . . . Watson, R. (2010). Global Biodiversity: Indicators of Recent Declines. *Science, 382(5982)*, 1164-1168. DOI: 10.1126/science.1187512

Carey, F.G., Scharold, J.V., & Kalmijn, A.J. (1990) Movements of blue sharks (*Prionace glauca*) in depth and course. *Marine Biology, 106*, 329–342. DOI: 10.1007/BF01344309

Clua, E., Chauvet, C., Read, T., Werry, J. M., & Lee, S. Y. (2013). Behavioural patterns of a Tiger Shark (*Galeocerdo cuvier*) feeding aggregation at a blue whale carcass in Prony

Bay, New Caledonia. *Marine and Freshwater Behaviour and Physiology, 46*(1), 1-20. DOI: 10.1080/10236244.2013.773127

Cooke, G. M. (2017). Stereotypic behaviour is not limited to terrestrial taxa: A response to Rose et al. *Journal of Veterinary Behaviour*, *22*, 17-18. DOI: 0.1016/j.jveb.2017.09.009

Cooke, S. J. (2008). Biotelemetry and biologging in endangered species research and animal conservation: relevance to regional, national, and IUCN Red List threat assessments. *Endangered Species Research, 4,* 165-185. DOI: 10.3354/esr00063

Cooke, S. J., Hinch, S. G., Wikelski, M., Andrews, R. D., Kuchel, L. J., Wolcott, T. G., & Butler, P. J. (2004) Biotelemetry – a mechanistic approach to ecology. *Trends in Ecology & Evolution, 19*(6), 334-343. DOI: 10.1016/j.tree.2004.04.003

Customised Animal Tracking Solutions, Australia. (2021). CATS-Diary. Available at: https://www.cats.is/products/cats-diary/ (Accessed 3rd May 2021).

Dicken, M. L., Hussey, N. E., Christiansen, H. M., Smale, M. J., Nkabi, N., Cliff, G., & Wintner, S. P. (2017). Diet and trophic ecology of the tiger shark (*Galeocerdo cuvier*) from South African waters. *PLOS ONE, 12*(6), e0177897. DOI: 10.1371/journal.pone.0177897

Drymon, J. M., Feldheim, K., Fournier, A. M. V., Seubert, E. A., Jefferson, A. E., Kroetz, A. M., & Powers, S. P., (2019). Tiger sharks eat songbirds: scavenging a windfall of nutrients from the sky. *Ecology, 100*(9), e02728. DOI: 10.1002/ecy.2728

Dulvy, N. K., Fowler, S. L., Musick, J. A., Cavanagh, R. D., Kyne, P. M., Harrison L. R., Carlson, J. K., Davidson, L. N. K., Fordham, S. V., Francis, M. P., Pollock, C. M., Simpfendorfer, C. A., Burgess, G. H., Carpenter, K. E., Compagno, L. J. V., Ebert, D. A., Gibson, C., Heupel, M. R., Livingstone, S. R., Sanciangco, J. C., Stevens, J. D., Valenti, S., & White, W. T. (2014). Extinction risk and conservation of the world's sharks and rays. *Elife*, *3,* e00590. DOI: 10.7554/eLife.00590

Ellwood, S. A., Wilson, R. P., & Addison, A. C. (2007) Technology in conservation: a boon but with small print. In: Macdonald, D. & Service, K (eds) *Key topics in conservation biology.* Blackwell Publishing Ltd, Oxford, 105-199.

Fedak, M. (2004). Marine animals as platforms for oceanographic sampling: A "win/win" situation for biology and operational oceanography. *Memoirs of National Institute of Polar Research. 58*, 133-147.

Ferreira, L. C., Thums, M., Heithaus, M. R., Barnett, A., Abrantes, K. G., Holmes, B. J., Zamora, L. M., Frisch, A. J., Pepperell, J. G., Burkholder, D., Vaudo, J., Nowicki, R., Meeuwig, J. & Meekan, M. G. (2017). The trophic role of a large marine predator, the tiger shark *Galeocerdo cuvier*. *Scientific Reports, 7(1),* 7641. DOI: 10.1038/s41598-017-07751-2

Ferretti, F., Worm, B., Britten, G. L., Heithaus, M. R., & Lotze, H. K. (2010). Patterns and ecosystem consequences of shark declines in the ocean. *Ecology Letters, 13,* 1055-1071. DOI: 10.1111/j.1461-0248.2010.01489.x

Gallagher, A. J., Serafy, J. E., Cooke, S. J., & Hammerschlag, N. (2014). Physiological stress response, reflex impairment, and survival of five sympatric shark species following

experimental capture and release. *Marine Ecology Progress Series, 496*, 207-218. DOI: 10.3354/meps10490

Garde, B., Wilson, R. P., Fell, A., Cole, N., Tatayah, V., Holton, M. D., Rose, K. A. R., Metcalfe, R. S., Robotka, H., Wikelski, M., Tremblay, F., Whelan, S., Elliott, K. H., Shepard, E. L. C. (2022). Ecological inference using data from accelerometers needs careful protocols. *Methods in Ecology and Evolution, 13,* 813-325. DOI: 10.1111/2041-210X.13804

Gardiner, J. M., & Atema, J. (2007). Sharks need the lateral line to locate odor sources: rheotaxis and eddy chemotaxis. *Journal of Experimental Biology, 210*(11), 1925-1934. DOI: 10.1242/jeb.000075

Gardiner, J. M., & Atema, J. (2010). The Function of Bilateral Odor Arrival Time Differences in Olfactory Orientation of Sharks. *Current Biology, 20*(13), 1187-1191. DOI: 10.1016/j.cub.2010.04.053

Gleiss, A. C., Dale, J. J., Holland, K. N., & Wilson, R. P. (2010). Accelerating estimates of activity-specific metabolic rate in fishes: Testing the applicability of acceleration data-loggers. *Journal of Experimental Marine Biology and Ecology, 385*(1-2), 85-91. DOI: 10.1016/j.jembe.2010.01.012

Gleiss, A. C., Jorgensen, S. J., Liebsch, N., Sala, J. E., Norman, B., Hays, G. C., Quintana, F., Grundy, E., Campagna, C., Trites, A. W., Block, B. A., & Wilson, R. P. (2011). Convergent evolution in locomotory patterns of flying and swimming animals. *Nature Communications, 2*(352). DOI: 10.1038/ncomms1350

Gleiss, A. C., Norman, B., Liebsch, N., Francis, C., & Wilson, R. P. (2009). A new prospect for tagging large free-swimming sharks with motion-sensitive data-loggers. *Fisheries Research, 97(1-2),* 11-16. DOI: 10.1016/j.fishres.2008.12.012

Gleiss, A. C., Norman, B., & Wilson, R. P. (2011). Moved by that sinking feeling: variable diving geometry underlies movement strategies in whale sharks. *Functional Ecology, 25(3)*, 595-607. DOI: 10.1111/j.1365-2435.2010.01801.x

Gleiss, A. C., Wilson, R. P., & Shepard, E. L. C. (2011). Making overall dynamic body acceleration work: On the theory of acceleration as a proxy for energy expenditure. *Methods in Ecology and Evolution*, *2*, 23–33. DOI: 10.1111/j.2041-210X.2010.00057.x

Gleiss, A C., Wright, S., Liebsch, N., Wilson, R. P., & Norman, B. (2013). Contrasting diel patterns in vertical movement and locomotor activity of whale sharks at Ningaloo Reef. *Marine Biology, 160*(11), pp.2981-2992. DOI: 10.1007/s00227-013-228

Godley, B. J., & Wilson, R. P., (2008). Tracking vertebrates for conservation: Introduction. *Endangered Species Research, 4*, 1-2. DOI: 10.3354/esr00081

Gordon, S. G., & Uetz, G. W. (2011). Multimodal communication of wolf spiders on different substrates: evidence for behavioural plasticity. Animal Behaviour, 81(2), pp.367-375. DOI: 10.1016/j.anbehav.2010.11.003

Grainger, R., Raubenheimer, D., Peddemors, V. M., Butcher, P. A., & Machovsky-Capuska, G. (2022). Integrating biologging and behavioural state modelling to identify cryptic behaviours and post-capture recovery processes: New insights from a threatened

marine apex predator. *Frontiers in Marine Science*, 2616473266. DOI: 10.3389/fmars.2021.791185

Greggor, A. L., Berger-Tal, O., Blumstein, D. T., Angeloni, L., Bessa-Gomes, C., Blackwell, B. F., St Clair, C. C., Crooks, K., de Silva, S., Fernández-Juricic, E., Goldenberg, S. Z., Mesnick, S. L., Owen, M., Price, C. J., Saltz, D., Schell, C. J., Suarez, A. V., Swaisgood, R. R., Winchell, C. S., & Sutherland, W. J. (2016). Research Priorities from Animal Behaviour for Maximising Conservation Progress. *Trends in Ecology & Evolution, 31*(12), 953-964. DOI: 10.1016/j.tree.2016.09.001

Gribble, N. A., McPherson, G., & Lane, B. (1998). Effect of the Queensland Shark Control Program on non-target species: whale, dugong, turtle and dolphin: a review. *Marine and Freshwater Research, 49(7),* 645-651. DOI: 10.1071/MF97053

Gunner, R. M., Holton, M. D., Scantlebury, M. D., van Schalkwyk, O. L., English, H. M., Williams, H. J., Hopkins, P., Quintana, F., Gómez-Laich, A., Börger, L., Redcliffe, J., Yoda, K., Yamamoto, T., Ferreira, S., Govender, D., Viljoen, P., Bruns, A., Bell, S. H., Marks, N. J., Bennett, N. C., Tonini, M. H., Duarte, C. M., van Rooyen, M. C., Bertelsen, M. F., Tambling, C. J., & Wilson, R. P. (2021). Dead-reckoning animal movements in R: a reappraisal using Gundog.Tracks. *Animal Biotelemetry*, *9*(1), 23. DOI: 10.1186/s40317-021-00245-z

Halsey, L. G., Shepard, E. L. C., & Wilson, R. P. (2011). Assessing the development and application of the accelerometry technique for estimating energy expenditure. *Comparative Biochemistry and Physiology Part A: Molecular & Integrative Physiology*, *158(3),* 305-314. DOI: 10.1016/j.cbpa.2010.09.002

Hart, A., Reynolds, Z., & Troxell-Smith, S. M. (2021). Using individual-specific conditioning to reduce stereotypic behaviours: A study on smooth dogfish *Mustelus cani*s in captivity. *Journal of Zoo & Research, 9*(3), 193-199. DOI: 10.19227/jzar.v9i3.536

Hart, N. S., Lisney, T. J., & Collin, S. P. (2006). Visual communication in elasmobranchs. In: Ladich, F., Collin, S. P., Moller, P., & Kapoor, B. G. (Eds). *Communication in Fishes.* Science Publishing, Plymouth, chapter 13, 337-392. ISBN: 978-1578084067

Hebblewhite, M., & Haydon, D. T. (2010). Distinguishing technology from biology: a critical review of the use of GPS telemetry data in ecology. *Philosophical Transactions of the Royal Society B: Biological Sciences, 365(1550)*, 2303-2312. DOI: 10.1098/rstb.2010.0087

Heithaus, M. R. (2001). The Biology of Tiger Sharks, *Galeocerdo Cuvier*, in Shark Bay, Western Australia: Sex Ratio, Size Distribution, Diet, and Seasonal Changes in Catch Rates. *Environmental Biology of Fishes, 61*(1), 25-36. DOI: 10.1023/A:1011021210685

Heithaus, M. R., Dill, L. M., Marshall, G. J., & Buhleier, B. (2002). Habitat use and foraging behaviour of tiger sharks (*Galeocerdo cuvier*) in a seagrass ecosystem. *Marine Biology, 140*(2), 237-248. DOI: 10.1007/s00227-001-0711-7

Herrera, J., & Nunn C. L. (2019). Behavioural ecology and infectious disease: implications for conservation of biodiversity. *Royal Society Philosophical Transactions B, 374*, 20180054. DOI: 10.1098/rstb.2018.0054

Hoffmann, M., Hilton-Taylor, C., Angulo, A., Böhm, M., Brooks, T., Butchart, S., . . . Stuart, S. (2010). The Impact of Conservation on the Status of the World's Vertebrates. *Science, 330(6010),* 1503-1509. DOI: 10.1126/science.1194442

Holland, K., Wetherbee, B., Lowe, C., & Meyer, C. (1999). Movements of tiger sharks (*Galeocerdo cuvier*) in coastal Hawaiian waters. *Marine Biology*, *134*(4), 665-673. DOI: 10.1007/s002270050582

IUCN (World Conservation Union) (2021). IUCN Red List of Threatened Species 2020-21. Available at: www.redlist.org (Accessed 28th April 2021).

Kawabe, R., Naito, Y., Sato, K., Miyashita, K., & Yamashita, N. (2004). Direct measurement of the swimming speed, tailbeat, and body angle of Japanese flounder (*Paralichthys olivaceus). ICES Journal of Marine Science, 61*(7), 1080-1087. DOI: 10.1016/j.icesjms.2004.07.014

Kawatsu, S., Sato, K., Watanabe, Y., Hyodo, S., Breves, J. P., Fox, B. K., Gordon Grau, E., & Miyazaki, N. (2010). A New Method to Calibrate Attachment Angles of Data Loggers in Swimming Sharks. *EURASIP Journal on Advances in Signal Processing, 2010*(1), ID 732586. DOI: 10.1155/2010/732586

Kelly, M. L., Collin, S. P., Hemmi, J. M., & Lesku, J. A. (2019). Evidence for Sleep in Sharks and Rays: Behavioural, Physiological, and Evolutionary Considerations. *Brain, Behaviour and Evolution, 94*(Suppl. 1-4), 37-50. DOI: 10.1159/000504123

Kelly, M. L., Spreitzenbarth, S., Kerr, C. C., Hemmi, J. M., Lesku, J. A., Radford, C. A., & Collin, S. P. (2020). Behavioural sleep in two species of buccal pumping sharks (*Heterodontus portusjacksoni* and *Cephaloscyllium isabellum*). *Journal of Sleep Research, 30*(3), e13139. DOI: 10.1111/jsr.13139

Kessel, S., & Hussey, N. (2015). Tonic immobility as an anaesthetic for elasmobranchs during surgical implantation procedures. *Canadian Journal of Fisheries and Aquatic Sciences*, *72*(9), 1287-1291. DOI: 10.1139/cjfas-2015-0136

Klimely, A. P. (1993). Highly directional swimming by scalloped hammerhead sharks, *Sphyrna lewini*, and subsurface irradiance, temperature, bathymetry, and geomagnetic field. *Marine Biology, 117,* 1-22. DOI: 10.1007/BF00346421

Lear, K. O., Gleiss, A. C., & Whitney, N. M. (2018). Metabolic rates and the energetic costs of external tag attachment in juvenile blacktip sharks *Carcharhinus limbatus*. *Journal of Fish Biology, 93,* 391-395. DOI: 10.1111/jfb.13663

Lear, K. O., & Whitney, N. M. (2016). Bringing data to the surface: recovering data loggers for large sample sizes from marine vertebrates. *Animal Biotelemetry, 4*, 12. DOI: 10.1186/s40317-016-0105-8

Lisney, T. J., Theiss, S. M., Collin, S. P., & Hart, N. S. (2012). Vision in elasmobranchs and their relatives: 21st century advances. *Journal of Fish Biology, 80*(5), 2024-2054. DOI: 10.1111/j.1095-8649.2012.03253.x

Lowe, C. G., Wetherbee, B. M., Crow, G. L., & Tester, A. L. (1996). Ontogenetic dietary shifts and feeding behaviour of the tiger shark, *Galeocerdo cuvier*, in Hawaiian waters. *Environmental Biology of Fishes, 47*(2), 203-211. DOI: 10.1007/BF00005044

Lyamin, O. I., Lapierre, J. L., Kosenko, P. O., Kodama, T., Bhagwandin, A., Korneva, S. M., Peever, J. H., Mukhametov, L. M., & Siegel, J. M. (2016). Monoamine Release during

Unihemispheric Sleep and Unihemispheric Waking in the Fur Seal. *Sleep, 39*(3), 625-636. 10.5665/sleep.5540

Lyamin, O. I., Manger, P. R., Ridgway, S. H., Mukhametov, L. M., & Siegel, J. M. (2008). Cetacean sleep: An unusual form of mammalian sleep. *Neuroscience & BiobehavioUral Reviews, 32*(8), 1451-1484. DOI: 10.1016/j.neubiorev.2008.05.023

Lyamin, O. I., Mukhametov, L. M., & Siegel, J. M. (2004). Relationship between sleep and eye state in Cetaceans and Pinnipeds. *Archives italiennes de biologie, 142*(4), 557–568. DOI: 10.4449/aib.v142i4.427

Lyamin, O. I., Mukhametov, L. M., Siegel, J. M., Nazarenko, E. A., Polyakova, I. G., & Shpak, O. V. (2002). Unihemispheric slow wave sleep and the state of the eyes in a white whale. *Behavioural Brain Research, 129*(1-2), 125-129. DOI: 10.1016/s0166-4328(01)00346-1

Meyer, C. G., Anderson, J. M., Coffey, D. M., Hutchinson, M. R., Royer, M. A., & Holland, K. N. (2018). Habitat geography around Hawaii's oceanic islands influences tiger shark (*Galeocerdo cuvier*) spatial behaviour and shark bite risk at ocean recreation sites. *Scientific Reports, 8*, 4945. DOI: 10.1038/s41598-018- 23006-0.

Meyer, C. G., O'Malley, J. M., Papastamatiou, Y. P., Dale, J. J., Hutchinson, M. R., Anderson, J. M., Royer, M. A., & Holland, K. N. (2014). Growth and Maximum Size of Tiger Sharks (*Galeocerdo cuvier*) in Hawaii. *PLoS ONE, 9*(1), p.e84799. DOI: 10.1371/journal.pone.0084799

Meyer, C. G., Papastamatiou, Y. P., & Holland, K. N. (2010). A multiple instrument approach to quantifying the movement patterns and habitat use of tiger (*Galeocerdo cuvier*) and Galapagos sharks (*Carcharhinus galapagensis*) at French Frigate Shoals, Hawaii. *Marine Biology, 157*(8), 1857-1868. DOI: 10.1007/s00227-010-1457-x

Morales, J. M., Haydon, D. T., Frair, J., Holsinger, K. E., & Fryxell, J. M. (2004). Extracting more out of relocation data: building movement models as mixtures of random walks. *Ecology, 85(9),* 2436-2445. DOI: 10.1890/03-0269

Myrberg, A. A., & Gruber, S. H. (1974). The Behaviour of the Bonnethead Shark, *Sphyrna tiburo. Copeia,* 2, p.358-374. DOI: 10.2307/1442530

Naito, Y., Bornemann, H., Takahashi, A., McIntyre, T., & Plötz, J. (2010). Fine-scale feeding behaviour of Weddell seals revealed by a mandible accelerometer. *Polar Science, 4(2)*, 309-316. DOI: 10.1016/j.polar.2010.05.009

Nakamura, I., Watanabe, Y. Y., Papastamatiou, Y. P., Sato, K., & Meyer, C. G. (2011) Yo-yo vertical movements suggest foraging strategy for tiger sharks *Galeocerdo cuvier. Marine Ecology Progress Series, 424,* 237-246.

Narazaki, T., Nakamura, I., Aoki, K., Iwata, T., Shiomi, K., Luschi, P., Suganuma, H., Meyer, C. G., Matsumoto, R., Bost, C. A., Handrich, Y., Amano, M., Okamoto, R., Mori, K., Ciccione, S., Bourjea, J., & Sato, K. (2021). Similar circling movements observed across marine megafauna taxa. *iScience, 24*(4), 102221. DOI: 10.1016/j.isci.2021.102221

Nathan, R., Spiegel, O., Fortmann-Roe, S., Harel, R., Wikelski, M., & Getz, W. M. (2012). Using tri-axial acceleration data to identify behavioural modes of free-ranging

animals: general concepts and tools illustrated for griffon vultures. *The Journal of Experimental Biology, 215,* 986-996. DOI: 10.1242/jeb.058602

Ocean Appliances, Australia. (2021). Innovative Commercial Fishing Equipment: Galvanised Timed Release. Available at: http://oceanappliances.com.au/index.php (Accessed 3rd May 2021).

Owen, K., Dunlop, R. A., Monty, J. P., Chung, D., Noad, M. J., Donnelly, D., Goldizen, A. W., & Mackenzie, T. (2016). Detecting surface-feeding behaviour by rorqual whales in accelerometer data. *Marine Mammal Science, 32(1),* 327-348. DOI: 10.1111/mms.12271

Pianka, E. R. (1976). Natural Selection of Optimal Reproductive Tactics. *American Zoologist, 16*(4), 775-784. DOI: 10.1093/icb/16.4.775

Qasem, L., Cardew, A., Wilson, A., Griffiths, I., Halsey, L., Shepard, E., Gleiss, A., & Wilson, R. (2012). Tri-Axial Dynamic Acceleration as a Proxy for Animal Energy Expenditure; Should We Be Summing Values or Calculating the Vector*? PLoS ONE, 7(2)*, e31187. DOI: 10.1371/journal.pone.0031187

Randall, J. E. (1977). Contribution to the biology of the white-tip reef shark (*Triaenodon obesus*). Pacific Science, 31, 143–164.

Rattenborg, N. C., van der Meij, J., Beckers, G. J. L., & Lesku, J. A. (2019). Local Aspects of Avian Non-REM and REM Sleep. *Frontiers in Neuroscience*, 13, 567. DOI: 10.3389/fnins.2019.00567

Rattenborg, N. C., Voirin, B., Cruz, S. M., Tisdale, R., Dell'Omo, G., Lipp, H.-P., Wikelski, M., & Vyssotski, A. L. (2016). Evidence that birds sleep in mid-flight. *Nature Communications, 7*(1). DOI: 10.1038/ncomms12468

Rihel, J. (2020). Sleep Across the Animal Kingdom. In: Mongomery-Downs, H. (Eds). *Sleep Science.* Oxford University Press, Oxford, chapter 2, 15-31. ISBN: 9780190923259

Ritter, E. K. (2020) Is the Shark Just Drifting, or Does It Take a Quick Nap? *Open Journal of Animal Sciences, 10*, 40-47. DOI: 10.4236/ojas.2020.101004

Ropert-Coudert, Y., & Wilson, R. P. (2005). Trends and perspectives in animal-attached remote sensing. *Frontiers in Ecology and the Environment*, *3*(8), 437-444. DOI: 10.2307/3868660

Roth II, T. C., Rattenborg, N. C., & Pravosudov, V. V. (2010). The ecological relevance of sleep: the trade-off between sleep, memory and energy conservation. Philosophical *Transactions of the Royal Society B: Biological Sciences*, *365*(1542), 945-959. DOI: 10.1098/rstb.2009.0209

Rutz, C., & Hays, G. C. (2009). New frontiers in biologging science. *Biology Letters, 5(3)*, 289-292. DOI: 10.1098/rsbl.2009.0089

Sakamoto, K. Q., Sato, K., Ishizuka, M., Watanuki, Y., Takahashi, A., Daunt, F., & Wanless, S. (2009). Can Ethograms Be Automatically Generated Using Body Acceleration Data from Free-Ranging Birds? *PLoS ONE, 4(4)*, e5379. DOI: 10.1371/journal.pone.0005379

Schneirla, T. C. (1950). The relationship between observation and experimentation in the field study of behaviour. *Annals of the New York Academy of Sciences, 51(6)*, 1022-1044. DOI: 10.1111/j.1749-6632.1950.tb27331.x

Sequeira, A. M. M., O'Toole, M., Keates, T. R., McDonnell, L. H., Braun, C. D., Hoenner, X., Jaine, F. R. A., Jonsen, I. D., Newman, P., Pye, J., Bograd, S. J., Hays, G. C., Hazen, E. L., Holland, M., Tsontos, V. M., Blight, C., Cagnacci, F., Davidson, S. C., Dettki, H., Duarte, C. M., Dunn, D. C., Eguíluz, V. M., Fedak, M., Gleiss, A. C., Hammerschlag, N., Hindell, M. A., Holland, K., Janekovic, I., McKinzie, M. K., Muelbert, M. M. C., Pattiaratchi, C., Rutz, C., Sims, D. W., Simmons, S. E., Townsend, B., Whoriskey, F., Woodward, B., Costa, D. P., Heupel, M R.., McMahon, C. R., Harcourt, R., & Weise, M. (2021). A standardisation framework for bio-logging data to advance ecological research and conservation. *Methods in Ecology and Evolution, 12(6)*, 996-1007. DOI: 10.1111/2041-210X.13593

Shepard, E. L. C., Wilson, R. P., Halsey, L. G., Quintana, F., Gómez Laich, A., Gleiss, A. C., Liebsch, N., Myers, A. E., & Norman, B. (2008b). Derivation of body motion via appropriate smoothing of acceleration data. *Aquatic Biology, 4*, 235-241. DOI: 10.3354/ab00104

Shepard, E. L. C., Wilson, R. P., Quintana, F., Gómez Laich, A., Liebsch, N., Albareda, D. A., Halsey, L. G., Gleiss, A. C., Morgan, D. T., Myers, A. E., Newman, C., & Macdonald, D. W. (2008a). Identification of animal movement patterns using tri-axial accelerometry. *Endangered Species Research, 10,* 47-60. DOI: 10.3354/esr00084

Shlesinger, M. F., Zaslavsky G. M., & Klafter, J. (1993). Strange Kinetics. *Nature, 363*(6424), 31-37. DOI: 10.1038/363031a0

Simpfendorfer, C. A., Goodreid, A. B., & McAuley, R. B. (2001). Size, Sex and Geographic Variation in the Diet of the Tiger Shark, *Galeocerdo Cuvier*, From Western Australian Waters. *Environmental Biology of Fishes, 61*(1), 37-46. DOI: 10.1023/A:1011021710183

Sims, D. W. (2003). Tractable models for testing theories about natural strategies: foraging behaviour and habitat selection of free-ranging sharks. *Journal of Fish Biology, 63*, 53-73. DOI: 10.1111/j.1095-8649.2003.00207.x

Sims, D. W. (2010). Swimming Behaviour and Energetics of Free-ranging Sharks: New Directions in Movement Analysis. In: Domenici, P. & Kapoor, B. G. (Eds). *Fish Locomotion: An Eco-ethological Perspective.* Enfield: Science Publishers, chapter 13, 407-435. ISBN: 978-1-57808-448-7

Sims, D. W., Southall, E. J., Humphries, N. E., Hays, G. C., Bradshaw, C. J. A., Pitchford, J. W., James, A., Ahmed, M. Z., Brierley, A. S., Hindell, M. A., Morritt, D., Musyl, M. K., Righton, D., Shepard, E. L. C., Wearmouth, V. J., Wilson, R. P., Witt, M. J., & Metcalfe, J. D. (2008). Scaling laws of marine predator search behaviour. *Nature, 451*(7182), 1098-1102. DOI: 10.1038/nature06518

South Pacific (2009) BBC Two, 10th May, episode 1: Ocean of Islands, 35:23 to 38:08.

Stankowich, T., & Blumstein, D. (2005). Fear in animals: a meta-analysis and review of risk assessment. *Proceedings of the Royal Society B: Biological Sciences, 272(1581)*, 2627-2634. DOI: 10.1098/rspb.2005.3251

Stevens, J. D., Bonfil, R., Dilvy, N. K., & Walker, P. A. (2000). The effects of fishing on sharks, rays, and chimaeras (chondrichthyans), and the implications for marine ecosystems. *ICES Journal of Marine Science*, *57(3),* 476–494. DOI: 10.1006/JMSC.2000.0724

Sutherland, W. J. (1998). The importance of behavioural studies in conservation biology. *Animal Behaviour, 56,* 801-809. DOI: 10.1.1.462.6457

Tanaka, H., Takagi, Y., & Naito, Y. (2001). Swimming speeds and buoyancy compensation of migrating adult chum salmon Oncorhynchus keta revealed by speed/depth/acceleration data logger. *Journal of Experimental Biology, 204*(22), 3895-3904. DOI: 10.1242/jeb.204.22.3895

Tinberben, N. (1960). Comparative Studies of the Behaviour of Gulls (Laridae): a Progress Report1). *Behaviour, 15*(1-2), 1-69. DOI: 10.1163/156853960x00098

Tomita, T., Touma, H., Murakumo, K., Yanagisawa, M., Yano, N., Oka, S., Miyamoto, K., Hanahara, N., & Sato, K. (2018). Captive Birth of Tiger Shark (Galeocerdo cuvier) Reveals a Shift in Respiratory Mode during Parturition. *Copeia, 106(2*), 292-296. DOI: 10.1643/CI-17-683

Tsuda, Y., Kawabe, R., Tanaka, H., Mitsunaga, Y., Hiraishi, T., Yamamoto, K., & Nashimoto, K. (2006). Monitoring the spawning behaviour of chum salmon with an acceleration data logger. *Ecology of Freshwater Fish, 15(3)*, 264-274. DOI: 10.1111/j.1600-0633.2006.00147.x

Tucker, J. P., Vercoe, B., Santos, I. R., Dujmovic, M., & Butcher, P. A. (2019). Whale carcass scavenging by sharks. *Global Ecology and Conservation, 19*, p.e00655. DOI: 10.1016/j.gecco.2019.e00655

Uetz, G. W., Roberts, J. A., & Taylor, P. W. (2009). Multimodal communication and mate choice in wolf spiders: female response to multimodal versus unimodal signals. *Animal Behaviour, 78*(2), 299-305. DOI: 10.1016/j.anbehav.2009.04.023

Valletta, J. J., Torney, C., Kings, M., Thornton, A., & Madden, J. (2017). Applications of machine learning in animal behaviour studies. *Animal Behaviour, 124*, 203-220. DOI: 10.1016/j.anbehav.2016.12.005

Vickers, N. J. (2000). Mechanisms of animal navigation in odour plumes. *The Biological Bulletin, 198*(2), 203-212. DOI: 10.2307/1542524

Wang, G. (2019). Machine learning for inferring animal behaviour from location and movement data. *Ecological Informatics, 49*, 69-76. DOI: 10.1016/j.ecoinf.2018.12.002

Weihs, D. (1973) Mechanically efficient swimming techniques for fish with negative buoyancy. *Journal of Marine Research, 31*

Whitney, N. M., Pratt Jr., H. L., Pratt, T. C., & Carrier, J. C. (2010). Identifying shark mating behaviour using three-dimensional acceleration loggers. *Endangered Species Research, 10*, 71-82. DOI: 10.3354/esr00247

Wildbyte Technologies Ltd. (2021) Animal tagging and motion experts. Available at: http://www.wildbytetechnologies.com/ (Accessed 28th August 2021).

Williams, H. J., Holton, M. D., Shepard, E. L. C., Largey, N., Norman, B., Ryan, P. G., Duriez, O., Scantlebury, M., Quintana, F., Magowan, E. A., Marks, N. J., Alagaili, A. N., Bennett, N. C., & Wilson, R. P. (2017). Identification of animal movement patterns using tri-axial magnetometry. *Movement Ecology, 5*, 6. DOI: 10.1186/s40462-017-0097-x

Wilson, R. P., Börger, L., Holton, M. D., Michael Scantlebury D. M., Gómez-Laich, A., Quintana, F., Rosell, F., Graf, P. M., Williams, H., Gunner, R., Hopkins, L., Marks, N., Geraldi, N. R., Duarte, C. M., Rebecca Scott, R., Strano, M. S., Robotka, H., Eizaguirre, C., Fahlman, A., & Shepard, E. C. L. (2020). Estimates for energy expenditure in free-living animals using acceleration proxies: A reappraisal. *Journal of Animal Ecology, 89,* 161-172. DOI: 10.1111/1365-2656.13040

Wilson, R. P., Griffiths, I. W., Legg, P. A., Friswell, M. I., Bidder, O. R., Halsey, L. G., Lambertucci, S. A., & Shepard, E. L. C. (2013). Turn costs change the value of animal search paths. *Ecology Letters*, *16*(9), 1145-1150. DOI: 10.1111/ele.12149

Wilson, R. P., Holton, M. D., di Virgilio, A., Williams, H. J., Shepard, E. L. C., Lambertucci, S., Quintana, F., Sala, J. E., Balaji, B., Lee, E. S., Srivastava, M., Scantlebury, D. M., & Duarte, C. M. (2018). Give the machine a hand: A Boolean time-based decision-tree template for rapidly finding animal behaviours in multisensor data. *Methods in Ecology and Evolution*, *9*(11), 2206-2215. DOI: 10.1111/2041-210X.13069

Wilson, R. P., & McMahon, C. (2006). Measuring devices on wild animals: what constitutes acceptable practice? *Frontiers in Ecology and the Environment, 4(3)*, 147-154. DOI: 10.1890/1540-9295(2006)004[0147:MDOWAW]2.0.CO;2

Wilson, R.P., Reynolds, S. D., Potts, J. R., Redcliffe, J., Holton, M. D., Buxton, A., Rose, K., & Norman, B. M. (in review). Energetically expensive travel; a proxy to highlight onerous behaviours.

Wilson, R. P., Shepard, E. L. C., & Liebsch, N. (2008) Prying into the intimate details of animal lives: use of a daily diary on animals. *Endangered Species Research, 4,* 123-137. DOI: 10/3354/esr00064

Wilson, R. P., Stewart, B. S., Polovina, J. J., Meekan, M. G., Stevens, J. D., & Galuardi, B. (2007) Accuracy and precision of archival tag data: a multiple-tagging study conducted on a whale shark (*Rhincodon typus*) in the Indian Ocean. *Fisheries Oceonography, 16*(6), 547-554. DOI: 10.1111/j.1365-2419.2007.00450.x

Wilson, R. P., White, C. R., Quintana, F., Halsey, L. G., Liebsch, N., Martin, G. R., & Butler, P. J. (2006). Moving towards acceleration for estimates of activity-specific metabolic rate in free-living animals: the case of the cormorant. *Journal of Animal Ecology, 75,* 1081-1090. DOI: 10.1111/j.1365-2656.2006.01127.x

Wright, S., Metcalfe, J., Hetherington, S., & Wilson, R. (2014). Estimating activity-specific energy expenditure in a teleost fish, using accelerometer loggers. *Marine Ecology Progress Series, 496,* 19-32. DOI: 10.3354/meps10528

Yoda, K., Naito, Y., Sato, K., Takahashi, A., Nishikawa, J., Ropert-Coudert, Y., Kurita, M., & Le Maho, Y. (2001). A new technique for monitoring the behaviour of free-ranging Adelie penguins. *Journal of Experimental Biology, 204*(4), 685-690. DOI: 10.1242/jeb.204.4.685

Yoda, K., Sato, K., Niizuma, Y., Kurita, M., Bost, C., Le Maho, Y., & Naito, Y. (1999). Precise monitoring of porpoising behaviour of Adelie penguins determined using acceleration data loggers. *Journal of Experimental Biology, 202(22)*, 3121-3126. DOI: 10.1242/jeb.202.22.3121

Yopak, K. E., Lisney, T. J. & Collin, S. P. (2014). Not all sharks are "swimming noses": variation in olfactory bulb size in cartilaginous fishes. *Brain Structure and Function, 220*(2), 1127-1143. DOI: 10.1007/s00429-014-0705-0

Zeki, S., Hulme, O. J., Roulston, B., & Atiyah, M. (2008). The Encoding of Temporally Irregular and Regular Visual Patterns in the Human Brain. *PLoS ONE* 3(5), e2180. DOI: 10.1371/journal.pone.0002180